

**PERFORMANCE ANALYSIS OF COMPOSITIONAL AND MODIFIED
BLACK-OIL MODELS FOR RICH GAS-CONDENSATE RESERVOIRS WITH
VERTICAL AND HORIZONTAL WELLS**

A Thesis

by

BULENT IZGEC

Submitted to the Office of Graduate Studies of
Texas A&M University
in partial fulfillment of the requirements for the degree of

MASTER OF SCIENCE

December 2003

Major Subject: Petroleum Engineering

**PERFORMANCE ANALYSIS OF COMPOSITIONAL AND MODIFIED
BLACK-OIL MODELS FOR RICH GAS-CONDENSATE RESERVOIRS WITH
VERTICAL AND HORIZONTAL WELLS**

A Thesis

by

BULENT IZGEC

Submitted to the Office of Graduate Studies of
Texas A&M University
in partial fulfillment of the requirements for the degree of

MASTER OF SCIENCE

Approved as to style and content by:

Maria A. Barrufet
(Chair of Committee)

Thomas Blasingame
(Member)

Rick Gibson
(Member)

Hans C. Juvkam-Wold
(Head of Department)

December 2003

Major Subject: Petroleum Engineering

ABSTRACT

Performance Analysis of Compositional and Modified Black-Oil Models for Rich Gas
Condensate Reservoirs with Vertical and Horizontal Wells. (December 2003)

Bulent Izgec, B.S., University of Ankara

Chair of Advisory Committee: Dr. Maria A. Barrufet

It has been known that volatile oil and gas condensate reservoirs cannot be modeled accurately with conventional black-oil models. One variation to the black-oil approach is the modified black-oil (MBO) model that allows the use of a simple, and less expensive computational algorithm than a fully compositional model that can result in significant timesaving in full field studies.

The MBO model was tested against the fully compositional model and performances of both models were compared using various production and injection scenarios for a rich gas condensate reservoir. The software used to perform the compositional and MBO runs were Eclipse 300 and Eclipse 100 versions 2002A.

The effects of black-oil PVT table generation methods, uniform composition and compositional gradient with depth, initialization methods, location of the completions, production and injection rates, k_v/k_h ratios on the performance of the MBO model were investigated. Vertical wells and horizontal wells with different drain hole lengths were used.

Contrary to the common belief that oil-gas ratio versus depth initialization gives better representation of original fluids in place, initializations with saturation pressure versus depth gave closer original fluids in place considering the true initial fluids in place are given by the fully compositional model initialized with compositional gradient.

Compared to the compositional model, results showed that initially there was a discrepancy in saturation pressures with depth in the MBO model whether it was initialized with solution gas-oil ratio (GOR) and oil-gas ratio (OGR) or dew point pressure versus depth tables. In the MBO model this discrepancy resulted in earlier condensation and lower oil production rates than compositional model at the beginning of the simulation.

Unrealistic vaporization in the MBO model was encountered in both natural depletion and cycling cases. Oil saturation profiles illustrated the differences in condensate saturation distribution for the near wellbore area and the entire reservoir even though the production performance of the models was in good agreement.

The MBO model representation of compositional phenomena for a gas condensate reservoir proved to be successful in the following cases: full pressure maintenance, reduced vertical communication, vertical well with upper completions, and producer set as a horizontal well.

DEDICATION

This effort is dedicated to:

My grandfather, Nusret Karaca

My mom, Fatos

My wife and brother, Hilal and Omer

And my cousin, Pinar

ACKNOWLEDGMENTS

I would like to express my sincerest appreciation to:

Dr. Maria Barrufet, chair of my advisory committee, for her help not only in constructing and completing this thesis, but also in my professional development.

Dr. Thomas Blasingame, for giving me the opportunity to be a part of the best petroleum engineering program and also for his invaluable support and encouragement throughout, and prior to, my studies at Texas A&M University.

Dr. Rick Gibson, for his service as member of my advisory committee.

TABLE OF CONTENTS

	Page
ABSTRACT.....	iii
DEDICATION	v
ACKNOWLEDGMENTS.....	vi
TABLE OF CONTENTS	vii
LIST OF TABLES	ix
LIST OF FIGURES.....	xi
 CHAPTER	
I INTRODUCTION.....	1
II BACKGROUND.....	8
2.1 Black-Oil Model	8
2.2 Compositional Model	16
2.2.1 Equation of State	19
2.2.2 Grouping and Splitting.....	22
2.2.3 Mechanisms of Retrograde Condensation and Vaporization.....	26
2.3 Modified Black-Oil Models	29
2.4 Compositional Gradient	31
III FLUID CHARACTERIZATION, SIMULATION MODEL AND GENERATION OF BLACK-OIL PVT TABLES.....	34
3.1 Experimental Fluid Description	34
3.2 Tuning the EOS	37
3.3 Simulation Model.....	43
3.3.1 Static Properties.....	44
3.3.2 Initialization	45
3.4 Black-Oil PVT Table Generation.....	46
IV METHODS.....	52

CHAPTER	Page
4.1 Natural Depletion	55
4.1.1 Effect of Initialization	55
4.1.1.1 Constant Composition with Depth	56
4.1.1.2 Initialization with Compositional Gradient.....	67
4.1.2 Effect of Completion	80
4.1.3 Effect of k_v/k_h Ratio	94
4.2 Gas Cycling Case	108
4.2.1 Effect of Initialization	108
4.2.2 Effect of k_v/k_h Ratio for Gas Cycling	116
4.2.3 Effect of Production and Injection Rates	122
4.2.4 Effect of Completion	126
4.3 Horizontal Wells....	133
4.3.1 Natural Depletion	133
4.3.2 Gas Cycling	140
V SUMMARY AND CONCLUSIONS.....	144
REFERENCES.....	153
APPENDIX A	158
APPENDIX B	159
VITA	180

LIST OF TABLES

	Page
Table 3.1 Sampling conditions.....	34
Table 3.2 Cusiana mixture extended composition	35
Table 3.3 Constant composition expansion data.....	36
Table 3.4 Separator test data	36
Table 3.5 Pseudocomponent grouping and composition	37
Table 3.6 Pseudocomponent properties	38
Table 3.7 Binary interaction coefficients	38
Table 3.8 Variation in parameters selected for regression	39
Table 3.9 Layer thickness, porosity and permeability values	45
Table 3.10 Fluids in place	46
Table 4.1 Fluid in place and CPU times for constant composition with depth.....	61
Table 4.2 Oil saturation values for gridblock 25, 25, 9.....	64
Table 4.3 Fluid in place and CPU times for compositional gradient	67
Table 4.4 Oil saturation values for gridblock 25, 25, 9.....	72
Table 4.5 Oil saturation values for gridblock 25, 25, 18.....	88
Table 4.6 Oil saturation values for gridblock 25, 25, 1.....	94
Table 4.7 Mole fractions of heavy and light components for k_v/k_h ratio of 0.1 in gridblock 25, 25, 18.....	97
Table 4.8 Mole fractions of heavy and light components for k_v/k_h ratio of 10^{-4} in gridblock 25, 25, 18	97
Table 4.9 Mole fractions of heavy and light components for k_v/k_h ratio of 0.1 in gridblock 25, 25, 9.....	97
Table 4.10 Mole fractions of heavy and light components for k_v/k_h ratio of 10^{-4} in gridblock 25, 25, 9	97
Table 4.11 Oil saturation values for gridblock 25, 25, 1.....	104
Table 4.12 Oil saturation values for gridblock 25, 25, 9.....	104

	Page
Table 4.13 Performance of different completions for reduced vertical Communication	107
Table 4.14 Layer thickness, porosity and permeability values for model with horizontal well	133

LIST OF FIGURES

	Page
Fig. 3.1 Cusiana gas condensate phase envelope	40
Fig. 3.2 Simulated and experimental relative volume data from CCE at 254 °F	40
Fig. 3.3 Simulated and experimental liquid saturation data from CCE at 254 °F	41
Fig. 3.4 Simulated and experimental gas density data from CCE at 254 °F	41
Fig. 3.5 C ₁ -N ₂ compositional gradient	42
Fig. 3.6 C ₇ ⁺ Compositional gradient	43
Fig. 3.7 3D Simulation Model.....	44
Fig. 3.8 Gas-oil ratio comparison from Coats versus Whitson and Torp methods	48
Fig. 3.9 Oil formation volume factor comparison from Coats versus Whitson and Torp methods	49
Fig. 3.10 Oil viscosity comparison from Coats versus Whitson and Torp methods.....	49
Fig. 3.11 Oil-gas ratio comparison from Coats versus Whitson and Torp methods.....	50
Fig. 3.12 Gas formation volume factor comparison generated from Coats versus Whitson and Torp methods	50
Fig. 3.13 Gas viscosity comparison from Coats versus Whitson and Torp methods.	51
Fig. 4.1 Steps followed during the study.....	54
Fig. 4.2 Average field pressure for the natural depletion case, constant composition with depth.....	57

	Page
Fig. 4.3 Average oil saturation for natural depletion case, constant composition.....	58
Fig. 4.4a Oil saturation distribution from compositional model for uniform composition case at t=175 days.....	59
Fig. 4.4b 2-D oil saturation distribution from compositional model for uniform composition case at t=175 days, slice between injector and producer.....	59
Fig. 4.5a Oil saturation distribution from MBO model for uniform composition case at t=175 days.....	60
Fig. 4.5b 2-D oil saturation distribution from MBO model for uniform composition case at t=175 days, slice between injector and producer.....	60
Fig. 4.6a Oil saturation distribution from compositional model for uniform composition case at t=1633 days.....	62
Fig. 4.6b 2-D oil saturation distribution from compositional model for uniform composition case at t=1633 days.....	62
Fig. 4.7a Oil saturation distribution from MBO model for uniform composition case at t=1633 days.....	63
Fig. 4.7b 2-D oil saturation distribution from MBO model for uniform composition case at t=1633 days.....	63
Fig. 4.8 Gas-oil ratio for the natural depletion case, constant composition.....	64
Fig. 4.9 Oil production rate for the natural depletion case, constant composition.....	65
Fig. 4.10 Recovery factor for the natural depletion case, constant composition.....	66
Fig. 4.11 Average field pressure with compositional gradient.....	68
Fig. 4.12 Average oil saturation with compositional gradient.....	69
Fig. 4.13 Differences in saturation pressures for both models at the beginning of simulation.....	69
Fig. 4.14a Oil saturation distribution from compositional model, with compositional gradient at t=190 days.....	70

	Page
Fig. 4.14b 2-D oil saturation distribution from compositional model, with compositional gradient at t=190 days	70
Fig. 4.15a Oil saturation distribution from MBO model with compositional gradient at t=190 days.....	71
Fig. 4.15b 2-D oil saturation distribution from MBO model with compositional gradient at t=190 days.....	71
Fig. 4.16 Molar production rate of heavy fraction (C_{17+}), group 6	73
Fig. 4.17a Oil saturation distribution from compositional model with compositional gradient at t= 1645 days	74
Fig. 4.17b 2-D oil saturation distribution from compositional model with compositional gradient at t= 1645 days	74
Fig. 4.18a Oil saturation distribution from MBO model with compositional gradient at t=1645 days.....	75
Fig. 4.18b 2-D oil saturation distribution from MBO model with compositional gradient at t=1645 days.....	75
Fig. 4.19 Oil saturation for well gridblock (25, 25, 1)	76
Fig. 4.20 Oil saturation for well gridblock (25, 25, 9)	76
Fig. 4.21 Oil saturation versus pressure for well gridblock (25, 25, 1).....	77
Fig. 4.22 Oil saturation versus pressure for well gridblock (25, 25, 9).....	77
Fig. 4.23 Oil production rate for the model initialized with compositional Gradient.....	79
Fig. 4.24 Gas-oil ratio for the model initialized with compositional gradient	79
Fig. 4.25 Recovery factor for the model initialized with compositional gradient	80
Fig. 4.26 Oil production rate for the well completed in the two upper layers	82
Fig. 4.27 Oil production rate for the well completed in the two bottom layers	82
Fig. 4.28a Oil saturation distribution from compositional model for bottom completion at t=175 days	83

	Page
Fig. 4.28b 2-D oil saturation profile from compositional model for bottom completion at t=175 days	83
Fig. 4.29a Oil saturation distribution from MBO model for bottom completion at t= 175 days	84
Fig. 4.29b 2-D oil saturation profile from MBO model for bottom completion at t= 175 days	84
Fig. 4.30 Recovery factor for the well completed in the two upper layers	85
Fig. 4.31 Recovery factor for the well completed in the two bottom layers	85
Fig.4.32a Oil saturation distribution from compositional model for bottom completion at the end of the simulation time	86
Fig.4.32b 2-D oil saturation distribution from compositional model for bottom completion at the end of the simulation time	86
Fig. 4.33a Oil saturation distribution from MBO model for bottom completion at the end of simulation time	87
Fig. 4.33b 2-D oil saturation profile from MBO model for bottom completion at the end of simulation time	87
Fig. 4.34 Average oil saturation for the well completed in the two upper layers	88
Fig. 4.35 Average oil saturation for well completed in the two bottom layers	89
Fig. 4.36a Oil saturation profile at 190 days when the well is completed at the top for the compositional model	90
Fig. 4.36b 2-D oil saturation distribution at 190 days when the well is completed at the top for the compositional model	90
Fig. 4.37a Oil saturation profile at 190 days when the well is completed at the top for the MBO model	91
Fig. 4.37b 2-D oil saturation profile at 190 days when the well is completed at the top for the MBO model	91
Fig. 4.38a Oil saturation profile at the end of the simulation time when the well is completed at the top for the compositional model	92

	Page
Fig. 4.38b Oil saturation profile at the end of the simulation time when the well is completed at the top for the compositional model.....	92
Fig. 4.39a Oil saturation profile at the end of the simulation time when the well is completed at the top for the MBO	93
Fig. 4.39b 2-D oil saturation profile at the end of the simulation time when the well is completed at the top for the MBO	93
Fig. 4.40 Average field pressure for k_v/k_h ratio of 0.0001	95
Fig. 4.41 Oil production rate for k_v/k_h ratio of 0.0001	95
Fig. 4.42 Oil saturation for well gridblock (25, 25, 1)	99
Fig. 4.43 Oil saturation for well gridblock (25, 25, 9)	99
Fig. 4.44a Oil saturation distribution from compositional model for k_v/k_h ratio of 0.0001 at $t= 127$ days.....	100
Fig. 4.44b 2-D oil saturation distribution from compositional model for k_v/k_h ratio of 0.0001 at $t= 127$ days.....	100
Fig. 4.45a Oil saturation distribution from MBO model for k_v/k_h ratio of 0.0001 at $t= 127$ days.....	101
Fig. 4.45b 2-D oil saturation distribution from MBO model for k_v/k_h ratio of 0.0001 at $t= 127$ days.....	101
Fig. 4.46a Oil saturation distribution from compositional model for k_v/k_h ratio of 0.0001 after 4 years.....	102
Fig. 4.46b 2-D oil saturation distribution from compositional model for k_v/k_h ratio of 0.0001 after 4 years.....	102
Fig. 4.47a Oil saturation distribution from MBO model for k_v/k_h ratio of 0.0001 after 4 years.....	103
Fig. 4.47b 2-D oil saturation distribution from MBO model for k_v/k_h ratio of 0.0001 after 4 years.....	103
Fig. 4.48 Gas-oil ratio for k_v/k_h ratio of 0.0001	105
Fig. 4.49 Recovery factor for k_v/k_h ratio of 0.0001	106

	Page
Fig. 4.50 Average reservoir pressure for different completion of layers for k_v/k_h ratio of 0.0001	107
Fig. 4.51 Average field pressure for gas cycling case.....	109
Fig. 4.52 Oil production rate for gas cycling case.....	110
Fig. 4.53 Average oil saturation for gas cycling case	110
Fig. 4.54 Gas-oil ratio for gas cycling case.....	111
Fig. 4.55 Saturation distribution for compositional model for layer 9, 3 gridblocks from the producer	112
Fig. 4.56 Saturation distribution for MBO model for layer 9, 3 gridblocks from the producer	112
Fig. 4.57 Saturation distribution for MBO model (Pd versus depth initialization) for layer 9, 3 gridblocks from the producer	113
Fig. 4.58 Saturation distribution for MBO model gridblock (25, 25, 4).....	114
Fig. 4.59 Saturation distribution for MBO model gridblock (25, 25, 5).....	114
Fig. 4.60 Recovery factor for cycling case.....	115
Fig. 4.61 Average field pressure for k_v/k_h ratio of 0.0001	116
Fig. 4.62 Oil production rate for k_v/k_h ratio of 0.0001	117
Fig. 4.63 Average field oil saturation for k_v/k_h ratio of 0.0001.....	117
Fig. 4.64 Gas-oil ratio for k_v/k_h ratio of 0.0001	118
Fig. 4.65 Saturation distribution from compositional model for k_v/k_h ratio of 0.0001 at the end of the simulation.....	118
Fig. 4.66 Saturation distribution from MBO model for k_v/k_h ratio of 0.0001 at the end of the simulation.....	119
Fig. 4.67 Oil-gas ratio versus pressure generated from different compositions.....	120
Fig. 4.68 Recovery factor for k_v/k_h ratio of 0.0001	121
Fig. 4.69 Average reservoir pressure for low production and injection rates	123
Fig. 4.70 Oil production rate for low production and injection rates.....	124
Fig. 4.71 Average oil saturation for low production and injection rates.....	124

	Page
Fig. 4.72 Gas-oil ratio for low production and injection rates	125
Fig. 4.73 Recovery factor for low production and injection rates.....	125
Fig. 4.74 Average field pressure with wells completed at the bottom of the model.....	128
Fig. 4.75 Average field pressure with wells completed at the top of the model.....	128
Fig. 4.76 Oil production rate with wells completed at the bottom of the model.....	129
Fig. 4.77 Oil production rate with wells completed at the top of the model.....	129
Fig. 4.78 Average oil saturation with wells completed at the bottom of the model	130
Fig. 4.79 Average oil saturation with wells completed at the top of the model.....	130
Fig. 4.80 Gas-oil ratio with wells completed at the bottom of the model.....	131
Fig. 4.81 Gas-oil ratio with wells completed at the top of the model	131
Fig. 4.82 Recovery factor with wells completed at the bottom of the model	132
Fig. 4.83 Recovery factor with wells completed at the top of the model.....	132
Fig. 4.84 Average field pressure with horizontal well in layer 3	135
Fig. 4.85 Oil production rate with horizontal well in layer 3.....	135
Fig. 4.86 Gas-oil ratio with horizontal well in layer 3	136
Fig. 4.87 Oil production rate with horizontal well in layer 16.....	137
Fig. 4.88 Gas-oil ratio with horizontal well in layer 16	137
Fig. 4.89 Oil production rate with horizontal well in layer 16 with longer drain hole.....	138
Fig. 4.90 Average oil saturation for horizontal well in layer 16	138
Fig. 4.91 Recovery factor for horizontal well in layer 16.....	139
Fig. 4.92 Oil production rate for gas cycling with horizontal well	140
Fig. 4.93 Gas-oil ratio for gas cycling with horizontal well	141
Fig. 4.94 Recovery factor for gas cycling with horizontal well.....	141
Fig. 4.95 Oil production rate for low production and injection rates for horizontal well.....	142
Fig. 4.96 Gas-oil ratio for low production and injection rates for horizontal well.....	142

Fig. 4.97 Recovery factor for low production and injection
rates for horizontal well..... 143

CHAPTER I

INTRODUCTION

Black-oil simulators represent more than three-fourths of all simulation applications and they can model immiscible flow under conditions such that fluid properties can be treated as functions of pressure only.

The validity of the black-oil model rests on the assumption that the reservoir fluid consists of only two pseudo-components, denoted as oil and gas. The gas phase consists of a gas component only, while the oil phase includes an oil component and a gas component in solution. The oil component cannot be dissolved in the gas phase, and this is the main constraint that prevents physically consistent simulations of volatile oil and gas condensate reservoirs.

The solubility of gas in the oil phase is taken into account by the solution gas-oil ratio (R_s) usually expressed in standard cubic feet of gas per stock tank barrel and the dissolved gas decreases with pressure below bubble point.

Black-oil models are inadequate, for studies that must account for mixing of fluids having significantly different properties, such as displacement of oil by miscible or conditionally miscible fluids, displacements involving chemicals that can affect fluid properties, nonisothermal flow, or combustion reactions.

A compositional study gives increased accuracy that can be obtained by a more realistic description of the fluid. Compositional simulation models assume that, reservoir fluid properties are dependent not only upon the reservoir temperature and pressure but also

on the composition of the reservoir fluid which changes during production, either by depletion or gas injection.

In contrast to the two component fluid representation, a compositional reservoir simulator represents the hydrocarbon phases as multicomponent mixtures and there are no restrictions in mutual solubilities. That is any component may exist in the gas or the oil phase.

Hydrocarbons, as single or two-phases, are at equilibrium at any point and at any time in the reservoir and this equilibrium determine the corresponding oil and gas saturations, phase densities and viscosities. The assumption of equilibrium, implies that the rate of mass transfer of components between phases is much greater than the rate at which individual components travel within the phases themselves.

Gas condensate reservoirs exhibit a complex thermodynamic behavior that cannot be described by simple pressure dependent functional relations. Compositions change continuously during production by pressure depletion, or by cycling above and below dew point pressures.

One variation to the black-oil approach is to treat the reservoir fluid as a gas condensate, consisting of a gas component and vaporized oil. The basic assumption for the pseudo two-component hydrocarbon system is, dry gas holds hydrocarbon liquid as a single-valued function of pressure. This assumption is essential to the characterization of a condensate gas as a two-component system and is based on the following facts; liquid condenses from a condensate gas by retrograde condensation when the pressure is reduced isothermally from the dew point, and retrograde liquid is vaporized by dry gas. Each pseudo-component is itself a multi component hydrocarbon fluid. The water phase, if present, constitutes a third component. However, usually water is considered immiscible in the oil and gas phases and exists as a single liquid phase.

Modified black-oil (MBO) simulation allows the use of a simple and less expensive model. The major question in the use of MBO approach is whether the two-component description can adequately represent the compositional phenomena during depletion or cycling of gas condensate reservoirs.

Coats¹ presented radial well simulations of a gas condensate that showed a modified black-oil PVT formulation giving the same results as a fully compositional EOS PVT formulation for natural depletion above and below dew point. Under certain conditions, he found that the modified black-oil model could reproduce the results of compositional simulation for cycling above the dew point. For cycling below the dew point, the two-component simulation gave results that were quite inaccurate; the two-component approach was incapable of modeling the large compositional gradients that developed.

According to Fevang and Whitson², results from Coats' example should be used with caution as EOS characterization uses seven components with one C₇₊ fraction. With a more detailed C₇₊ split, oil viscosity differences between black-oil and compositional formulations often yield noticeable differences in well deliverability.

Fevang *et al.*³ obtained results which mostly support the conclusions by Coats.¹ However, they found significant differences in oil recovery predicted by compositional and MBO models when the reservoir is a very rich gas condensate and has increasing permeability downwards. According to their final conclusions, a black oil simulator may be adequate where the effect of gravity is negligible, and for gas injection studies a black oil model can only be used for lean to medium-rich gas condensate reservoirs undergoing cycling above dew point.

El-Banbi and McCain^{4, 5} suggested that the MBO approach could be used regardless of the complexity of the fluid. Their paper presented the results of a full field simulation study for a rich gas condensate reservoir. The MBO models performance was compared

with the performance of a compositional model in the presence of water influx and also a field wide history match study was conducted for above and below the dew point. Their paper presents an accurate match of average reservoir pressure and water production rates. However gas-oil ratio, condensate saturation plots were not provided and initial condensate production rates do not represent a clear match for 500 days.

The objectives of this research are to investigate the performance of a modified black-oil model for a rich gas condensate reservoir under natural depletion and gas cycling scenarios.

We performed simulations for natural depletion and gas cycling scenarios for a rich a gas condensate reservoir with full compositional and MBO models. Modified black-oil simulation results were evaluated by comparison with results to the results from the fully compositional simulation.

In MBO model, initializations with saturation pressure versus depth gave closer original fluids in place values compared to the initializations with oil-gas ratio versus depth, especially with the compositional gradient case, which was taken as the reference.

For the uniform composition with depth case original fluids in place were represented by the same value in both initialization methods and also no difference in performance of the models were observed for this particular case for natural depletion.

However it was observed that in the region of higher heavier fractions, initialization with saturation pressure versus depth resulted in erroneous oil saturations for the particular fluid used in this study.

For natural depletion cases as the reservoir gas gets leaner, the initial differences between the models, due to saturation pressure changes with depth disappear and a better

match can be obtained, especially for the poor vertical communication. Accordingly if the perforations are placed in the upper part of the reservoir, when the compositional gradient takes part, the performance of two models get closer. At the top of the reservoir, gas gets leaner due to reduction in heavy component amount that leads to less condensation when the pressure is reduced.

No effect of production rate effect was observed on the performance of models for natural depletion cases.

For the gas cycling cases the models were in good agreement as long as the reservoir was produced with rates high enough to minimize condensation. If the model is initialized with compositional gradient, lower production and injection rates and bottom completions created differences between the performances of the models.

Almost all the cases showed differences in condensate saturation distribution around the wellbore area and the entire reservoir. In MBO model, the runs with the horizontal wells exhibited closer performances with compositional model compared to the runs with vertical wells. The minimum difference between the models is 5 % in terms of average field oil saturation and this was obtained for gas injection with the reduced vertical communication. However, the saturation differences between models depend on the case and the time interval studied. As can be seen in bottom completion for gas injection case, at 1000 days, the condensate saturation difference between two models can be as high as 60 % although they converge to the same value at the end of the simulation.

An additional bank away from to producer closer to the upper boundary of the producing formation was observed which is important in locating the injector to enhance productivity of the producer well. The extent of this bank gets larger if the reservoir has no compositional gradient. MBO model was not able to produce the same banking.

The changes in oil-gas ratio of the cycling gas showed that, it is not possible to accurately represent the changing PVT properties of recycled gas with a single PVT table in the MBO model since every time the produced gas passes through the separators and is injected back into the reservoir its oil-gas ratio and accordingly vaporization characteristics changes.

For this study a representative gas condensate fluid was selected and a fluid model was built by calibrating the EOS to the available experimental data, which consisted of constant composition expansion (CCE) with relative volume, liquid saturations and gas density values.

By using the calibrated EOS black-oil PVT tables were generated for MBO model by using Whitson and Torp⁶ method.

The compositional model was run either with compositional gradient or uniform composition. The compositional gradient in MBO model was given by depth variation of OGR (R_v) and GOR (R_s) or saturation pressure versus depth tables.

MBO model was tested against a compositional model and performances of models were compared for different scenarios. The parameters, which were expected to create differences on the performance of models, are as follows;

- Initialization with compositional gradient/uniform composition in compositional model and correspondingly initialization with saturation pressure and oil-gas ratio versus depth or uniform oil-gas ratio and uniform saturation pressure with depth in MBO model
- PVT tables for MBO model created with different methods
- Size and location of the completions
- Production and injection rates

- k_v/k_h ratio
- The effects of vertical and horizontal wells

An analysis of the effects of different parameters on the performance of modified black-oil model provided guidelines and recommendations for future field wide simulation studies.

The end result is an answer to the major question of whether a complex thermodynamic phenomenon can be represented by simple pressure dependent relationships or would more adjustments have to be done for different scenarios.

CHAPTER II

BACKGROUND

This chapter presents a review of the current literature regarding black-oil, compositional and modified black-oil models, compositional gradients and generation of PVT data for modified black-oil models.

The mechanisms of condensate dropout, vaporization and compositional changes during depletion and gas cycling processes, and the equations of state proposed to characterize this type of fluids are also included.

2.1 Black-Oil Model

The use of reservoir simulation as a predictive tool has become a standard in the petroleum industry due to success in history matching. Its widespread acceptance can be attributed to advances in computing facilities, advances in numerical techniques for solving partial-differential equations, the generality built into reservoir simulators, which makes them useful in modeling field cases, advances in reservoir characterization techniques, and the development of increasingly complicated oil recovery techniques.

A set of algebraic mathematical equations developed from a set of partial differential equations with appropriate initial and boundary conditions approximates reservoir behavior in the reservoir simulation approach. These equations incorporate the most important physical processes taking place in the reservoir system, including, the flow of fluids partitioned into as many as three phases (oil, gas, water), and mass transfer between the various phases. The effects of viscous, capillary, and gravity forces on the fluid flow are taken into consideration by use of a generalized form of Darcy's law.

Many derivations of the oil, water, and gas fluid flow equations exist in the literature, e.g. Crichlow⁷ and Peaceman⁸.

Consequently, only a brief discussion will be presented here beginning with conservation of mass.

We begin by considering the flow of fluid in and out of a single reservoir block (**Figure 2.1**). Assume fluid flows into the block at x (J_x) and out of the block at $x + \Delta x$ ($J_{x + \Delta x}$). J denotes the fluid flux and is defined as the rate of flow of mass per unit cross-sectional area normal to the direction of flow, which is the x-direction in the present case.

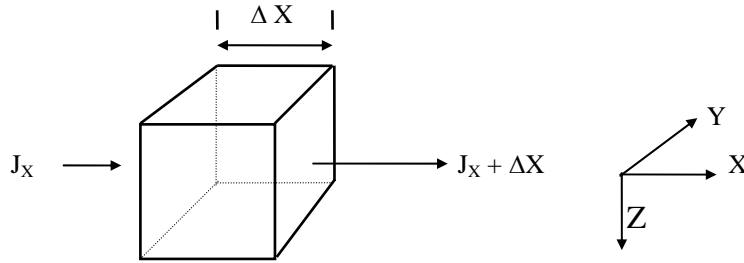
By conservation of mass, we have the equality:

$$\begin{aligned} & \text{mass entering the block} - \text{mass leaving the block} \\ & = \text{accumulation of mass within the block} \dots \dots \dots (2.1) \end{aligned}$$

If the block has length Δx , width Δy , and depth Δz , then we can write the mass entering the block in a time interval Δt as

$$[(J_x)_x \Delta y \Delta z + (J_y)_y \Delta x \Delta z + (J_z)_z \Delta x \Delta y] \Delta t = \text{mass in} \dots \dots \dots (2.2)$$

where we have generalized to allow flux in the y and z directions as well. The notation $(J_x)_x$ denotes the x-direction flux at location x , with analogous meanings for the remaining terms.



Corresponding to mass entering is a term for mass exiting which has the form

$$\begin{aligned}
 & [(J_x)_{x+\Delta x} \Delta y \Delta z + (J_y)_{y+\Delta y} \Delta x \Delta z + (J_z)_{z+\Delta z} \Delta x \Delta y] \Delta t \\
 & + q \Delta x \Delta y \Delta z \Delta t = \text{Mass out} \dots\dots\dots(2.3)
 \end{aligned}$$

where we have added a source/sink term q , which represents mass flow into (source) or out of (sink) a well. A producer is represented by $q > 0$, and an injector by $q < 0$.

Accumulation of mass in the block is the change in concentration of component p (C_p) in the block over the time interval Δt . If the concentration C_p is defined as the total mass of component p (oil, water, or gas) in the entire reservoir block divided by the block volume, then the accumulation term becomes

$$[(C_p)_{t+\Delta t} - (C_p)_t] \Delta x \Delta y \Delta z \dots\dots\dots(2.4)$$

Using Equations (2.1) through (2.4) in the mass conservation equality

$$\text{Mass in} - \text{Mass out} = \text{Mass accumulation}$$

gives

$$[(J_x)_x \Delta y \Delta z + (J_y)_y \Delta x \Delta z + (J_z)_z \Delta x \Delta y] \Delta t$$

$$\begin{aligned}
& - [(J_x)_{x+\Delta x} \Delta y \Delta z + (J_y)_{y+\Delta y} \Delta x \Delta z + (J_z)_{z+\Delta z} \Delta x \Delta y] \Delta t - q \Delta x \Delta y \Delta z \Delta t \\
& = [(C_p)_{t+\Delta t} - (C_p)_t] \Delta x \Delta y \Delta z \dots\dots\dots(2.5)
\end{aligned}$$

Dividing equation (2.5) by Δx , Δy , Δz , Δt and taking the limit as Δx , Δy , Δz and Δt go to zero equation (2.5) becomes the continuity equation

$$-\frac{\partial J_x}{\partial x} - \frac{\partial J_y}{\partial y} - \frac{\partial J_z}{\partial z} - q = \frac{\partial C_p}{\partial t} \dots\dots\dots(2.6)$$

The oil, water, and gas phases each satisfy a mass conservation equation having the form of Equation (2.6).

The flow equations for an oil, water, and gas system are determined by specifying the fluxes and concentrations of the conservation equations for each of the three phases. A flux in a given direction can be written as the density of the fluid times its velocity in the given direction. Letting the subscripts o, w, and g denote oil, water, and gas, respectively, the fluxes become:

$$(\vec{J})_o = \frac{\rho_{osc}}{B_o} \vec{v}_o \dots\dots\dots(2.7)$$

$$(\vec{J})_w = \frac{\rho_{wsc}}{B_w} \vec{v}_w \dots\dots\dots(2.8)$$

$$(\vec{J})_g = \frac{\rho_{gsc}}{B_g} \vec{v}_g + \frac{R_{so} \rho_{gsc}}{B_o} \vec{v}_o + \frac{R_{sw} \rho_{gsc}}{B_w} \vec{v}_w \dots\dots\dots(2.9)$$

where R_{so} and R_{sw} are gas solubilities in the oil and gas phases respectively in SCF/STB, B_o , B_w , and B_g are formation volume factors in units of reservoir volume/standard volume, the subscripts sc denote standard conditions (usually 60°F and 14.7 psia), and ρ denotes fluid densities. The velocities v are assumed to be Darcy velocities and their x-components are

$$v_{xo} = -K_x \lambda_o \frac{\partial}{\partial x} \left[P_o - \frac{\rho_o g z}{144 g_c} \right]^* \dots\dots\dots(2.10)$$

$$v_{xw} = -K_x \lambda_w \frac{\partial}{\partial x} \left[P_w - \frac{\rho_w g z}{144 g_c} \right] \dots\dots\dots(2.11)$$

$$v_{xg} = -K_x \lambda_g \frac{\partial}{\partial x} \left[P_g - \frac{\rho_g g z}{144 g_c} \right] \dots\dots\dots(2.12)$$

where g is the acceleration of gravity in ft/sec², and g_c is 32.174 ft/sec².

The phase mobility λ_p is defined as the ratio of the relative permeability to flow of the phase divided by its viscosity, thus

$$\lambda_p = k_{rp} / \mu_p \dots\dots\dots(2.13)$$

The phase densities are related to formation volume factors and gas solubilities by

$$\rho_o = \frac{1}{B_o} [\rho_{osc} + R_{so} \rho_{gsc}] \dots\dots\dots(2.14)$$

* Similar expressions can be written for the y and z components.

$$\rho_w = \frac{1}{B_w} [\rho_{wsc} + R_{sw} \rho_{gsc}] \dots\dots\dots(2.15)$$

$$\rho_g = \frac{\rho_{gsc}}{B_g} \dots\dots\dots(2.16)$$

Besides fluxes, we also need concentrations. These are given by

$$C_o = \phi \rho_{osc} S_o / B_o, \dots\dots\dots(2.17)$$

$$C_w = \phi \rho_{wsc} S_w / B_w, \dots\dots\dots(2.18)$$

$$C_g = \phi \rho_{gsc} \left[\frac{S_g}{B_g} + \frac{R_{so} S_o}{B_o} + \frac{R_{sw} S_w}{B_w} \right] \dots\dots\dots(2.19)$$

where ϕ is the porosity and S_p is the saturation of phase p . The saturations satisfy the constraint

$$S_o + S_w + S_g = 1 \dots\dots\dots(2.20)$$

Combining Equations 2.6, 2.7 through 2.9, and 2.17 through 2.19 provides a mass conservation equation for each phase:

Oil

$$\begin{aligned}
& \left[\frac{\partial}{\partial x} \left(\frac{\rho_{osc}}{B_o} v_{xo} + R_v \frac{\rho_{osc}}{B_g} v_{xg} \right) + \right. \\
& \left. - \frac{\partial}{\partial y} \left(\frac{\rho_{osc}}{B_o} v_{yo} + R_v \frac{\rho_{osc}}{B_g} v_{yg} \right) + \right. \\
& \left. \frac{\partial}{\partial z} \left(\frac{\rho_{osc}}{B_o} v_{zo} + R_v \frac{\rho_{osc}}{B_g} v_{zg} \right) \right] - q_o = \frac{\partial}{\partial t} (\phi \rho_{osc} S_o / B_o) \dots\dots\dots(2.21)
\end{aligned}$$

Water

$$\left[\frac{\partial}{\partial x} \left(\frac{\rho_{wsc}}{B_w} v_{xw} \right) + \frac{\partial}{\partial y} \left(\frac{\rho_{wsc}}{B_w} v_{yw} \right) + \frac{\partial}{\partial z} \left(\frac{\rho_{wsc}}{B_w} v_{zw} \right) \right] - q_w = \frac{\partial}{\partial t} (\phi \rho_{wsc} S_w / B_o) \dots\dots(2.22)$$

Gas

$$\begin{aligned}
& - \frac{\partial}{\partial x} \left(\frac{\rho_{gsc}}{B_g} v_{xg} + \frac{R_{so} \rho_{gsc}}{B_o} v_{xo} + \frac{R_{sw} \rho_{gsc}}{B_w} v_{xw} \right) - \frac{\partial}{\partial y} \left(\frac{\rho_{gsc}}{B_g} v_{yg} + \frac{R_{so} \rho_{gsc}}{B_o} v_{yo} + \frac{R_{sw} \rho_{gsc}}{B_w} v_{yw} \right) \\
& - \frac{\partial}{\partial z} \left(\frac{\rho_{gsc}}{B_g} v_{zg} + \frac{R_{so} \rho_{gsc}}{B_o} v_{zo} + \frac{R_{sw} \rho_{gsc}}{B_w} v_{zw} \right) - q_g \qquad \qquad \qquad (2.23) \\
& = \frac{\partial}{\partial t} \left[\phi \rho_{gsc} \left(\frac{S_g}{B_g} + \frac{R_{so} S_o}{B_o} + \frac{R_{sw} S_w}{B_w} \right) \right]
\end{aligned}$$

The densities at standard conditions are constants and can, therefore, be divided out of the above equations. This reduces the equations to the following form:

Oil

$$-\left[\begin{aligned} &\frac{\partial}{\partial x} \left(\frac{v_{xo}}{B_o} + R_v \frac{v_{xg}}{B_g} \right) + \frac{\partial}{\partial y} \left(\frac{v_{yo}}{B_o} + R_v \frac{v_{yg}}{B_g} \right) \\ &+ \frac{\partial}{\partial z} \left(\frac{v_{zo}}{B_o} + R_v \frac{v_{zg}}{B_g} \right) \end{aligned} \right] - \frac{q_o}{\rho_{osc}} = \frac{\partial}{\partial t} (\phi S_o / B_o) \dots\dots\dots(2.24)$$

Water

$$-\left[\frac{\partial}{\partial x} \left(\frac{v_{xw}}{B_w} \right) + \frac{\partial}{\partial y} \left(\frac{v_{yw}}{B_w} \right) + \frac{\partial}{\partial z} \left(\frac{v_{zw}}{B_w} \right) \right] - \frac{q_w}{\rho_{wsc}} = \frac{\partial}{\partial t} (\phi S_w / B_w) \dots\dots\dots(2.25)$$

Gas

$$-\frac{\partial}{\partial x} \left(\frac{v_{xg}}{B_g} v_{xg} + \frac{R_{so}}{B_o} v_{xo} + \frac{R_{sw}}{B_w} v_{xw} \right) - \frac{\partial}{\partial y} \left(\frac{v_{yg}}{B_g} + \frac{R_{so}}{B_o} v_{yo} + \frac{R_{sw}}{B_w} v_{yw} \right) \\ - \frac{\partial}{\partial z} \left(\frac{v_{zg}}{B_g} + \frac{R_{so}}{B_o} v_{zo} + \frac{R_{sw}}{B_w} v_{zw} \right) - \frac{q_g}{\rho_{gsc}} = \frac{\partial}{\partial t} \left[\phi \left(\frac{S_g}{B_g} + \frac{R_{so} S_o}{B_o} + \frac{R_{sw} S_w}{B_w} \right) \right] \dots\dots\dots(2.26)$$

Equations (2.10) through (2.16), (2.20), and (2.24) through (2.26) are the basic fluid flow equations, which are numerically solved in a modified black-oil simulator. Setting the oil-gas ratio term equal to zero in the oil equations reduces the model to the conventional black oil model.

Many reservoirs contain fluids, which have simple type of phase behavior and physical properties. It is sufficient accurate for these fluids, to represent the amount of gas in

solution as an empirical function of pressure only. The densities of gas and reservoir oil are related to surface densities through formation volume factors which are pressure-dependent functions named B_o , B_g and R_s . Viscosities are also functions of pressure. Such simple systems are called black oil systems.

Black-oil simulators are used in situations where recovery processes are insensitive to compositional changes in the reservoir fluids. In black-oil simulators, mass transfer is assumed to be strictly pressure dependent.

Primary oil recovery mechanisms, such as solution-gas drive, gas-cap expansion, gravity drainage, and water drive, and also some secondary recovery mechanisms such as water or immiscible gas injection can all be modeled with conventional black-oil simulators.

As long as the phase behavior and physical properties are simple enough to be represented as functions of pressure black-oil models can be used.

However, for many reservoirs and recovery processes, black-oil models are not representative of the actual phase behavior and fluid properties. The primary limitation of black-oil simulators is that they do not account for liquids that condense out of the vapor phase.

2.2 Compositional Model

The fundamental difference between compositional reservoir simulators and black-oil reservoir simulators lies in their treatment of fluid properties and phase behavior. Compositional simulators are used when recovery processes are sensitive to compositional changes. These situations include primary depletion of volatile oil and gas-condensate reservoirs, as well as pressure maintenance operations for these reservoirs. Also, multiple contact miscible processes are generally modeled with compositional simulators.

In some cases a compositional model may also be required to accurately simulate immiscible gas injection in a black-oil reservoir. For example, injection of a very lean gas may cause significant vaporization of residual oil, resulting in higher recoveries than a black-oil model would predict.

A compositional study gives increased accuracy that can be obtained by a more realistic description of the fluids. It computes changing compositions of liquid and gaseous phases using the principles of mass conservation and phase equilibrium.

Although the mathematical equations are more complicated than for black-oil reservoir simulation, the concepts can be simplified by saying that we are simultaneously modeling; three-phase Darcy flow, the movement of each individual hydrocarbon component, and phase equilibrium at each point in the reservoir. When we consider black oil models each phase (oil, water, gas) has its own corresponding mass balance equation. For compositional models we must keep track of the mass of individual hydrocarbon components.⁹

The pressure of three fluid phases is related by capillary pressure.

Hydrocarbon components can exist in either gas or oil phase. The mass balance equation and other conditions applicable for component i are:

1-) Mass balance equation for hydrocarbon components:

$$\nabla x(\hat{y}_i \rho_g \bar{u}_g) + \nabla x(\hat{x}_i \rho_o \bar{u}_o) = -\frac{\partial}{\partial t} [\phi(S_o \rho_o \hat{x}_i + S_g \rho_g \hat{y}_i)] \dots\dots\dots(2.27)$$

$\hat{y}_i, \hat{x}_i =$ mass fractions of vapor, liquid

2-) the saturation relationship is:

$$\sum S_{o,g,w} = 1.0 \quad \dots\dots\dots(2.28)$$

3-) Darcy's Law and Martin's Equation apply and the phase behavior is:

$$\rho_o = f_o(p, T, x_i) \quad \dots\dots\dots(2.29)$$

$$\rho_g = f_g(p, T, y_i) \quad \dots\dots\dots(2.30)$$

$$\mu_o = q_o(p, T, x_i) \quad \dots\dots\dots(2.31)$$

$$\mu_g = q_g(p, T, y_i) \quad \dots\dots\dots(2.32)$$

The simplest compositional models use the same mass balance equation for water as used in black oil models. This assumes no hydrocarbon components dissolve in the water and this is generally a good assumption. However at high temperatures and pressures or if there is a significant amount of carbon dioxide in the reservoir water in oil solubility and the solubility of hydrocarbon components in water should be accounted for.

The compositional simulator assumes equilibrium at all times when two phases are present and this equilibrium determines the corresponding oil and gas saturations. According to this assumption the rate of mass transfer of components between phases are much greater than the rate at which individual components travel within the phases themselves. The equilibrium between oil and gas phases is determined by a flash calculation from thermodynamic flash calculations using an EOS or from correlated or empirically derived equilibrium ratios or K -values.

2.2.1 Equation of State

An equation of state (EOS) is a mathematical expression among volume, pressure, temperature, composition and can be used to describe the volumetric and phase behavior of hydrocarbon mixtures.

Experimental data obtained from constant volume depletion tests (CVD) and constant composition expansion tests (CCE) done with bottom hole samples at high pressures is not always available. Properties and compositions measured from recombining samples at standard conditions to obtain separator oil compositions can involve inexact predictions. Additionally sampling a gas condensate reservoir is costly and subject to errors such as inaccurate initial reservoir pressure and temperature values.

Equations of state provide an efficient way to describe the volumetric and phase behavior of hydrocarbon mixtures. Once the EOS is tuned to match the experimental data of the given fluid it is assumed that it will represent the phase behavior of that fluid at any pressure and temperature.

The Soave Redlich Kwong^{10, 11} equation is one of the most widely used because of its simplicity although it underestimates liquid densities of petroleum mixtures. However it is an excellent tool for systems where accurate predictions of vapor-liquid equilibria (VLE) and vapor properties are required.

A better liquid density prediction was then the goal, especially in the vicinity of the critical region. Looking for an improved equation, Peng Robinson^{10, 11, 12} developed the following expression (PR EOS):

$$p = \frac{RT}{v-b} - \frac{a\alpha}{v(v+b)+b(v-b)} \dots\dots\dots(2.33)$$

The parameters a and b are determined by imposing the critical point constraints at T_c and p_c :

$$a = \Omega_a \frac{R^2 T_c^2}{p_c} \quad \text{with} \quad \Omega_a = 0.45724 \dots\dots\dots(2.34)$$

$$b = \Omega_b \frac{RT_c}{p_c} \quad \text{with} \quad \Omega_b = 0.07780 \dots\dots\dots(2.35)$$

$$\alpha = \left[1 + m(1 - \sqrt{T_R}) \right]^2 \dots\dots\dots(2.36)$$

$$m = 0.37464 + 1.54226\omega - 0.26992\omega^2 \quad \omega \leq 0.5 \dots\dots\dots(2.37)$$

Zudkevitch and Joffe¹⁰ suggested that the constants a and b should be corrected as functions of temperature to match saturated liquid densities and liquid fugacities.

Their equation of state is more accurate for predictions of both liquid and vapor properties but its main disadvantage is the complexity of the functions used to represent temperature dependent corrections for the constants a and b .

Peng and Robinson (PR) proposed a modified expression for m that is recommended for heavier components ($\omega > 0.49$).

$$m = 0.379642 + 1.48503\omega - 0.164423\omega^2 + 0.016666\omega^3 \dots\dots\dots(2.38)$$

To calculate the constants a and b for mixtures the following mixing rules are recommended:

$$b = \sum_j y_j b_j \quad a = \sum_i \sum_j y_i y_j (a_i a_j)^{1/2} (1 - \delta_{ij}) \dots\dots\dots(2.39)$$

where:

Subscripts j and i refer to components

y_i = gas molar fraction of component i

δ_{ij} = binary interaction coefficient between component i and j

The estimation of a universal critical compressibility factor of 0.307, which is lower than the Redlich Kwong value of 1/3 and is closer to experimental values for heavier hydrocarbons is the most significant improvement of the Peng Robinson equation with respect to the Redlich Kwong equation. A two-parameter equation of state, which includes the critical pressure and critical temperature, predicts densities of saturated liquids and critical volumes with significant differences from their experimental values. Therefore cubic equations with three parameters such as the Peng Robinson EOS and the Soave Redlich Kwong EOS that include the critical properties along with the acentric factor, are widely used for their simplicity and accuracy.

The four parameter Peng Robinson equation of state was introduced when a method was developed to improve volumetric predictions introducing a fourth EOS constant, c , the volume correction parameter. Jhaveri and Youngren¹³ found in the application of the Peng Robinson equation of state to predict the gas phase compressibility, error ranged from 3% to 5% and the error in the liquid density predictions was from 6% to 12%. Then they developed a correlation for characterizing the volume correction parameter c . This relation can be expressed as follows:

$$c_i = S_i b_i \dots\dots\dots(2.40)$$

where:

S_i = Dimensionless parameter, “Shift Parameter”, characteristic of every component

b_i = Peng Robinson co-volume as given by equation (2.35)

A significant improvement in the volumetric predictions can be obtained by this equation. This correction does not affect phase equilibria predictions. The corrected hydrocarbon phase volume are given by the following expressions:

$$v^L_{corr} = v^L - \sum_{i=1}^{N_c} (x_i c_i) \quad v^V_{corr} = v^V - \sum_{i=1}^{N_c} (y_i c_i) \dots\dots\dots(2.41)$$

where:

v^L, v^V = Molar volumes of the liquid phase and gas phase calculated by unmodified PR EOS, ft³/lbmole.

v^L_{corr}, v^V_{corr} = Corrected volumes of the liquid and gas phase, ft³/lbmole.

2.2.2 Grouping and Splitting

Grouping

A typical crude oil contains thousands of different chemical compounds. When a fluid is described by a long list of components it is impractical to use all of them in a reservoir simulation. Since the material balance equation must be solved for each component in a compositional reservoir simulation, computer storage requirements and time will be significant. For each grid block the principles of component mass conservation and phase equilibrium are used to calculate the phase pressures, saturations, and compositions at each time step.

A significant speedup can be accomplished in simulation processes by using fewer components. These equivalent pseudocomponents must be selected such that the predicted reservoir performance is equivalent to that obtained with more components. Therefore pseudoization is a common practice for compositional simulations.

This procedure allows us to obtain new components called “pseudocomponents”, that consist of a subset of the N_c original components. At the same time pseudocomponent properties such as critical pressure, critical temperature, Ω_a , Ω_b , and binary interaction coefficients are computed in such a way that when these are properly combined a good match with the measured properties of the original mixture can be achieved.

According to Wattenbarger⁹, modeling depletion of volatile oil or gas condensate reservoirs requires that all components through hexane be included, with the heptane-plus fraction being lumped. If depletion is by gas cycling, the model must include a breakdown of the composition of heptane-plus fraction because an important part of the process is vaporization of heavy components. If this detailed breakdown is not used, the model will eventually compute that all the oil has vaporized which is physically unrealistic. There are several rules of thumb to group these components depending upon their composition, nature of the molecules and production strategies planned.

Coats¹ developed a pseudoization procedure for a gas condensate where the sample was lumped into 7 pseudocomponents system of N_2+C_1 , CO_2 , C_3+C_4 , C_5+C_6 and 3 heavy components. He concluded a minimum of six components was needed.

Li, Nghiem, and Siu¹⁴ presented a method where lumping is based on the K values of an original fluid description taken from a flash at reservoir temperature and the average operating pressure. They also suggested the use of phase diagrams and compositional simulation to verify the appropriateness of the grouping.

Splitting

The existing chemical separation techniques are not able to identify all the components found in reservoir fluids. Critical properties and other EOS parameters of compounds heavier than approximately C_{20} cannot be accurately known. However, an approximate characterization of the heavier compounds, dividing the C_7^+ fraction into a number of fractions with specified molar compositions, molecular weights, specific gravities, boiling points and critical properties of each C_7^+ fraction, can solve this problem. Three important requirements should be satisfied when applying any splitting models.

First Constraint: The sum of the mole fractions of the individual pseudocomponents is equal to the mole fraction of C_7^+ .

$$\sum_{i=7}^{N^+} z_i = z_{C_7^+} \dots\dots\dots(2.42)$$

Second Constraint: The sum of the products of the mole fraction and the molecular weight of the individual pseudocomponents is equal to the product of the mole fraction and molecular weight of C_7^+ .

$$\sum_{i=7}^{N^+} z_i Mw_i = z_{C_7^+} Mw_{C_7^+} \dots\dots\dots(2.43)$$

Third Constraint: The sum of the product of the mole fraction and molecular weight divided by the specific gravity of each individual component is equal to that of C_7^+ .

$$\sum_{i=7}^{N^+} \frac{z_i Mw_i}{\gamma_i} = \frac{z_{C_7^+} Mw_{C_7^+}}{\gamma_{C_7^+}} \dots\dots\dots(2.44)$$

where:

i = number of carbon atoms

N^+ = last hydrocarbon group in the C_7^+ with n carbon atoms, e.g., 20 +

It is assumed that the molecular weight and specific gravity of the C_7^+ are measured.

Whitson¹⁵ proposed a splitting method based on molecular weights. He suggested that the plus fraction can be represented by a number of Multi Carbon Number groups, which can be determined from the following expression:

$$N_g = \text{Int}\{1 + 3.31\log(N - n)\} \dots\dots\dots(2.45)$$

where:

N_g = Number of MCN groups

Int = Integer

N = Number of carbon atoms of the last component in the hydrocarbon system

n = Number of carbon atoms of the first component in the plus fraction

Lee *et al*¹⁶ suggested that C_7^+ fractions can be split according to a factor computed from averaging slopes of the curves obtained when plotting molecular weight and specific gravity vs. boiling point. Behrens and Sandler¹⁷ proposed a splitting method for C_7^+ fractions based on application of the Gaussian-quadrature method to continuous thermodynamics. Although this method uses a simple exponential distribution with two quadrature points the method can be applied to any molar distribution model and for any number of C_7^+ groups.

Once the pseudocomponents have been determined tuning the equation of state is a prerequisite for a compositional simulation. Tuning the selected equation of state

provides a reduced component characterization that matches the experimental PVT data. Studies done with the untuned Peng Robinson equation of state with the original number of components have shown that errors in computed saturation pressures can reach values higher than 25%. However since there is not a general guide to choose the parameters of the equation of state that should be altered or regressed, the types and number of regression variables depend on the experience of the engineer in charge of the fluid characterization. Coats¹ defined as standard regression variables the Ω_a 's, Ω_b 's of methane and heaviest fraction and the binary interaction parameter between methane and the heaviest fraction. Sometimes the Ω 's of CO₂ and N₂ can be selected as regression variables if these components are present in large quantities in the original mixture.¹⁵ Stepwise regression is the best approach to determine the number and properties of pseudocomponents that can accurately describe a reservoir fluid's phase behavior. These steps are repeated until the scheme resulting from the regression is the one that shows the closest phase behavior between the reduced pseudocomponent characterization and the original fluid characterization. If stepwise regression is not possible, standard grouping of the light and intermediates (N₂ + C₁, CO₂ + C₂, *i*-C₄ + *n*-C₄, and *i*-C₅ + *n*-C₅) and Gaussian quadrature (or equal mass fractions) for C₇⁺ is recommended.¹⁵

2.2.3 Mechanisms of Retrograde Condensation and Vaporization

Kuenen¹⁸ discovered the phenomenon of retrograde condensation in 1892. Since then researchers have been fascinated by the near critical phenomena because of the atypical condensation behavior that takes place in this type of fluid. The behavior is atypical since a pressure drop causes condensation rather than vaporization, as would normally occur. For complex hydrocarbon mixtures few studies have been done, although for pure substances, binary, and ternary fluid systems, more detailed studies are available in the literature.

Gas condensate fluids present a very complex behavior in the reservoir, but especially near the wellbore, where pressure variations can substantially affect the performance of the reservoir. Once the reservoir pressure drops below the saturation pressure, or dewpoint pressure, at temperatures between the cricondentherm and critical point, liquid precipitates from gas condensate systems. As the pressure drops further liquid builds up decreasing the gas relative permeability and causing large pressure drops in the near well zone. This wellbore flow behavior acts as a condensate blockage¹. As a consequence the well productivity is reduced.

Fevang and Whitson² identified the existence, at any time of depletion, of one, two or three flow regions, depending on the values of flowing bottomhole pressure and reservoir pressure.

If the flowing bottomhole pressure is above the initial in-situ fluid dew point, the whole reservoir is single phase. If the flowing bottom hole pressure is below dew point, then the reservoir may contain three flow regions. Region one is defined as a zone closer to the inner near-wellbore where both gas and oil flow simultaneously at different velocities. The size of region one increases with time.

Outward into the reservoir, region two contains a condensate buildup where only gas is flowing. The size of this region is larger at early times just after the reservoir pressure falls below the dewpoint, and it decreases with time due to expansion of region one.

Finally contiguous to region two, region three, which extends to the limits of the reservoir, exists only if the reservoir pressure is higher than the dew point pressure and only a single gas phase is present. Composition is constant and equal to the original reservoir gas composition.

The size of the each region changes with time as the reservoir depletes. The three regions will coexist whenever the bottom hole flowing pressure is slightly lower than the dewpoint pressure.

The authors also discussed the phase behavior characteristics in each region and noted that region one behaves like constant composition expansion (CCE) cell, whereas region two acts like a constant volume depletion (CVD) cell. Based on this, they argued that the produced well stream has the same composition, as the single-phase gas entering region one and thus the flowing GOR must be constant throughout region one.

An effective way to enhance condensate recovery is to maintain reservoir pressure above the dewpoint as long as possible is by gas injection or gas cycling. Once the well is produced at a pressure below the dewpoint, it is not possible to remove all the liquid precipitated in the reservoir unless a complete revaporization takes place in the reservoir. However, gas cycling will increase the original dewpoint of the mixture and form a leaner mixture; as a result condensate production will decline over time. The formation of the condensate region near the well bore will be prevented or delayed since the cycling process reduces the loss of condensate by maintaining pressure and vaporizing the liquid hydrocarbon phase into the injected gas.

During the initial stages of dry gas injection, the rich gas is displaced by the dry gas towards the producing wells. Pressure is partially maintained and the rising of the producing gas-oil ratio is slowed. The displacement of the rich gas is a miscible process and the interface between dry gas and rich gas is dispersed due to convection dispersion and molecular diffusion. Due to normal sweepout, the dry gas breaks through the producing wells and the producing gas-oil ratios begin to climb.

The liquid normally does not move because it is below the residual oil saturation. However, the oil does vaporize behind the displacement front. The lighter ends of the oil vaporize because of the contact with the dry injection gas instead of the rich reservoir

gas that is previously contacted. As this vaporization continues, the oil saturation decreases and a significant amount of the oil components are transported to the producing wells in the gas phase. This vaporization process is important because the vaporized components have an impact on the plant economics and because it tends to make the remaining oil heavier and more difficult to move.

This miscible process is referred to as a multiple contact miscible process as opposed to a first contact miscible process. Two fluids are considered first contact miscible if all possible mixtures of the two yield a single-phase fluid at a given pressure and temperature. If the path connecting the injected gas composition and the reservoir composition does not pass through the two-phase region, the process is termed first contact miscible. This path is known as the dilution path and represents the composition changes as the injected gas displaces reservoir oil.

2.3 Modified Black-Oil Models

It has been known that volatile oil and gas condensate reservoirs cannot be modeled accurately with conventional black-oil models. Conventional black-oil models use the three pressure-dependent functions B_o , B_g and R_s . The primary limitation of these techniques is that they do not account for the liquid that condenses out of the vapor phase. It is also known that these reservoir fluids can be modeled accurately with full compositional models.

However, compositional simulation is more difficult, time-consuming and costly than black-oil models. Several studies have been conducted to show that full compositional simulation may not be needed in all cases. It is desirable to find an intermediate model between black-oil and compositional approaches.

Modified black-oil models have an additional pressure dependent function, R_v . This parameter accounts for the amount of oil carried in vapor phase. The amount of oil carried in the gas phase is a function of pressure below the dew point. The modified black-oil representation is based on fixed densities of surface gas and oil just like black oil models. A compositional simulation of the same fluid will result in gravities of the surface oil and gas that vary as the reservoir is depleted, which more closely models what actually happens in the field.^{19, 20, 21}

The compositional variation in MBO model is given by the depth variation of solution gas-oil ratio and oil-gas ratio. These two black-oil PVT properties represent in fact composition and should, accordingly, be used to initialize the reservoir model. Despite an initialization of composition with depth in a black-oil model, where solution gas-oil and oil-gas ratio are taken directly from the compositional EOS mode, we know that the saturation pressure versus depth will not be represented properly in the black-oil model. Because a single PVT table is used for a MBO model and fluid at each depth has its own set of PVT tables.³

In MBO model the first dry gas injected will vaporize liquid according to the liquid content, oil-gas ratio. As the vaporizing gas flows through the reservoir its ability to vaporize oil diminishes. Thus for this gas, oil-gas ratio is not simply a function of pressure but depends upon the path it takes and the oil with which it comes into contact.

²²

According to Cook *et al.*²³, the percentage rate of vaporization for the individual components of heavy fractions of oil, during the first part of cycling is a direct function of their equilibrium ratios. The lighter hydrocarbons tend to vaporize first and the reservoir oil becomes denser and less volatile as gas cycling continues. After a small amount of cycling, all of the components with the lower K -values are vaporized beginning with those of lower molecular weights.

In modified black-oil model the primary compositional effect, the stripping of the liquid components in inverse proportion to their molecular weight is completely ignored and by doing this the standard black-oil model disregards the compositional dependence of PVT properties. The kind of formulation used in MBO model allows the dry gas to pick up oil until the gas becomes saturated, which is an optimistic approximation to the actual reservoir behavior.²⁴

As a consequence, when dry gas is injected into a condensate reservoir below its dew point the gas continues to re-vaporize liquid at a rate governed only by the pressure. In reality the liquid saturation profiles should vary smoothly with increasing distance from the injector.

2.4 Compositional Gradient

In thick reservoirs (sometimes more than 6500 ft) gravity forces may generate and stabilize variations in composition along the hydrocarbon column. From the top to the bottom of the reservoir the mole fraction of lighter components decreases, whereas the fraction of heavier components increases.²⁵

In a reservoir at thermodynamic equilibrium, a segregation profile will be established under the influence of gravitational forces.

Complete thermodynamic equilibrium will never be achieved since a uniform temperature, which does not occur in reality, would be required. Theory indicates that the natural temperature gradient will enhance compositional grading.²⁶

The thermodynamic expression for work in a multicomponent system under a gravitational field must include not only the term representing expansion or compression

by the system on the surroundings, but also the work associated with displacing a differential amount of mass in the vertical direction.^{27, 28}

The Gibbs free energy under a gravitational field as given by Firoozabadi²⁹ is

$$dG_i = -S_i dT + V_i dP + \sum_{i=1}^{N_c} (\hat{\mu}_i + M w_i g h) dn_i + mg dh \dots\dots\dots(2.46)$$

At equilibrium dG vanishes. Pressure and position (z) are related through the hydrostatic equation as

$$V_i dP + mg dh = 0 \dots\dots\dots(2.47)$$

$$dP = -\rho g dh \dots\dots\dots(2.48)$$

For an isothermal system

$$dT = 0 \dots\dots\dots(2.49)$$

Equation (2.43) becomes

$$\hat{\mu}_i + M w_i g h = 0 \dots\dots\dots(2.50)$$

This expression provides the Gibbs sedimentation equation

$$(d\hat{\mu}_i + M w_i g dh)_T = 0 \dots\dots\dots(2.51)$$

Expressing the chemical potential in terms of fugacities and integrating from reference depth of zero to h gives

$$\hat{f}_i = \hat{f}_i^o \exp\left(-\frac{Mw_i}{RT} gh\right) \dots\dots\dots(2.52)$$

Equation (2.49) gives the fugacity coefficient of component “i” in a given phase as a function of vertical position, given the pressure and compositions at a reference depth.

Volatile oil and gas condensate reservoirs may present a strong vertical compositional segregation due to gravity field and temperature gradients. Compared to an oil column, the compositional variations in the gas column are rather small but seem to have a marked effect on the dew-point pressure. Both reservoir pressure and dew point pressure increase with increasing height.

Such a compositional grading can have significant influence on various aspects of reservoir development. Also, when considering gas injection, one must be aware that compositional effects, such as the development of miscibility change with depth.

Without including the compositional gradient, the original oil and original gas in place can be underestimated or overestimated and these variations depend on the depth of the sample.²⁹

CHAPTER III

FLUID CHARACTERIZATION, SIMULATION MODEL AND GENERATION OF BLACK-OIL PVT TABLES

The fluid selected for our study is a very rich gas condensate taken from Cusiana Field located 125 miles northeast of Bogotá, Colombia in the Llanos basin. Data was taken from Jaramillo.²⁹

Sampling conditions are presented in **Table 3.1**.

Table 3.1 Sampling conditions

Sampling Conditions	
Choke (1/64")	24
Well Head Pressure (psia)	2,270
Well Head Temperature (°F)	124
Separator Pressure (psia)	313
Separator Temperature (°F)	84
Oil Rate (STB/D)	870
Oil Density (°API)	42.1
GOR (SCF/STB)	5,855
Gas Specific Gravity	0.716

3.1 Experimental Fluid Description

A compositional analysis with hydrocarbon components that includes a heavy fraction of C_{30}^+ , and a set of experimental data obtained from a constant composition expansion and a separator test were used to characterize the fluid.

Table 3.2 presents the extended compositional description of the fluid.

Table 3.2 Cusiana mixture extended composition

Component	Symbol	Mol %
Carbon Dioxide	CO ₂	4.57
Nitrogen	N ₂	0.52
Methane	C ₁	68.97
Ethane	C ₂	8.89
Propane	C ₃	4.18
Isobutane	iC ₄	0.99
N-Butane	nC ₄	1.4
Isopentane	iC ₅	0.71
N-Pentane	nC ₅	0.6
Hexanes	C ₆	0.99
Heptanes	C ₇	1.02
Octanes	C ₈	1.28
Nonanes	C ₉	0.97
Decanes	C ₁₀	0.73
Undecanes	C ₁₁	0.53
Dodecanes	C ₁₂	0.44
Tridecanes	C ₁₃	0.48
Tetradecanes	C ₁₄	0.41
Pentadecanes	C ₁₅	0.36
Hexadecanes	C ₁₆	0.28
Heptadecane	C ₁₇	0.26
Octadecanes	C ₁₈	0.24
Nonadecanes	C ₁₉	0.19
Eicosanes	C ₂₀	0.16
C21's	C ₂₁	0.13
C22's	C ₂₂	0.11
C23's	C ₂₃	0.1
C24's	C ₂₄	0.08
C25's	C ₂₅	0.07
C26's	C ₂₆	0.06
C27's	C ₂₇	0.06
C28's	C ₂₈	0.05
C29's	C ₂₉	0.04
C30+	C ₃₀₊	0.13

Peng-Robinson EOS was selected and tuned to the data obtained from the constant composition expansion at 254°F, which includes the liquid saturation, gas density and the relative volume. This process is discussed in the next section. **Table 3.3** presents the data from this experiment. Additionally data from a separator test is presented in **Table 3.4**.

Table 3.3 Constant composition expansion data

CCE @ 254°F			
Pressure (psia)	Relative Volume (fraction)	Liquid Saturation (fraction)	Gas Density lbm/ft ³
6358	0.9612	0.000	26.0075
6255	0.9665	0.000	25.8639
6157	0.9716	0.000	25.7266
6055	0.9773	0.000	25.5767
5959	0.9830	0.000	25.4269
5892	0.9869	0.000	25.3270
5842	0.9898	0.000	25.2584
5794	0.9927	0.000	25.1772
5744	0.9958	0.000	25.1023
5695	0.9990	0.000	25.0211
Pd =5680	1.0000	0.000	24.9962
5644	1.0030	1.650	0.0000
5545	1.0100	5.939	0.0000
5446	1.0190	9.128	0.0000
5347	1.0280	11.720	0.0000
5254	1.0370	13.800	0.0000
5056	1.0570	16.760	0.0000
4740	1.0930	20.460	0.0000
4437	1.1360	21.170	0.0000
4144	1.1870	21.420	0.0000
3847	1.2490	21.190	0.0000
3544	1.3280	20.480	0.0000
3241	1.4260	19.390	0.0000
2937	1.5500	17.950	0.0000
2660	1.6940	16.410	0.0000
2351	1.9010	14.440	0.0000
2044	2.1790	12.390	0.0000
1738	2.5680	10.270	0.0000
1435	3.1240	8.199	0.0000
1133	4.0040	6.165	0.0000

Table 3.4 Separator test data

Separator Test @ 254°F			
Pressure (psig)	Temperature °F	GOR (SCF/STB)	Gas Specific Gravity
500	180	6696.5	0.7728
30	150	208.2	1.205
15	80	68.07	2.078

3.2 Tuning the EOS

As mentioned in Chapter II section 2.3 it is necessary to reduce the number of components to reduce the computer storage requirements and the time of the simulation. Therefore following the procedure proposed by Whitson¹⁵ discussed in section 2.3, where the groups are separated by molecular weight we used six pseudocomponents and one non-hydrocarbon, CO₂. The pseudocomponents were defined as two pseudo-gases, GRP1 and GRP2, one gasoline group, GRP3 and three heavy pseudocomponents, GRP4, GRP5 and GRP6, in the same way that Jaramillo²⁹ proposed when he characterized this fluid. For the purposes of CO₂ injection, this component was kept as a separate group.

The first pseudocomponent GRP1 is composed of methane and nitrogen. The amount of nitrogen in the original fluid is not significant; therefore for injection purposes it is assumed that this pseudocomponent contains only methane. The second pseudo-gas contains ethane and propane. The gasoline group GRP3 contains butanes, pentanes and hexanes. GRP4 contains heptanes to C₁₀'s, GRP5 contains C₁₁'s to C₁₆'s, and GRP6 contains C₁₇₊ components. **Table 3.5** shows the final molar composition for the pseudocomponents.

Table 3.5 Pseudocomponent grouping and composition

Pseudocomponent	Components	Molar Percentage
	CO ₂	4.570
GRP1	N ₂ -C ₁	69.490
GRP2	C ₂ -C ₃	13.070
GRP3	C ₄ -C ₆	4.690
GRP4	C ₇ -C ₁₀	4.000
GRP5	C ₁₁ -C ₁₆	2.500
GRP6	C ₁₇ -C ₃₄	1.680

Once the pseudocomponents were defined we proceeded with the EOS tuning process. The EOS selected for this study is the four parameter Peng Robinson equation of state. This is the most recommended and widely used for characterizing gas condensate fluids. The software used to characterize the fluid was PVTi (Geoquest²) version 2001a. The variables used as regression parameters were binary interaction coefficients, and shift factors for selected groups. The final values for these variables are presented in **Table 3.6**. Binary interaction coefficients values after tuning are presented in **Table 3.7**. **Table 3.8** presents the initial and final values of the regressed variables.

Table 3.6 Pseudocomponent properties

Component	Molecular Weight	p_c (psig)	T_c (°F)	Z_c	v_c (ft ³ /lb-mol)	s-Shifts
CO ₂	44.01	1056.6	88.79	0.27407	1.50573	-0.045792
GRP1	16.132	651.77	-117.46	0.28471	1.56885	-0.144168
GRP2	34.556	664.04	127.15	0.28422	2.63712	-0.095027
GRP3	67.964	490.47	350.279	0.27197	4.67964	-0.041006
GRP4	112.52	384.19	591.912	0.25668	7.26188	0.003672
GRP5	178.79	269.52	781.912	0.23667	11.09534	0.00893404
GRP6	303.64	180.2	1001.13	0.21972	17.67366	0.0115616

Table 3.7 Binary interaction coefficients

	CO ₂	GRP ₁	GRP ₂	GRP ₃	GRP ₄	GRP ₅	GRP ₆
CO ₂							
GRP ₁	0.0657	0					
GRP ₂	0.0657	0	0				
GRP ₃	0.0657	0.0657	0.0000	0			
GRP ₄	0.0657	0.0248	0.0066	0	0		
GRP ₅	0.0657	0.1052	0.0226	0	0	0	
GRP ₆	0.0657	0.1231	0.0226	0	0	0	0

Table 3.8 Variation in parameters selected for regression

Parameter	Initial Value	Final Value	% Change
$\delta_{\text{GRP6-GRP1}}$	0.0544	0.1231	-126.28
$\delta_{\text{GRP6-GRP2}}$	0.01	0.0226	-126
$\delta_{\text{GRP5-GRP1}}$	0.0464	0.1052	-126.72
$\delta_{\text{GRP5-GRP2}}$	0.01	0.0226	-126
$\delta_{\text{GRP4-GRP1}}$	0.0377	0.0248	34.21
$\delta_{\text{GRP4-GRP2}}$	0.01	0.0066	34
$\delta_{\text{CO2-GRP1}}$	0.1	0.0657	34.3
$\delta_{\text{CO2-GRP2}}$	0.1	0.0657	34.3
$\delta_{\text{CO2-GRP3}}$	0.1	0.0657	34.3
$\delta_{\text{CO2-GRP4}}$	0.1	0.0657	34.3
$\delta_{\text{CO2-GRP5}}$	0.1	0.0657	34.3
$\delta_{\text{CO2-GRP6}}$	0.1	0.0657	34.3
S_{CO2}	0.0066	-0.0458	793.93
S_{GRP4}	0.0525	0.0037	92.95
S_{GRP5}	0.0714	0.0089	87.53
S_{GRP6}	0.095	0.0116	87.78

After these regressions were done a very good match between the experimental and simulated data was obtained. The experimental saturation pressure of the sample was 5,680 psia according to CCE and the predicted saturation pressure once the tuning was done was 5,670 psia. **Fig. 3.1** presents the corresponding phase envelope.

Due to the complexity in the characterization of a near critical fluid such as the one that we are studying the phase envelope does not close completely. It does not mean that the tuning of the fluid is not correct. Although the bubble line presents a tendency that is not likely this does not affect our simulations since we are focused on the changes that occur along the dewpoint line. This is the typical behavior when the binary interaction parameters are too high but this behavior is outside the expected temperature and pressure ranges for the reservoir under study.

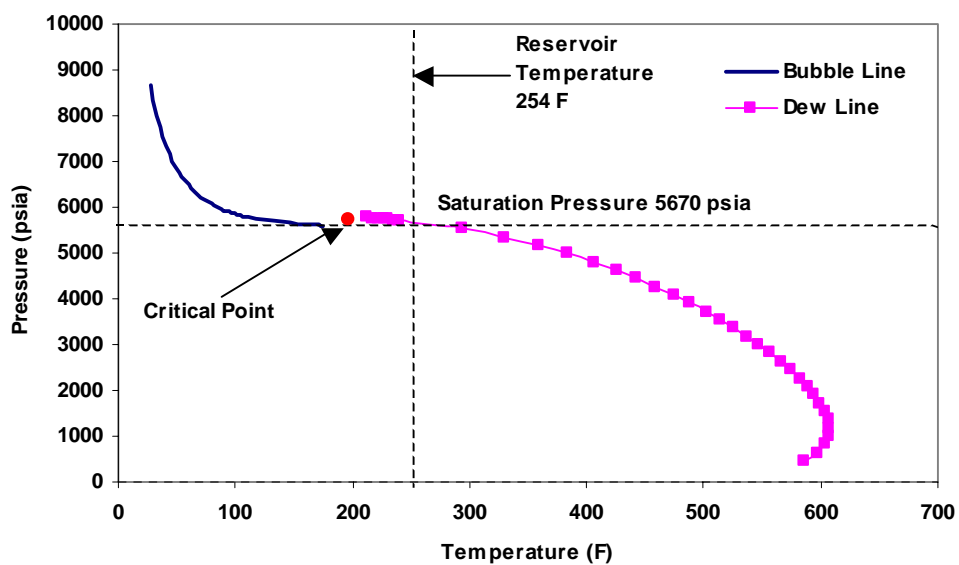


Fig. 3.1 Cusiana gas condensate phase envelope

Figs. 3.2 through 3.4 illustrates the match between the experimental and the simulated data. A very good agreement between the values can be observed on the plots.

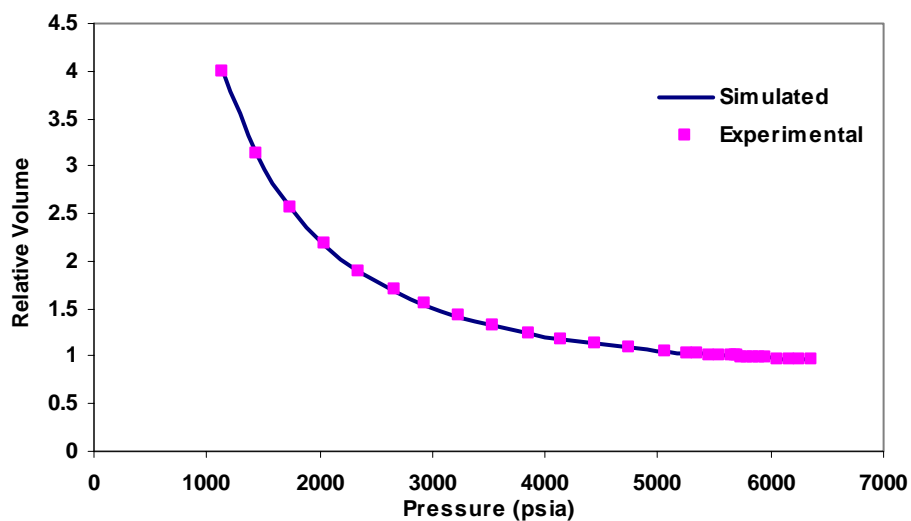


Fig. 3.2 Simulated and experimental relative volume data from CCE at 254 °F

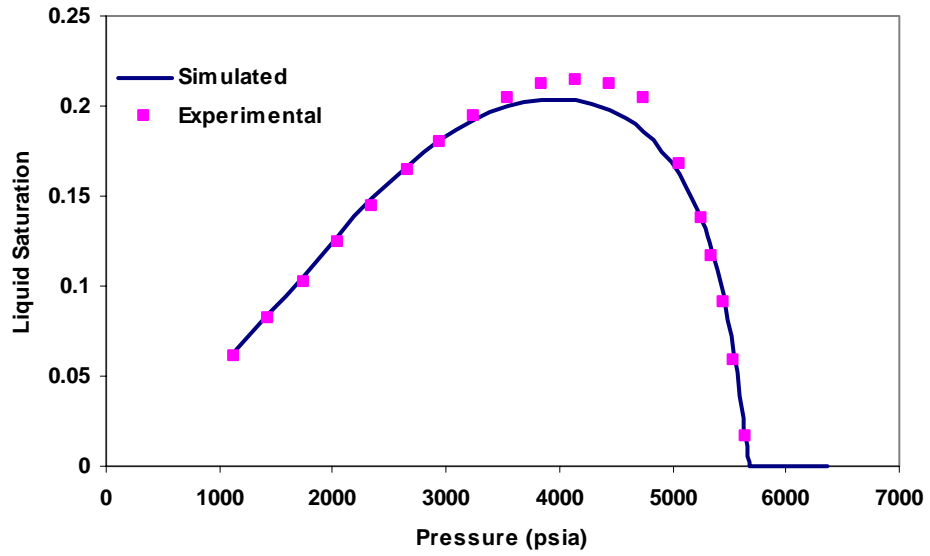


Fig. 3.3 Simulated and experimental liquid saturation data from CCE at 254 °F

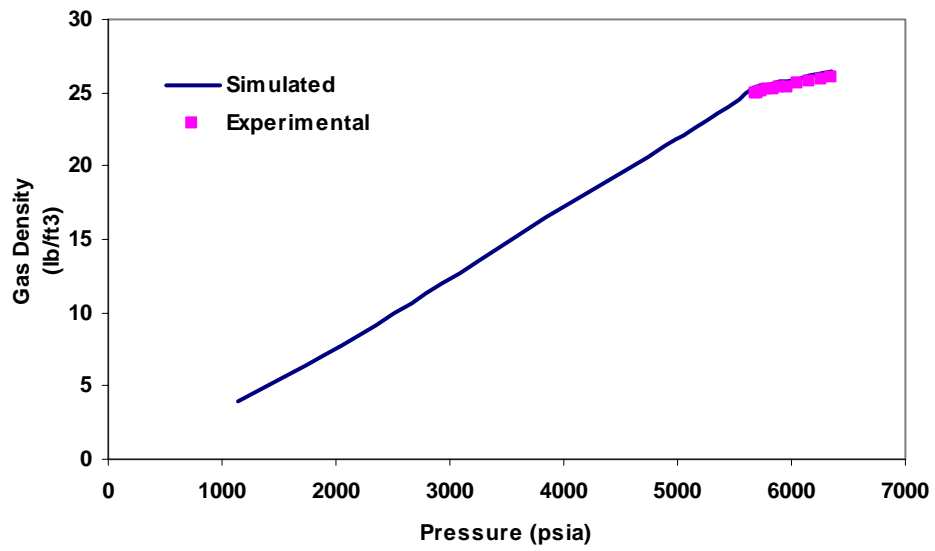


Fig. 3.4 Simulated and experimental gas density data from CCE at 254 °F

The absolute average error was calculated using equation 3.1. The calibrated results for relative volume indicate an absolute average error of 0.15%. Results for liquid saturation have an absolute average error of 3.33%. Gas density values showed an average error of 1.5%.

$$Error_i = \left(\frac{Observed_i - Calculated_i}{Observed_i} \right) \times \frac{100}{n} \dots\dots\dots(3.1)$$

A compositional gradient was also considered since this has a significant impact upon the estimated hydrocarbons in place, fluid property predictions, and gas and liquid recoveries. Variation of the composition of C_1-N_2 and C_7^+ with depth is presented in **Figs. 3.5 and 3.6**.

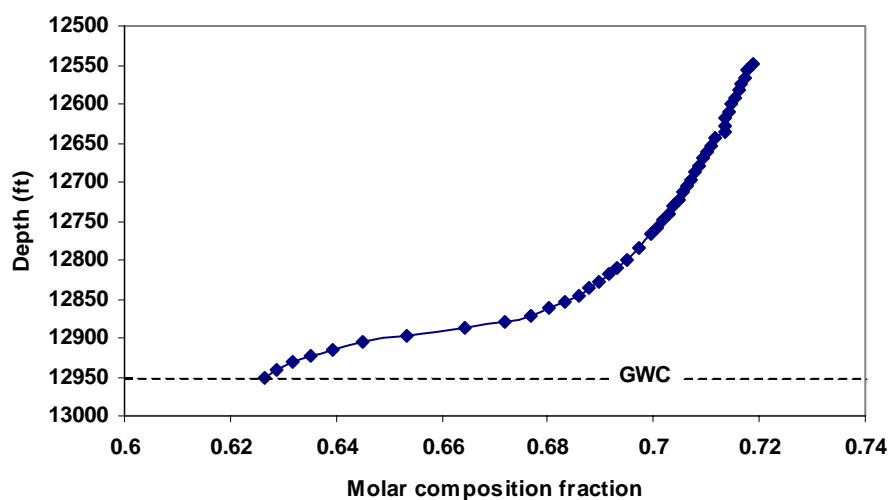


Fig. 3.5 C_1-N_2 compositional gradient

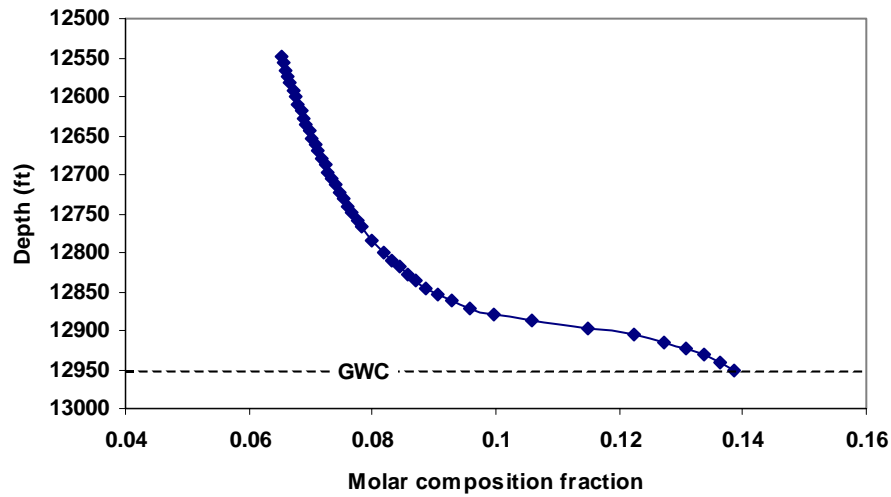


Fig. 3.6 C_7^+ compositional gradient

3.3 Simulation Model

A quarter five spot model was built as a sector model that can be scaled for representations of an entire field. The model is a synthetic reservoir that includes the fluid description of a real gas condensate. This synthetic model has Cartesian coordinates with length 800 ft in both the X and Y directions and thickness 359 ft in the Z direction. The top of the model is at 12,540 ft with an initial pressure of 5,868 psia at a reference depth of 12,800 ft. The gas water contact is at 12,950 ft. The number of grids selected are 25x25x18 with a total of 11,250 blocks **Fig. 3.7** illustrates the model.

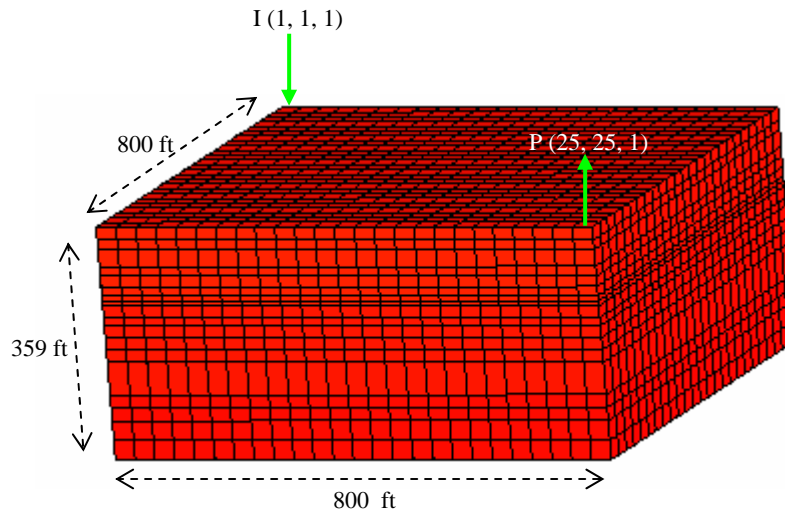


Fig. 3.7 3D Simulation model

The injector well I was located in block 1,1,1 while the producer well P is located in block 25, 25, 1 with the nine upper layers open.

3.3.1 Static Properties

Tables with relative permeability, saturation and capillary pressure data for water, oil, and gas were taken from the third SPE comparative case.³⁰ **Table 3.9** presents the rock properties used in the model. k_v/k_h ratio was chosen as 0.1 throughout the study except during the evaluation of vertical communication effect, a lower value of 0.0001 was used.

Table 3.9 Layer thickness, porosity and permeability values

Layer	Thickness	Porosity	Permeability (md)
1	20	0.087	180
2	15	0.097	180
3	26	0.111	100
4	15	0.16	100
5	16	0.13	50
6	14	0.17	50
7	8	0.17	50
8	8	0.08	50
9	18	0.14	80
10	12	0.13	80
11	19	0.12	80
12	18	0.105	150
13	20	0.12	150
14	50	0.116	180
15	20	0.157	180
16	20	0.157	180
17	30	0.157	180
18	30	0.157	180

3.3.2 Initialization

To initialize the model, we performed a run with the producer well shut in. The original hydrocarbon volume stays constant with time, which means that material balance is correct and no mass losses are present. Also the pressure distribution remains constant.

Once the initialization was done original fluids in place report was obtained for the compositional model. **Table 3.10** presents the original fluid in place with the compositional gradient.

Table 3.10 Fluids in place

Compositional Model	
Average Pressure	5855 psia
Total Pore Volume	5.36 MM rb
Hydrocarbon Pore Volume	4.37 MM rb
Average Oil Saturation	0
Reservoir Volume of Oil	0
Average Water Saturation	0.18
Reservoir Volume of Water	995 M rb
Average Gas Saturation	0.81
Reservoir Volume of Gas	4.37 MM rb
Surface Oil Volume	941 M stb

3.4 Black-Oil PVT Table Generation

Black-oil PVT properties in this study have been generated with an EOS model using the Whitson and Torp⁶ procedure. In this approach a depletion type experiment is simulated, either a CCE, CVD or DLE test. At each step in the depletion test, the equilibrium gas and oil phases are taken separately through a multistage separator. The surface oil and surface gas products from reservoir oil phase are used to define the oil formation volume factor and solution gas-oil ratio. The surface oil and surface gas products from the reservoir gas phase are used to define the dry gas formation volume factor and solution oil-gas ratio. The MBO properties are calculated according to the definitions given.

$$B_o = \frac{V_o}{V_{oo}} \dots\dots\dots(3.2)$$

$$R_s = \frac{V_{go}}{V_{oo}} \dots\dots\dots(3.3)$$

$$B_{gd} = \frac{V_g}{V_{gg}} \dots\dots\dots(3.4)$$

$$R_v = \frac{V_{og}}{V_{gg}} \dots\dots\dots(3.5)$$

where:

V_o = Reservoir oil volume

V_{oo} = Volume of stock tank oil produced from reservoir oil

V_{go} = Volume of surface gas produced from reservoir oil

V_g = Reservoir gas volume

V_{gg} = Volume of surface gas produced from reservoir gas

V_{og} = Stock tank oil produced from reservoir gas

Also a single set of constant surface gas and surface oil densities are used to calculate reservoir densities. Proper selection of surface component densities can ensure improved accuracy in black-oil reservoir density calculations.³

Coats¹ developed another black-oil PVT table generation method. Instead of flashing the equilibrium liquid and vapor compositions separately to obtain B_o , R_s , B_g , R_v directly as Whitson and Torp did, Coats determines only one of these properties R_v , from flash separation and determines the remaining three using equations that force the PVT properties to satisfy mass conservation equations and yield correct reservoir liquid density.

In determining R_v from the surface separation at each CVD pressure step Coats uses the surface oil and gas molecular weights and densities obtained from the separation of the “original fluid” mixture. McVay³² found better agreement between compositional and MBO simulations models if the surface oil, gas molecular weights and densities are

obtained from the separation of the mixture at each CVD pressure step to calculate R_v at each pressure. Also by using Coats' method it is not possible to obtain the PVT properties of the liquid phase at the saturation pressure. Coats defined the first CVD pressure step to be 0.1 or 1 psi below the saturation pressure and used the values calculated at this pressure as the PVT properties at the saturation pressure. Standard extrapolation of sub-dew point properties to dew point can lead to situations where the oil has non-physical negative compressibility.

Fig. 3.8 through **3.13** gives the saturated oil, and gas PVT properties obtained by Whitson and Torp and Coats methods. Notice that gas formation volume factors at lower pressure values are quite different for two methods. This probably resulted errors in the MBO model simulation.

Coats method was not preferred for this study since it created convergence problems in MBO model and the run was automatically terminated due to number of errors encountered.

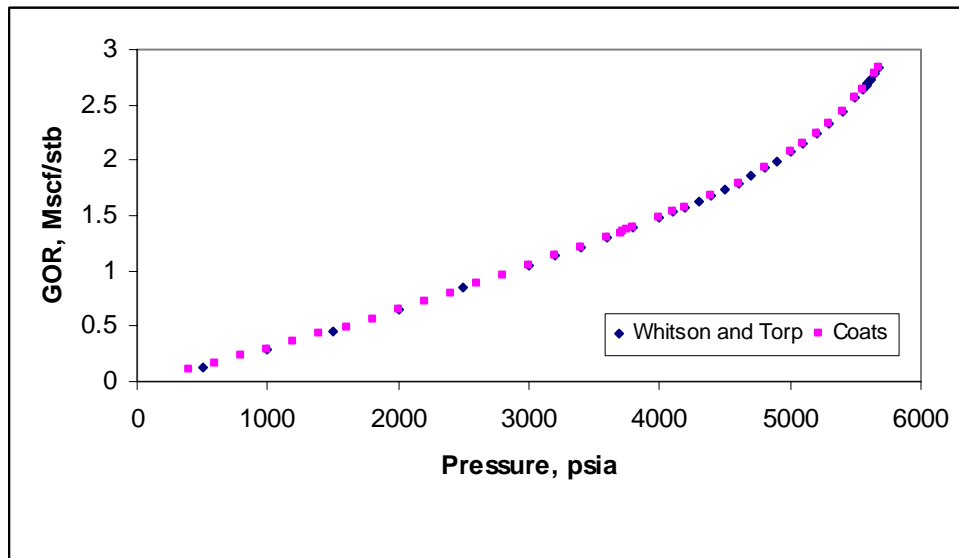


Fig. 3.8 Gas-oil ratio comparison from Coats versus Whitson and Torp methods

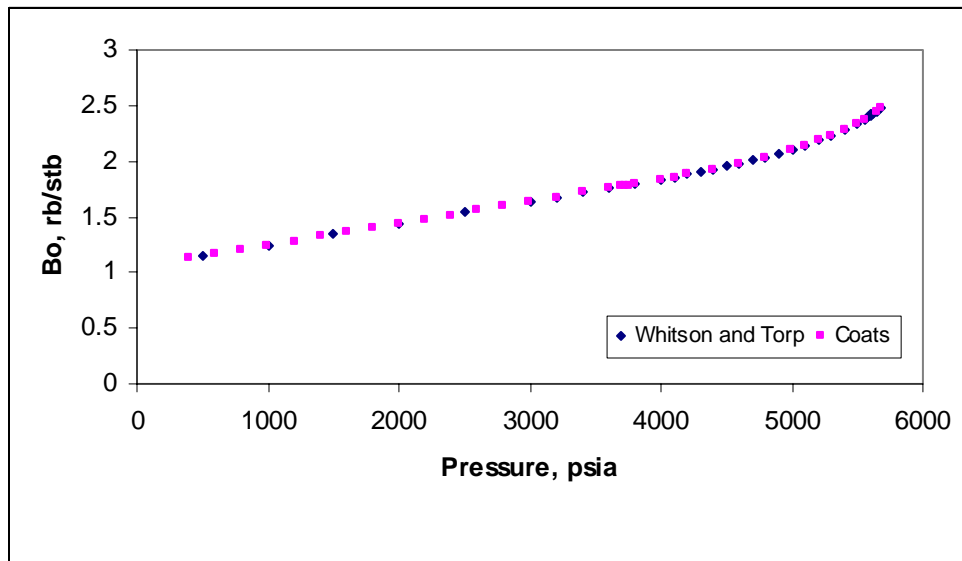


Fig. 3.9 Oil formation volume factor comparison from Coats versus Whitson and Torp methods

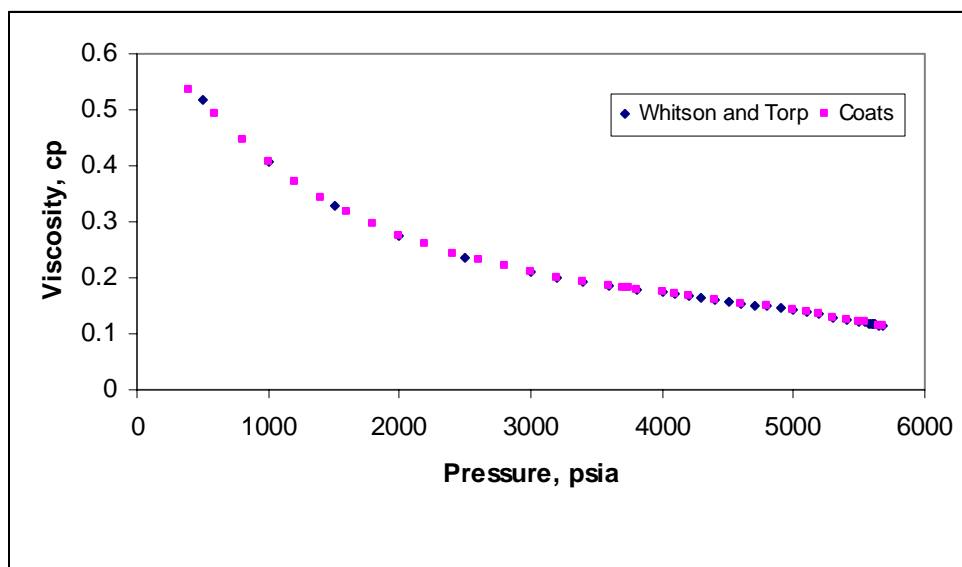


Fig. 3.10 Oil viscosity comparison from Coats versus Whitson and Torp methods

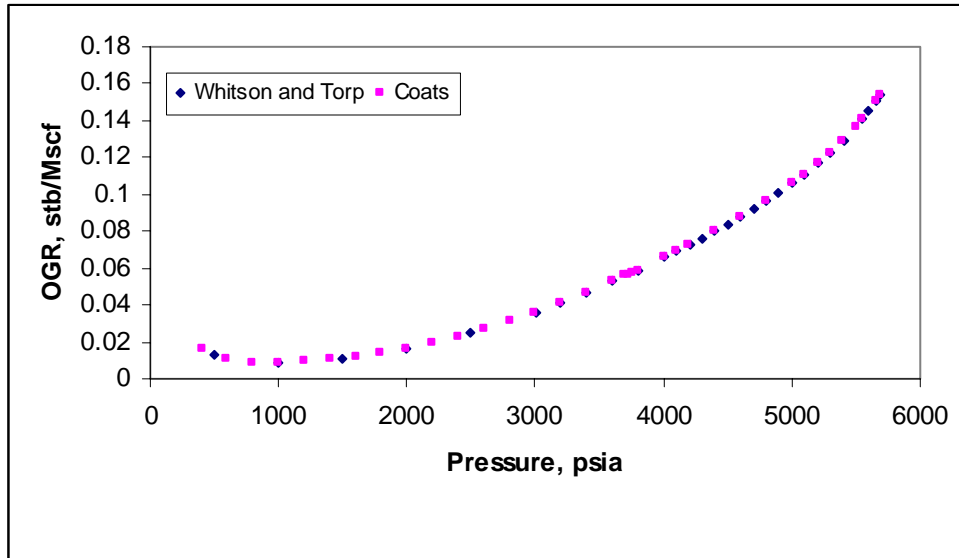


Fig. 3.11 Oil-gas ratio comparison from Coats versus Whitson and Torp methods

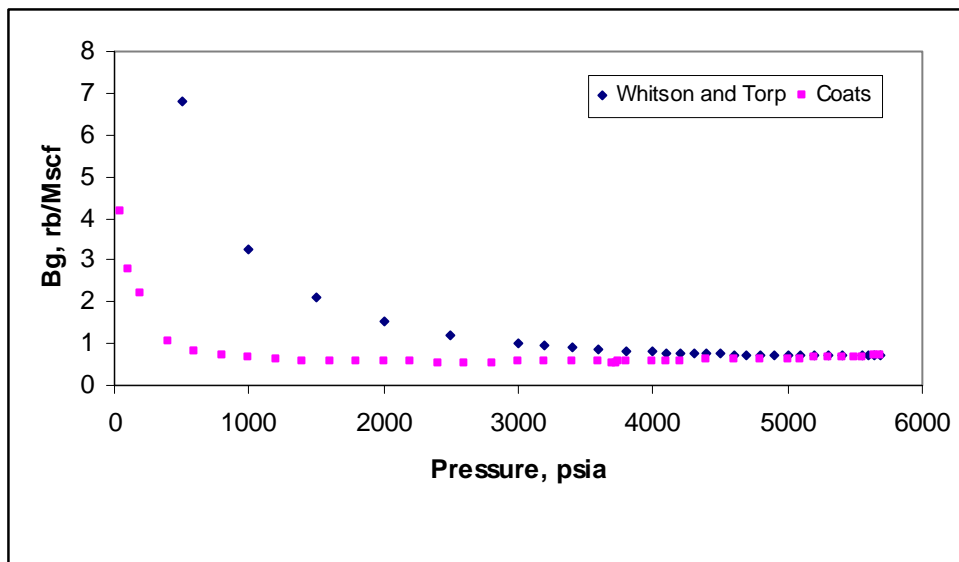


Fig. 3.12 Gas formation volume factor comparison from Coats versus Whitson and Torp methods

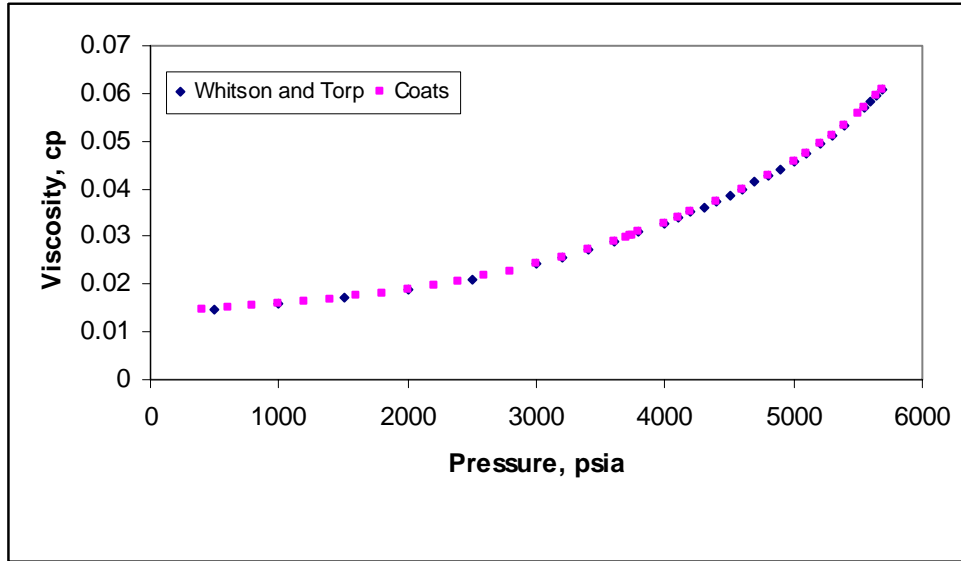


Fig. 3.13 Gas viscosity comparison generated from Coats versus Whitson and Torp methods

CHAPTER IV

METHODS

Reservoir simulation is a versatile tool for reservoir engineering. Full field simulation models and history matching the field performance help finalize the critical management decisions such as number of wells and the location to be drilled, pressure maintenance schemes, design of facilities.

However, CPU-time is the limiting factor when the simulation model is made. Modified black-oil approach, instead of a full compositional approach, may result in significant timesaving especially in full field studies of volatile oil and rich gas condensate reservoirs.

The major question in the use of MBO approach is whether the two-component description can adequately represent the compositional phenomena during the depletion or the cycling of rich gas condensate reservoirs.

We performed simulations for natural depletion and cycling scenarios in a gas condensate reservoir with full compositional and MBO models. Compositional model is considered as the basis of this study and it is compared with the MBO model by changing the following parameters:

- Initialization with compositional gradient/uniform composition in compositional model and correspondingly initialization with saturation pressure and oil-gas ratio versus depth or uniform oil-gas ratio and uniform saturation pressure with depth in MBO model
- Size and location of the completions
- Production and injection rates

- k_v/k_h ratio
- The effects of vertical and horizontal wells

The producer well was operating under the constraint of a fixed gas production rate of 3,000 MSCF/D but when the minimum bottom hole pressure of 1,000 psia was reached the constraint changed to fixed bottom hole pressure.

The injection rate was chosen as 2,500 MSCF/D. Injection was started from the first day of production.

The following chart (**Fig. 4.1**) represents the steps taken in this study. The same scheme was followed for both vertical and horizontal wells except the initial part of the study, which consists of the fluid characterization, lumping and EOS tuning.

The constant composition case was only run for the natural depletion to show that initialization methods do not make any difference if compositional gradient is not used in the model. For constant composition with depth case MBO model was initialized with either oil-gas ratio versus depth or saturation pressure versus depth tables, which corresponded to composition at reference depth of 12,800 ft.

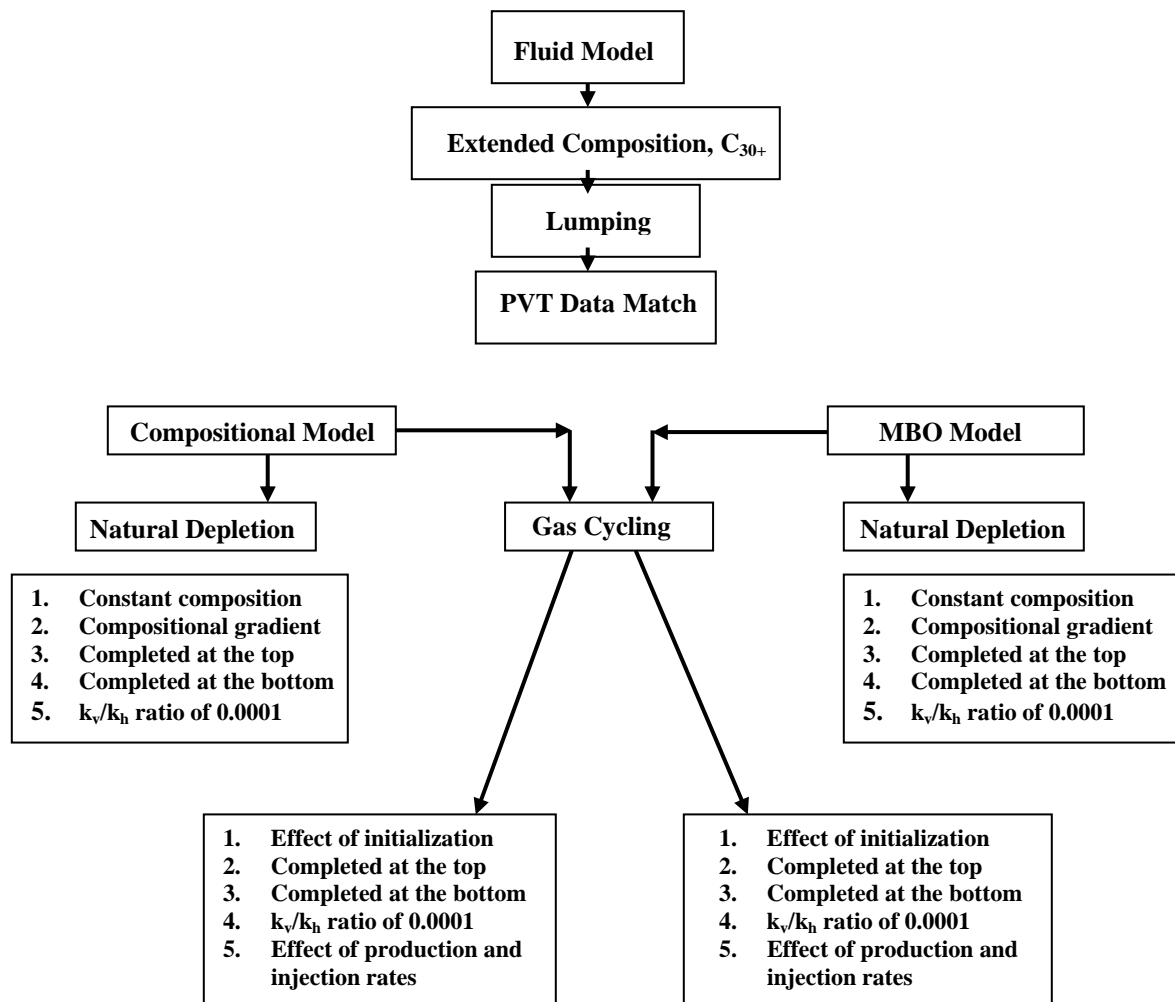


Fig. 4.1 Steps followed during the study

For all the other cases compositional model was run with compositional gradient. Correspondingly MBO model was run with both initialization methods mentioned above since it is very well known that the systems in the vicinity of the critical condition exhibit significant compositional variations with depth that affect the field development considerably.^{25, 26, 27, 28}

Oil production rates, gas-oil ratios, pressure and oil saturation distributions and recovery factors were monitored to compare the performance of models.

4.1 Natural Depletion

In the natural depletion case we analyzed certain variables that might create differences on the performance of modified black-oil and compositional models. These included the effects of initialization methods, uniform composition with depth and compositional grading, k_v/k_h ratios and the location of the completions. Production rates were not included since no effect of production rate on the performance of models was observed in natural depletion case.

4.1.1 Effect of Initialization

To obtain the correct and consistent initial fluids in place for black-oil and compositional models it is important to initialize the models properly. This involves proper treatment of phase definitions, PVT models, compositional gradients, and the importance of initial fluids in place versus ultimate recoveries for the relevant recovery mechanisms.

For obtaining accurate initial fluids in place and description of reservoir recovery processes, modified black-oil PVT properties and compositional gradients must be selected carefully. The initial reservoir fluid composition is either constant with depth or

shows a vertical compositional gradient where the effect of gravity is not negligible. The compositional gradient in black-oil model is taken into account by depth variation of solution gas-oil ratio (GOR) in the oil zone and solution oil-gas ratio (OGR) in the gas zone. Depending on the type of the reservoir fluid, the model should be initialized either with solution GOR/ OGR versus depth or saturation pressure versus depth to minimize the errors for initial fluids in place. Although initialization with saturation pressure versus depth gives more accurate representation of fluids in place, at the bottom of the reservoir where amount of heavy fraction increases, this initialization method gives higher condensate saturations, especially for gas cycling, compared to the compositional model and MBO model initialized with GOR/ OGR versus depth.

4.1.1.1 Constant Composition with Depth

For the constant composition case modified black-oil model was initialized with both solution oil-gas ratio versus depth and saturation pressure versus depth. If the displacement process is gravity stable or where the effect of gravity is negligible, both initialization methods give the same initial fluids in place. The error in initial fluids in place is calculated as 4 % for MBO model.

The average field pressure from both models with constant composition with depth is given in **Fig 4.2**.

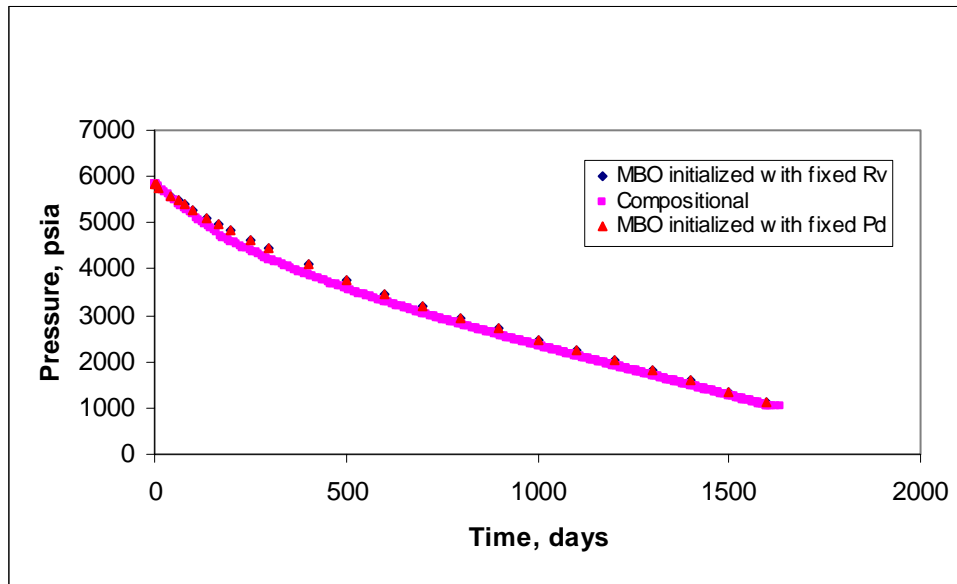


Fig. 4.2 Average field pressure for the natural depletion case, constant composition with depth

The average field pressure in the modified black-oil model is slightly higher than the compositional model at the beginning of the simulation (for about 250 days). Early condensate drop-out and accumulation around the wellbore reduces relative permeability to gas and slows down the gas production, so the pressure drop in MBO model is smaller compared to compositional model. As the reservoir is depleted, part of the liquid condenses out of the gas phase and also oil saturation begins to increase in compositional model. This results in a leaner gas phase over time in the reservoir and a better match between two models. The same pattern can be observed with the producing solution gas-oil ratios, oil production rates and average oil saturation plots. According to **Fig. 4.3**, the average oil saturation plot, MBO model is giving condensate drop-out earlier than the compositional model. For the MBO model, changes in saturation pressure with depth cannot be represented properly. Liquid content of the gas is a function of pressure, the compositional effects are ignored and in relation to that assumption liquid drop-out is observed as soon as the saturation pressure is reached. The

oil-gas ratio plot generated by the EOS determines the revaporization process in MBO model and this allows gas to pick-up oil until it reaches to the value determined by the PVT table. The presence of more gas would have caused excess amount of revaporization in MBO model.

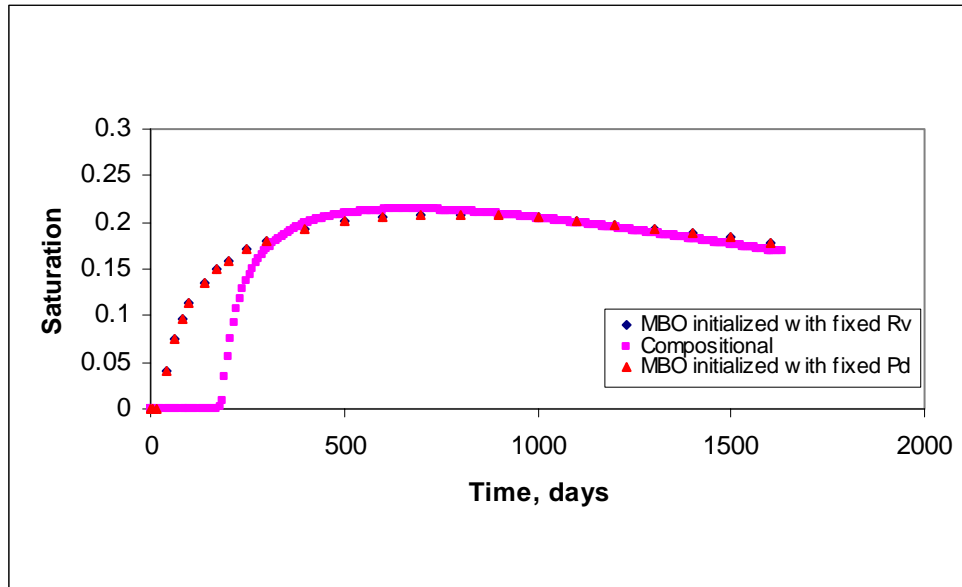


Figure 4.3 Average oil saturation for natural depletion case, constant composition

Fig. 4.4 and **Fig. 4.5** compare the oil saturation distribution in the reservoir at the time of first condensation observed in compositional model ($t=175$ days). First liquid drop-out is observed around the wellbore, then upper layers are affected and finally the bottom layers. Condensation follows a different path if composition is not uniform with depth.

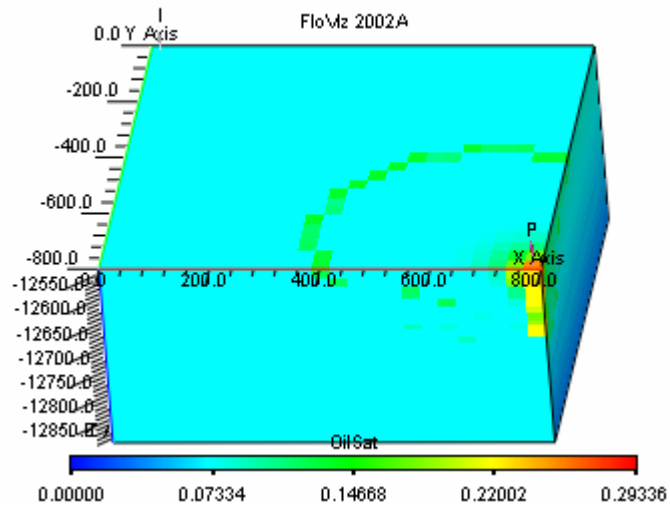


Fig. 4.4a Oil saturation distribution from compositional model for uniform composition case at t = 175 days

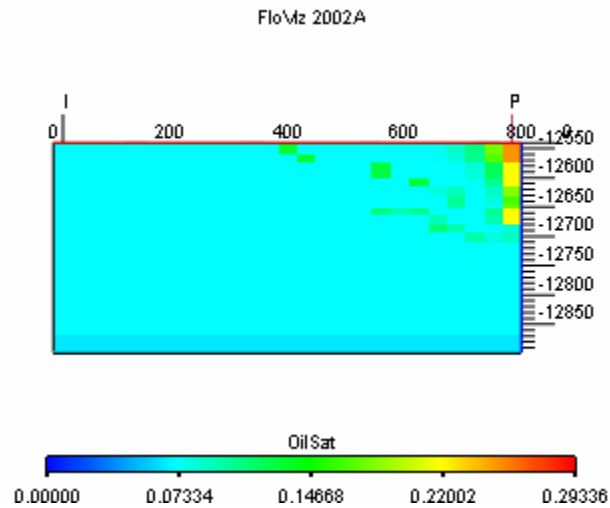


Fig. 4.4b 2-D oil saturation distribution from compositional model for uniform composition case at t = 175 days, slice between injector and producer

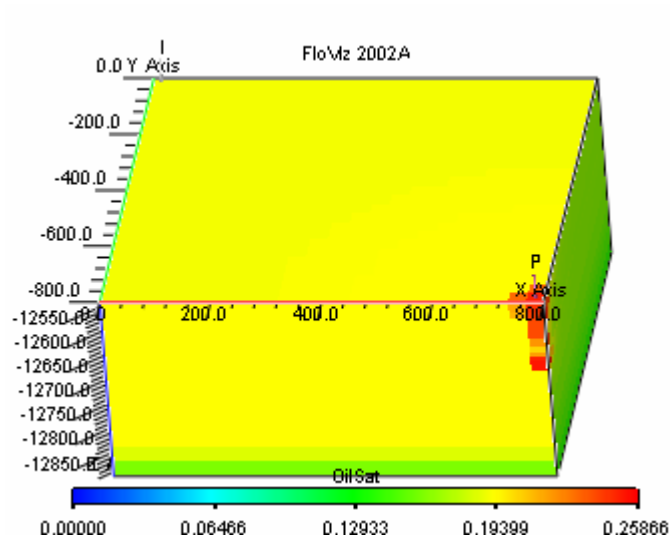


Fig. 4.5a Oil saturation distribution from MBO model for uniform composition case at $t = 175$ days

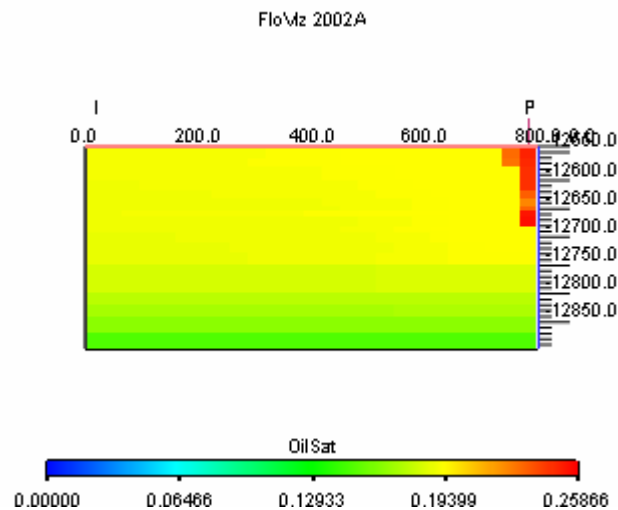


Fig. 4.5b 2-D oil saturation distribution from MBO model for uniform composition case at $t = 175$ days, slice between injector and producer

Fig. 4.6 and **Fig. 4.7** compare the oil saturation distribution in the reservoir at the end of the simulation. Compositional model gives less oil saturation around the wellbore and throughout the reservoir at the end of four years. This results in lower producing gas-oil ratios in compositional model after 1,500 days since most of the oil in the reservoir is vaporized and carried by gas. In MBO model higher amounts of oil are left in the reservoir resulting in higher gas-oil ratios (**Fig. 4.8**) and lower recoveries than compositional model.

This may be misleading when forecasting the field production and identifying new development locations. The effect of early condensation can also be observed from the recoveries. **Fig. 4.9** represents the oil production rates for both models. MBO model is giving lower oil production rate at the beginning. In the compositional model, oil is carried to the production well in the rich gas phase resulting in a higher and constant oil production rate for 170 days. Gas-oil ratio in modified black-oil model is slightly higher for that period since less oil is produced. Then it is almost the same as the compositional model for the rest of the simulation time.

Table 4.1 shows the oil in places values for compositional and MBO models initialized with two different methods. Initialization methods did not create any differences in the production performance or initial fluids in place values. However, according to **Table 4.2**, there is 11 % difference in saturations in wellbore gridblock (25, 25, 9) between two models. Notice that MBO model is 12 times faster than the compositional model.

Table 4.1 Fluid in place and CPU times for constant composition with depth

	OOIP, stb	CPU, sec.	Error in OOIP, %
Compositional	999916.20	785.91	-
Rv vs Depth	958733.40	64.47	4.11
Pd vs Depth	958733.40	65.00	4.11

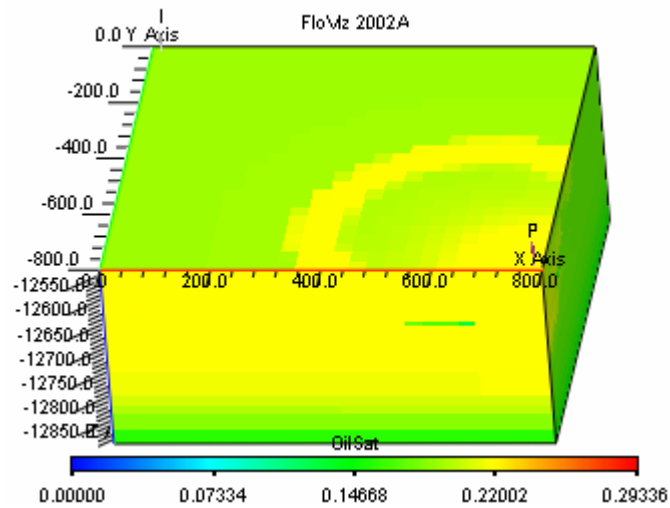


Fig. 4.6a Oil saturation distribution from compositional model for uniform composition case at $t = 1633$ days

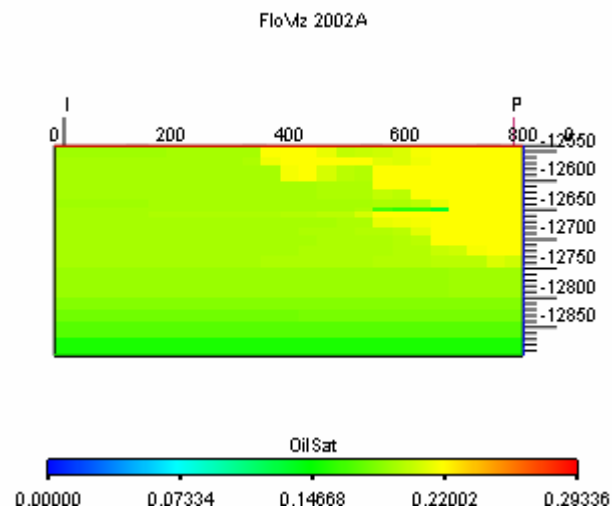


Fig. 4.6b 2-D oil saturation distribution from compositional model for uniform composition case at $t = 1633$ days

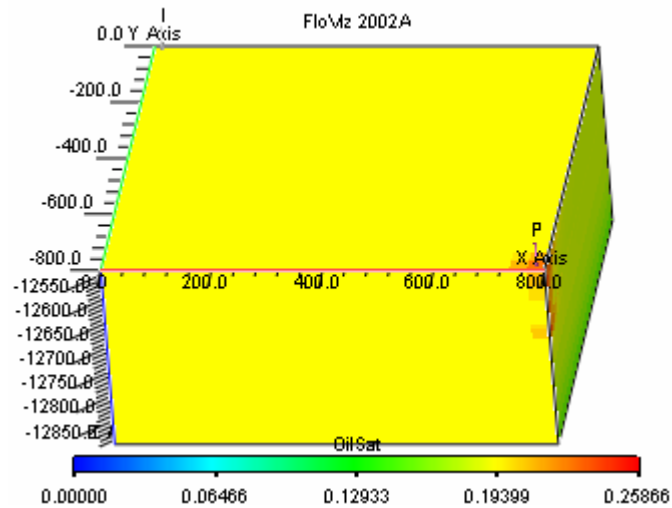


Fig. 4.7a Oil saturation distribution from MBO model for uniform composition case at $t = 1633$ days

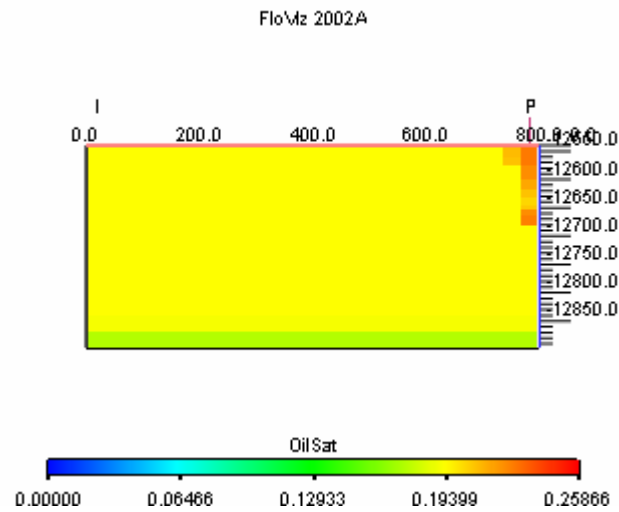


Fig. 4.7b 2-D oil saturation distribution from MBO model for uniform composition case at $t = 1633$ days

Table 4.2 Oil saturation values for gridblock 25, 25, 9

Time, days	MBO	Compositional	Difference, %
	So	So	
100	0.25	0.00	-100.00
200	0.26	0.23	-10.75
400	0.26	0.27	5.00
600	0.26	0.28	7.75
800	0.25	0.27	6.94
1000	0.25	0.26	3.59
1200	0.24	0.24	-1.43
1400	0.24	0.23	-4.94
1633	0.24	0.22	-11.42

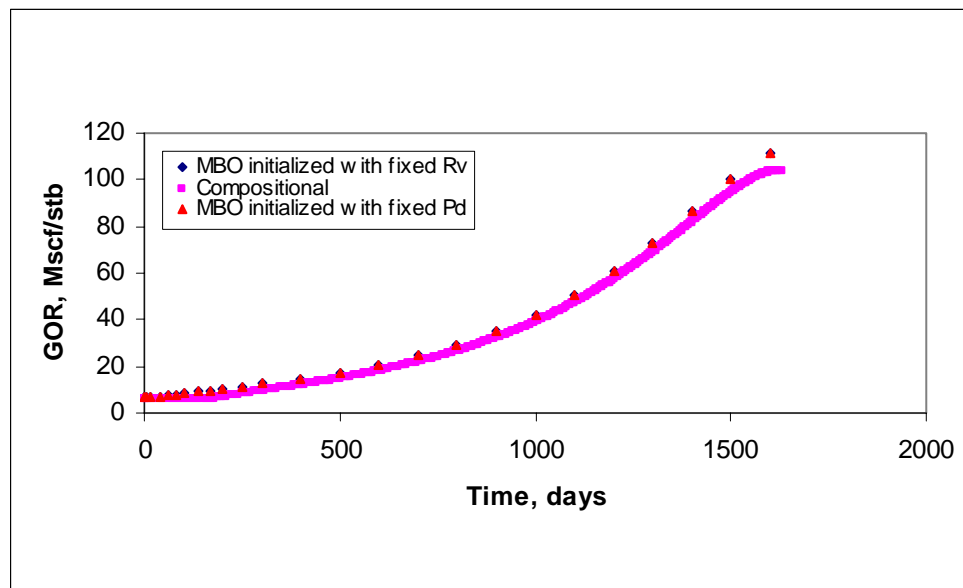


Fig. 4.8 Gas oil ratio for the natural depletion case, constant composition

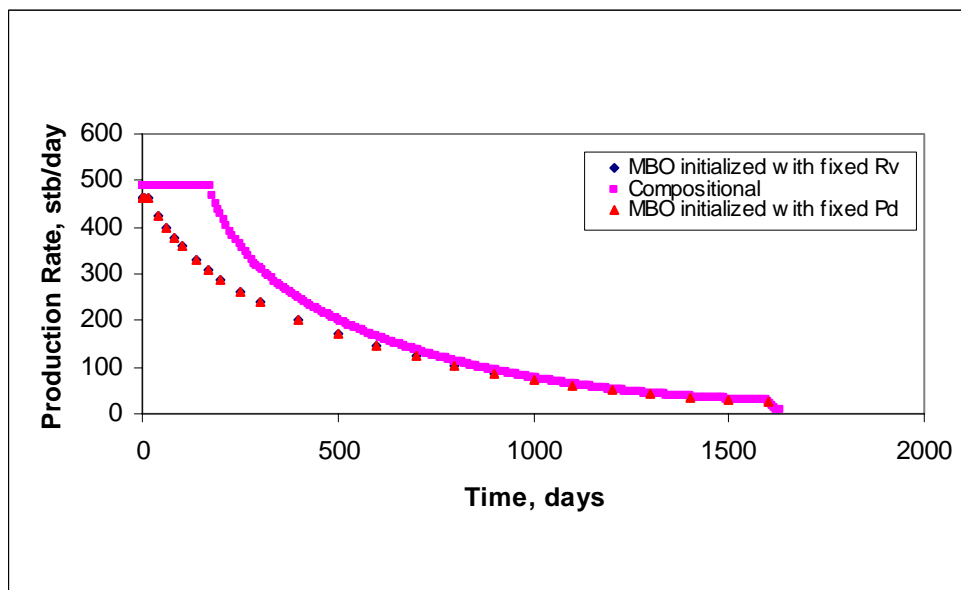


Fig. 4.9 Oil production rate for the natural depletion case, constant composition

Fig. 4.10 shows the recovery factor for MBO and compositional models. MBO model final recovery factor is 22 % and compositional model is given as 27 %.

The difference between the two models is created by the higher oil production rate in the compositional model in relation to the early condensate drop-out in MBO model. Also after the reservoir gas gets leaner revaporization effects in compositional model contribute to higher recoveries. In MBO model reservoir gas has limited capacity to revaporize the condensate, especially at lower pressures due to smaller values of oil-gas ratio (liquid content of gas). In the simulator oil-gas ratio tables obtained from EOS model determine this. The revaporization capacity of recycled reservoir gas will be further investigated with changing R_v values as shown in **Fig 4.67**.

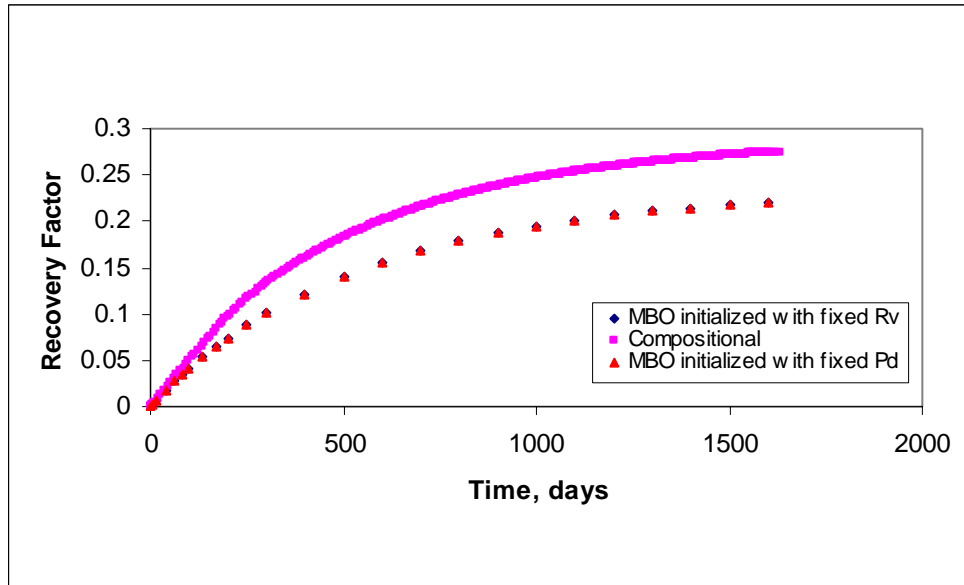


Fig. 4.10 Recovery factor for the natural depletion case, constant composition

4.1.1.2 Initialization with Compositional Gradient

Beginning from this part of the study all models, both compositional and MBO were run with compositional gradients. Compositional model was initialized with depth versus composition. MBO model was initialized with solution gas-oil and oil-gas ratio versus depth tables and saturation pressure versus depth tables to investigate the effects of different initialization methods. **Table 4.3** shows that when the black-oil model was initialized with saturation pressure versus depth, a better representation of initial fluids in place could be obtained. With the use of compositional gradient, initialization methods exhibited different performances and gave different initial fluids in place values. The error in initial fluids in place can be as low as 2 % with saturation pressure initialization.

Table 4.3 Fluid in place and CPU times for compositional gradient

	OOIP, stb	CPU, sec.	Error in OOIP, %
Compositional	941669.40	745.56	-
Rv vs Depth	888033.20	72.22	5.69
Pd vs Depth	922730.10	64.28	2.01

Fig. 4.11 shows the average field pressure for both cases and it gives slightly higher-pressure values for the modified black-oil model initially, which is similar to the constant composition case presented previously.

Fig. 4.12 shows the comparison of two different initialization methods for the average oil saturation in each model. When the MBO model is initialized with saturation pressure versus depth table, the model becomes more sensitive to pressure drop in the reservoir and tends to give more condensate in the reservoir at early times.

Fig. 4.13 shows the differences in saturation pressure changes with depth initially for both models. In this case MBO is initialized with saturation pressure versus depth table. Since the MBO model has higher saturation pressures throughout the column, it is expected to give early condensation compared to the compositional model. The difference is 1044 psia and 900 psia at the bottom and the top of the reservoir.

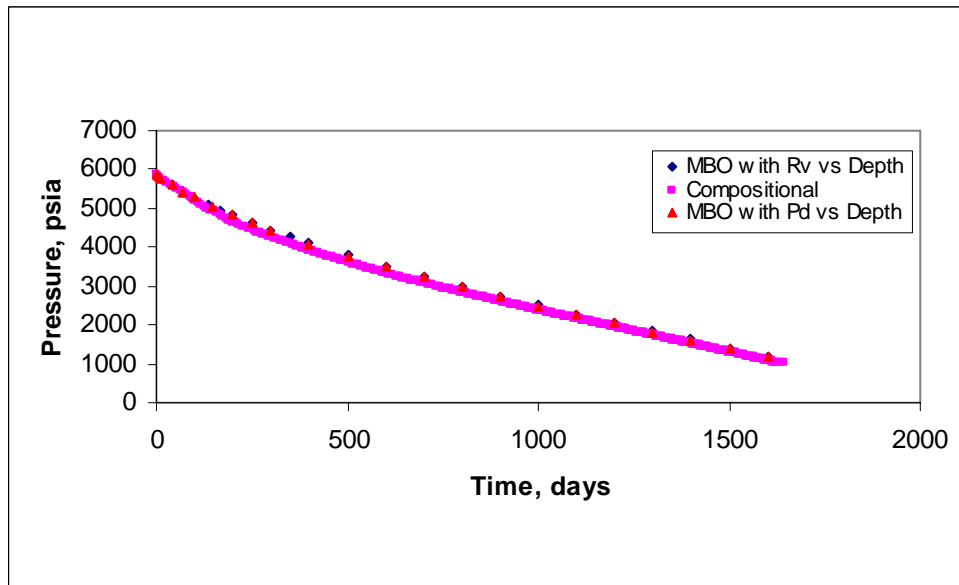


Fig. 4.11 Average field pressure with compositional gradient

Fig. 4.14 and **Fig. 4.15** show the oil saturation distribution from two simulation models, initialized with R_v versus depth at 190 days. This is the first time liquid drop-out is observed in compositional model.

The result of gravitational segregation is that a gas condensate gets richer at greater depths, with increasing C_{7+} mole fraction and as well as dew point pressure. Unlike the case without compositional gradient, oil saturation is first observed in the bottom layers for both models. Later on it progresses upwards with time. Due to inability of MBO model to represent the changes in dew point pressure with depth properly, it gives earlier and smaller amounts oil saturation in the bottom layer compared to the compositional model. MBO gives more oil saturation around the wellbore area at the end of the simulation (**Table 4.4**).

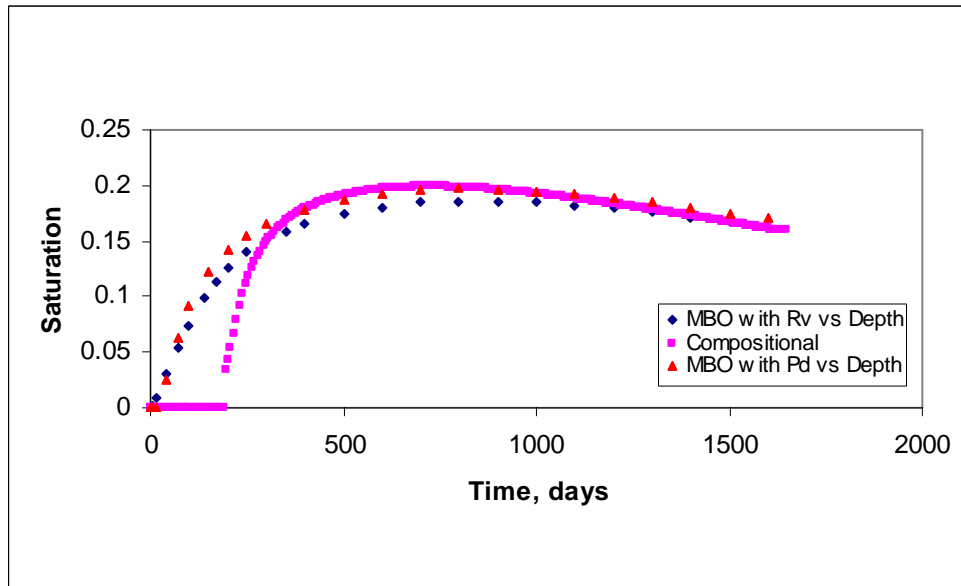


Fig. 4.12 Average oil saturation with compositional gradient

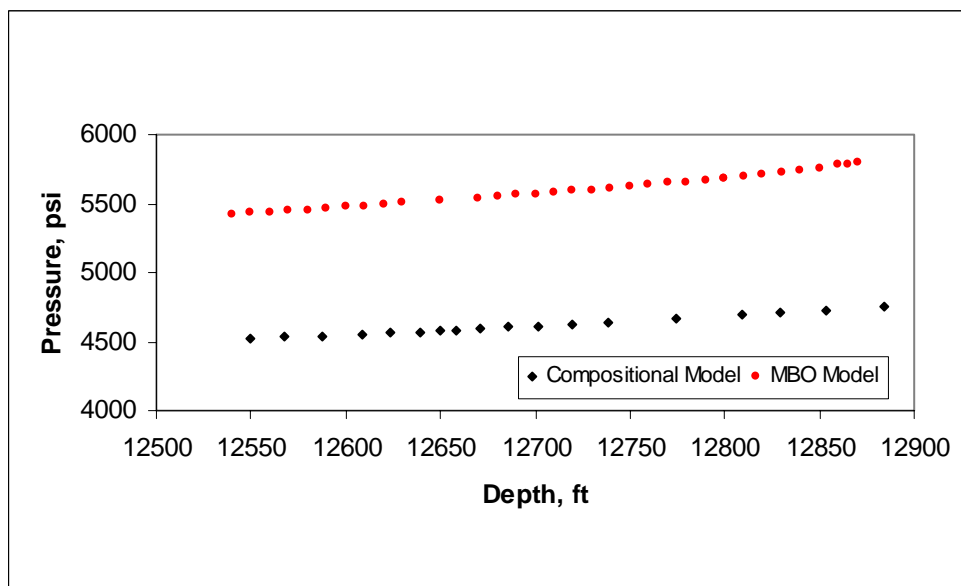


Fig. 4.13 Differences in saturation pressures for both models at the beginning of simulation

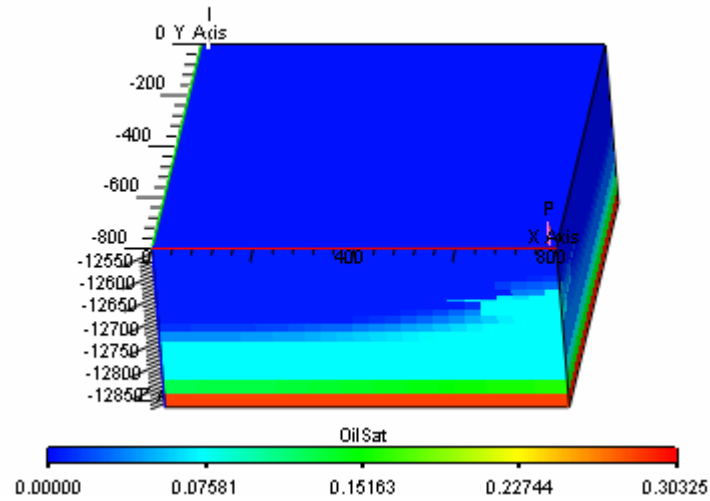


Fig. 4.14a Oil saturation distribution from compositional model with compositional gradient at $t = 190$ days

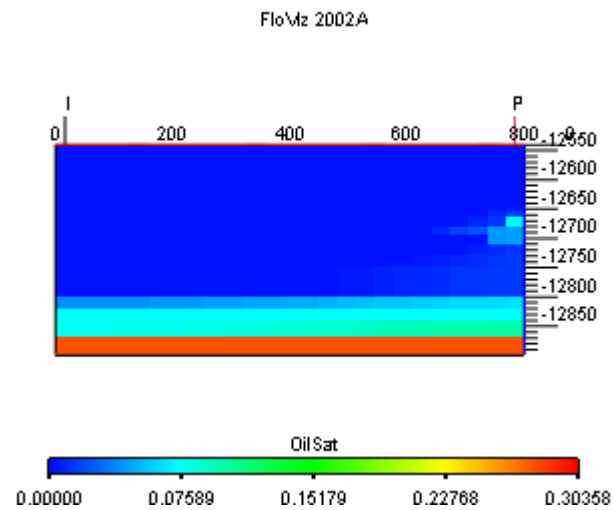


Fig. 4.14b 2-D oil saturation distribution from compositional model with compositional gradient at $t = 190$ days

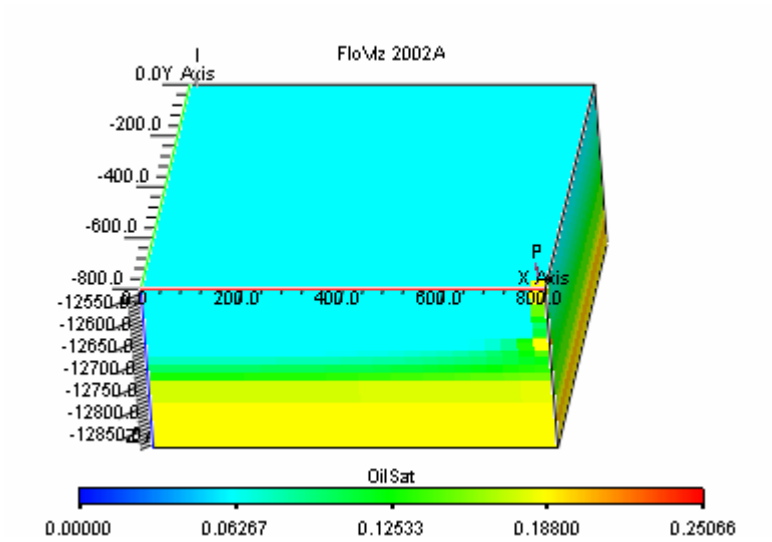


Fig. 4.15a Oil saturation distribution from MBO model with compositional gradient at $t = 190$ days

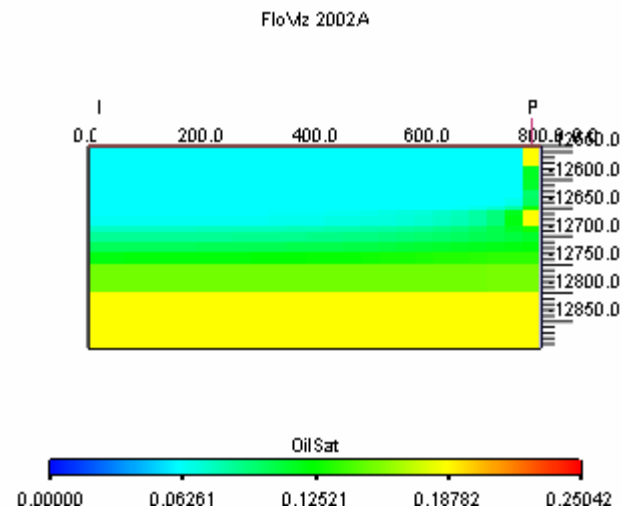


Fig. 4.15b 2-D oil saturation distribution from MBO model with compositional gradient at $t = 190$ days

Table 4.4 Oil saturation values for gridblock 25, 25, 9

Time, days	MBO	Compositional	Difference, %
	So	So	
100	0.09	0.00	-100.00
200	0.20	0.05	-325.18
400	0.25	0.26	3.63
600	0.25	0.26	4.30
800	0.25	0.25	2.05
1000	0.25	0.24	-0.73
1200	0.24	0.24	-2.37
1400	0.24	0.23	-6.37
1645	0.24	0.21	-12.71

Fig. 4.16 shows the decrease in molar production of heavy fraction, C_{17+} (Group 6) with time.

Fig. 4.17 and **Fig. 4.18** give the oil saturation distribution for both models at the end of the simulation time. Notice that the bottom layer has higher oil saturation for the compositional model. Also in compositional model an additional condensate bank away from the producer is observed in **Fig. 4.17**. The same bank cannot be observed in the MBO model. The models are completed in the first nine layers and the drainage of the fluids is faster from these layers. At the top of the reservoir even though the gas is not as rich as in the bottom layers because of compositional grading, condensation is still effective due to faster drainage. At some distance away from the producer, closer to the top of the reservoir where no flow boundary conditions dominate, quick drainage, pressure drop and lack of pressure support from the neighbor layers in the region may form this kind of banking. If the injector well is completed inside this additional bank or outside the bank but in the lower layers, it will only be effective around the wellbore region and production from top layers will be negatively affected. This bank would be much more effective in the case of uniform composition since the percentage of heavy components in the upper layers become larger. According **Fig. 4.17** and **Fig. 4.6** the oil saturations in this bank are similar but the size of the bank in the case of uniform composition is much larger.

This situation can be investigated further from **Fig. 4.19** through **Fig. 4.22** by using data from individual wellbore gridblocks, bottom and top completions of the well.

After the reservoir pressure begins to go down, significant condensate saturation builds up and the gas that arrives to the wellbore becomes leaner and drops less condensate, which also helps vaporization of the previously accumulated liquid in the near wellbore region.

At the beginning of the simulation both models are giving the same pressure drop. After the first condensate drop-out in MBO model, the productivity of the well goes down for some time and causes less pressure drop compared to the compositional model.

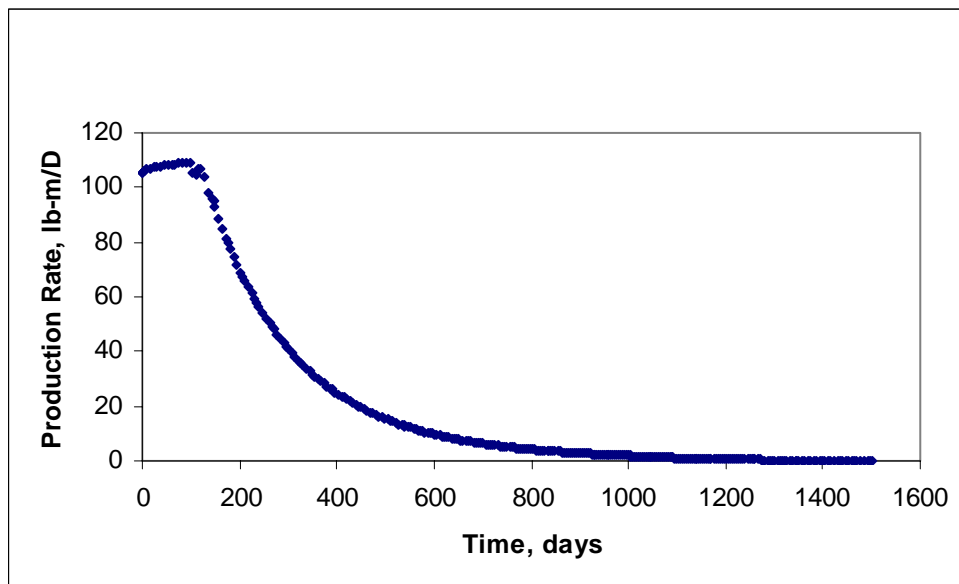


Fig. 4.16 Molar production rate of heavy fraction (C_{17+}), group 6

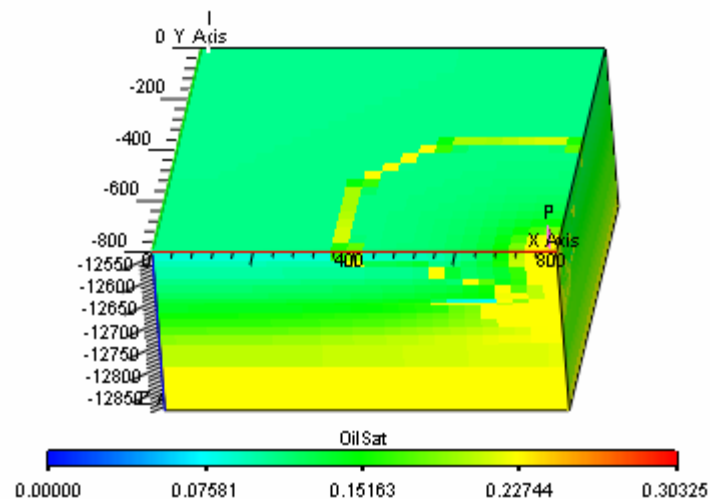


Fig. 4.17a Oil saturation distribution from compositional model with compositional gradient at $t = 1645$ days

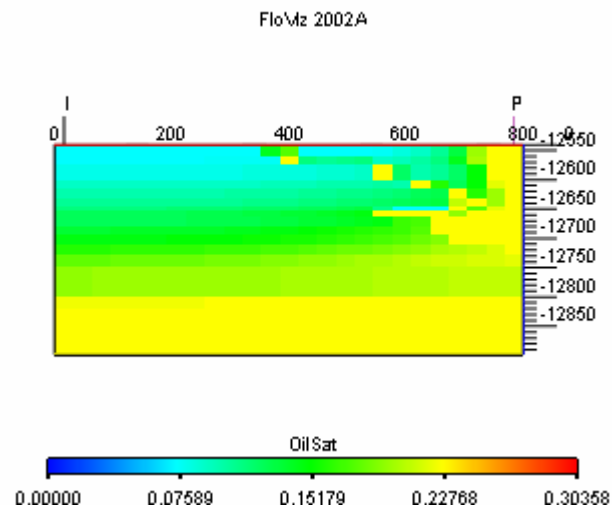


Fig. 4.17b 2-D oil saturation distribution from compositional model with compositional gradient at $t = 1645$ days

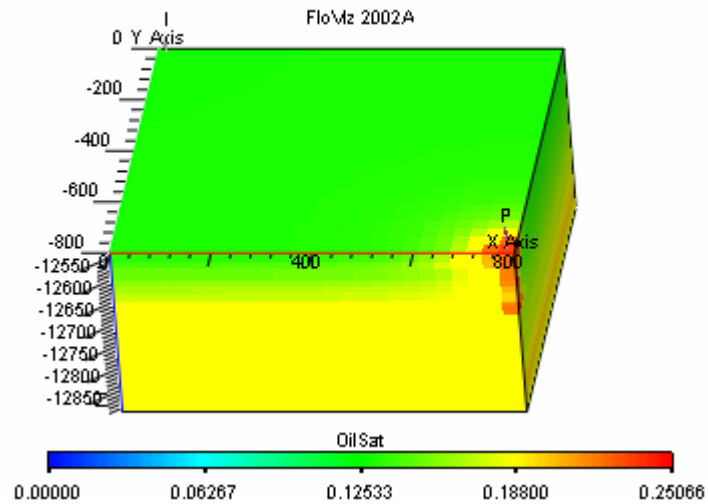


Fig. 4.18a Oil saturation distribution from MBO model with compositional gradient at $t = 1645$ days

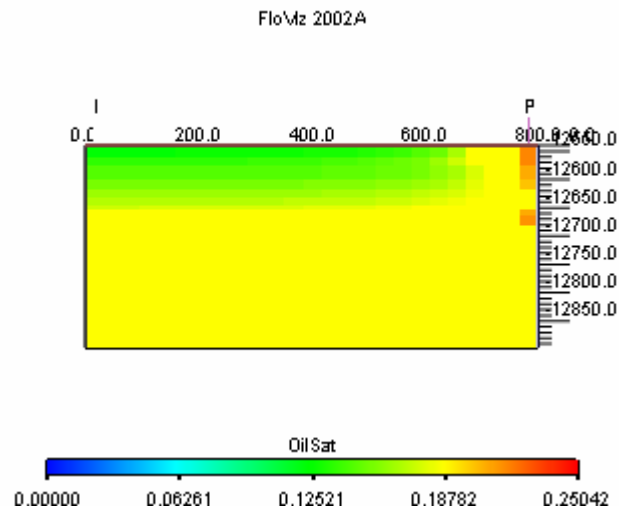


Fig. 4.18b 2-D oil saturation distribution from MBO model with compositional gradient at $t = 1645$ days

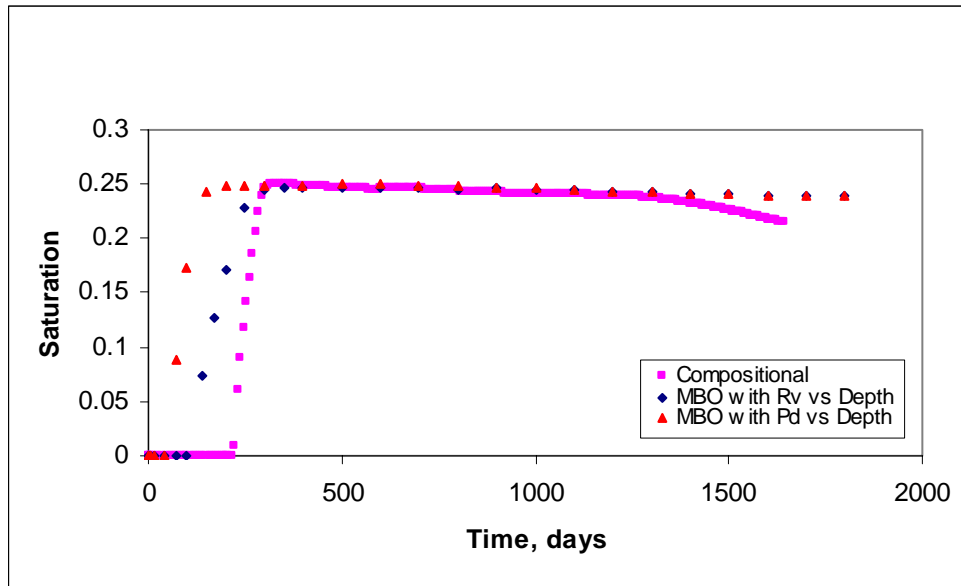


Fig. 4.19 Oil saturation for well gridblock (25, 25, 1)

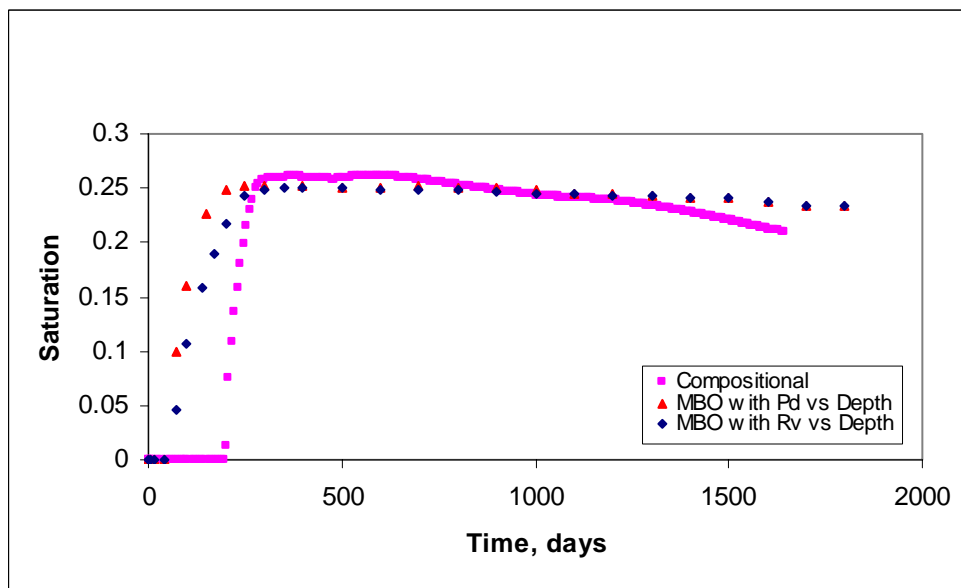


Fig. 4.20 Oil saturation for well gridblock (25, 25, 9)

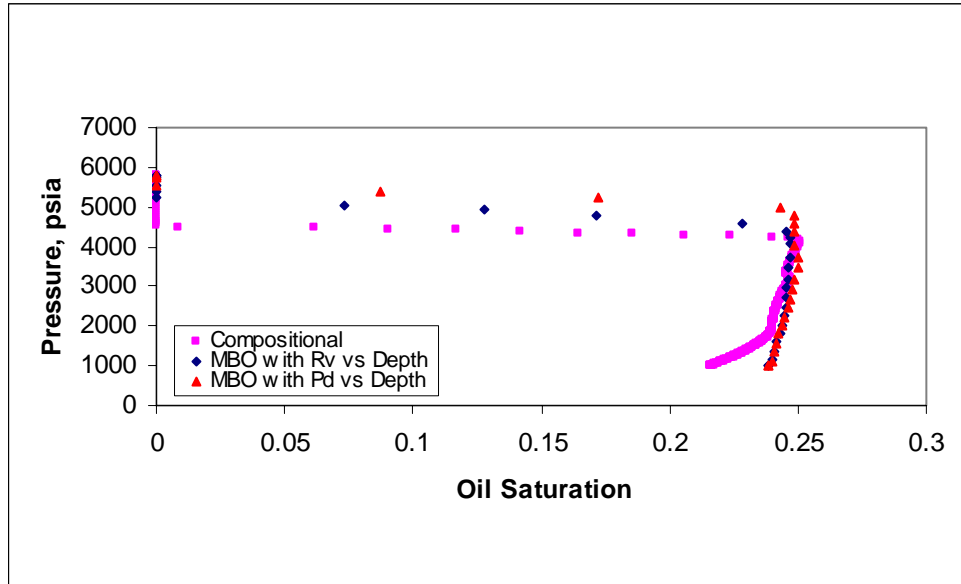


Fig. 4.21 Oil saturation versus pressure for well gridblock (25, 25, 1)

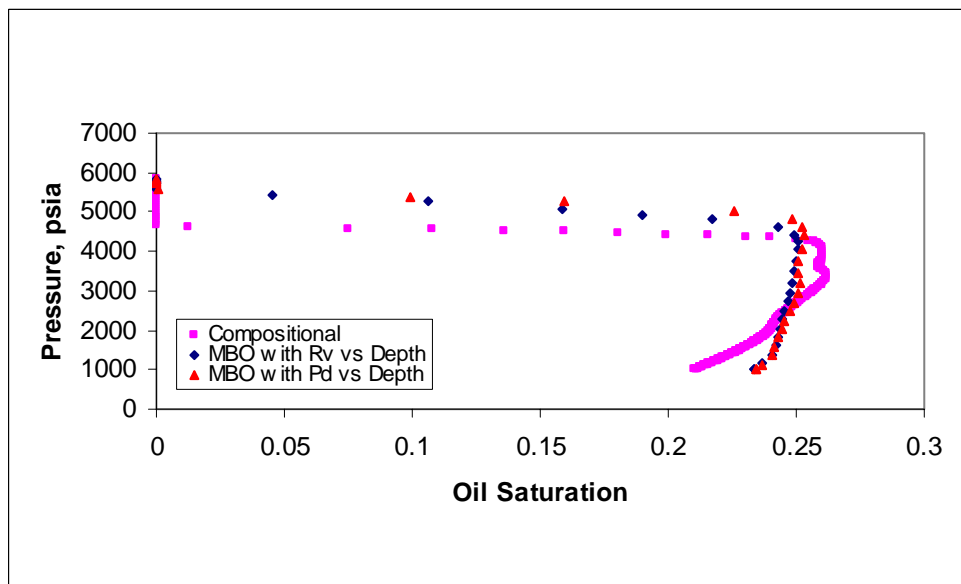


Fig. 4.22 Oil saturation versus pressure for well gridblock (25, 25, 9)

When the compositional model begins to give liquid drop-out, the accumulation around the wellbore area causes also less pressure drop in compositional model and the two models begin to give similar pressure drop plots again. The reservoir gas is becoming leaner with the continuing depletion process, which also reduces the compositional effects. From the individual wellbore gridblock data, it can be inferred that revaporization takes place after some time in compositional model and the oil saturation decreases. However, this process cannot be represented properly in the modified black-oil model. None of the initialization methods can represent the vaporization process properly. Especially at the top of the model where lower pressure values are encountered the modeling of revaporization process is poor.

Since the liquid holding tendency of the gas in modified black-oil model is dependent on the pressure, this amount gets smaller in the regions of low pressures. On the other hand, towards the bottom part of the model where higher-pressure values dominate, a better approximation of the revaporization process can be observed. This can be evaluated by observing the oil saturation values below critical saturation that is 0.24. Above this point a reduction in oil saturation is due to mobilization of liquid phase. In the MBO model initialized with saturation pressure versus depth, oil saturation exceeds the critical oil saturation and the condensate becomes mobile for the bottom layers. Also it gives higher saturations for top completions. Mobile condensate results in higher oil production rates than the compositional model as shown in **Fig. 4.23**. Early condensation results in lower oil rates for the MBO model. Compared to the constant composition case, oil production rate is constant for some time. Since the model is initialized with compositional gradient, it has less oil compared to the constant composition case. **Fig. 4.24** and **Fig. 4.25** give the gas-oil ratio and recovery factors consequently.

Initialization methods and their affect on revaporization will be investigated further for the injection purposes.

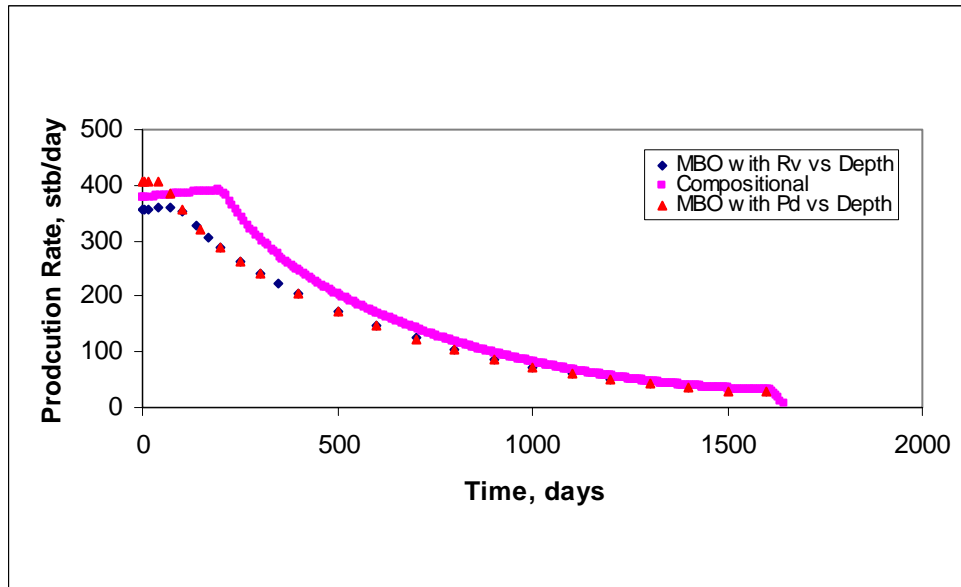


Fig. 4.23 Oil production rate for the model initialized with compositional gradient

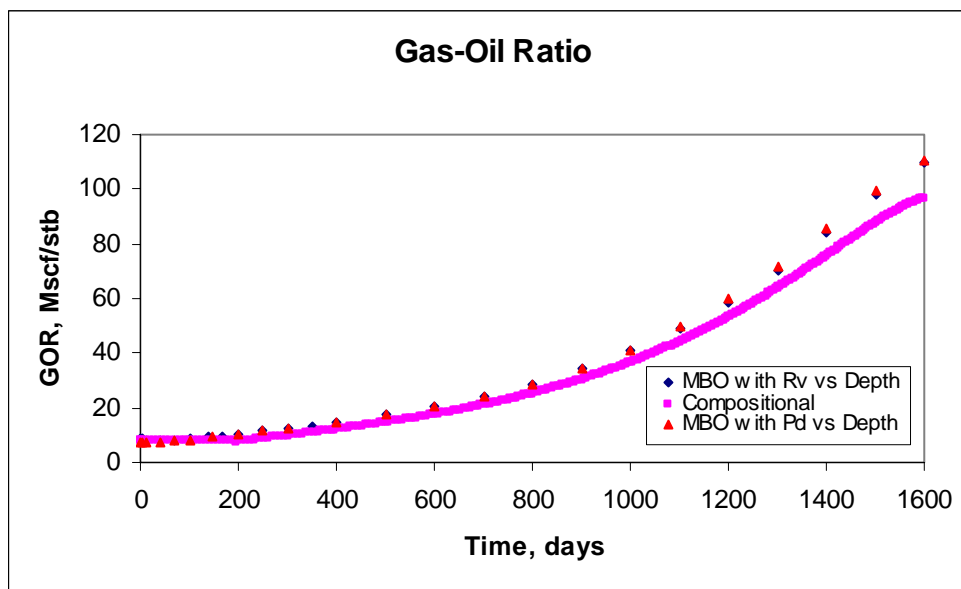


Fig. 4.24 Gas-Oil ratio for the model initialized with compositional gradient

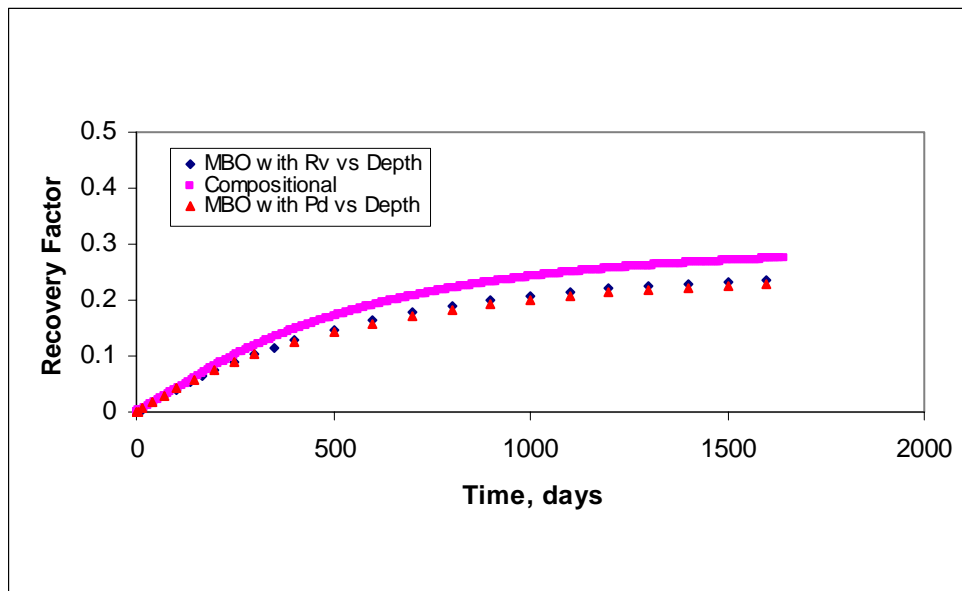


Fig. 4.25 Recovery factor for the model initialized with compositional gradient

4.1.2 Effect of Completion

To investigate the effect of different completion strategies two runs were conducted. The first one with the well completed in the first two layers and the second with the well completed in last two layers. The models were initialized with saturation pressure with depth and oil-gas ratio versus depth tables.

For the two runs conducted, average field pressure and gas-oil ratio plots from two models exhibited exactly the same patterns as the plots previously presented.

Fig. 4.26 and **Fig. 4.27** represent the oil production rate for two layers completed at the top and bottom of the model respectively. Due to compositional grading, the heavy fraction amount increases towards the bottom of the reservoir and also the dew point pressure. The model with the lower completions gives more oil production and earlier condensate drop-out (**Table 4.5**). The effect of initialization with saturation pressure

versus depth table can be observed in the model with upper layers completed from the plots. However, initialization with different methods does not make a major difference in the performance of models when the bottom layers are completed. Modified black-oil and compositional models agreed better when the layers are completed at the top of the reservoir since the fraction of the lighter components is higher in the region (**Table 4.6**). This confirms the fact that MBO models work better for leaner gases.

Fig. 4.28 and **Fig. 4.29** give the oil saturation distribution after the first condensate formation in compositional model for bottom completion. Notice that condensate saturation in the compositional model, around the wellbore is higher than for the MBO model for approximately 2 years.

Fig. 4.30 and **Fig. 4.31** represent the recovery factor plots for two layers completed at the top and the bottom of the model respectively. Recovery factor for the compositional model is always higher; in MBO models most of the oil is left in the reservoir due to early condensation and poor revaporization. The differences between two models for upper and lower completion are 4 % and 7 %.

Fig. 4.32 through **Fig. 4.35** shows oil saturation distribution and average saturations at the end of the simulation. Compositional model has higher condensation around the wellbore. However in MBO model condensation occurs throughout the reservoir causing lower recovery factors. For the bottom completion recovery factor is slightly lower if the model is initialized with saturation pressure versus depth table. MBO model tends to give higher oil saturation if initialized with saturation pressure and this effect can be observed clearly if fraction of the heavy component is higher around the region of completions. **Fig. 4.36** through **Fig. 4.39** gives the condensate distribution for upper layer completion.

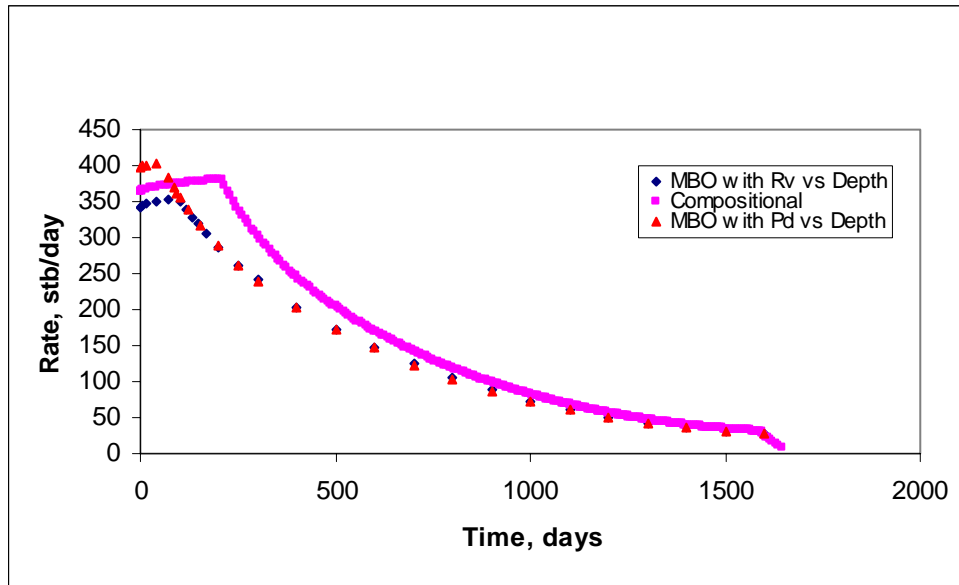


Fig. 4.26 Oil production rate for the well completed in the two upper layers

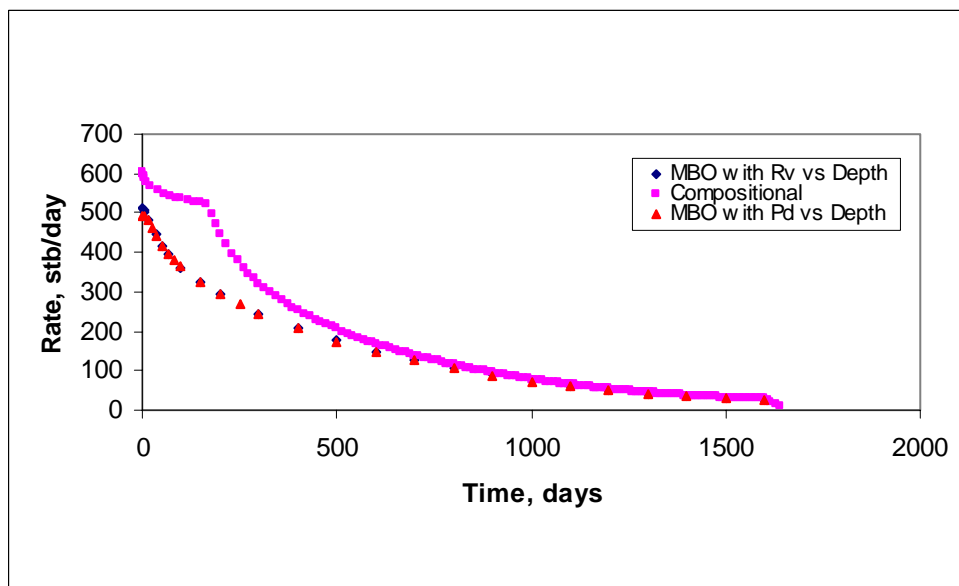


Fig. 4.27 Oil production rate for the well completed in the two bottom layers

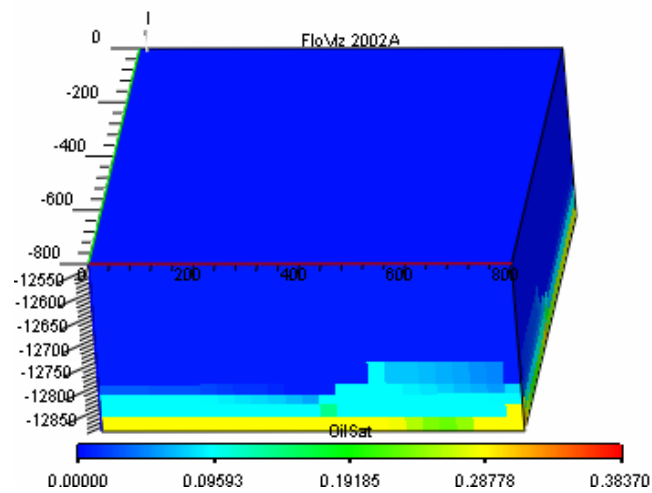


Fig. 4.28a Oil saturation distribution from compositional model for bottom completion at $t = 175$ days

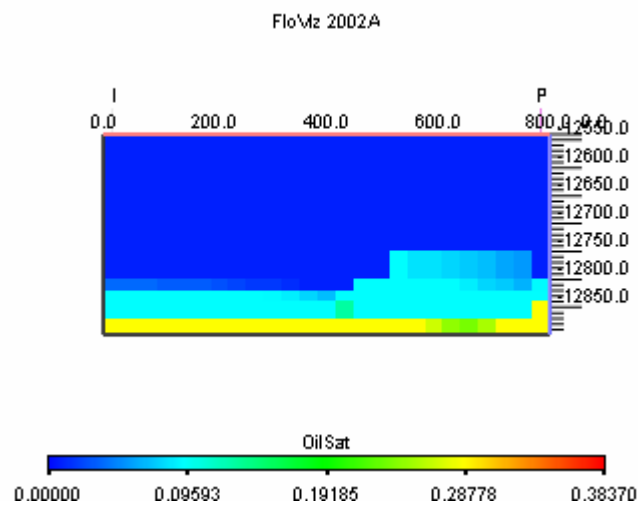


Fig. 4.28b 2-D oil saturation profile from compositional model for bottom completion at $t = 175$ days

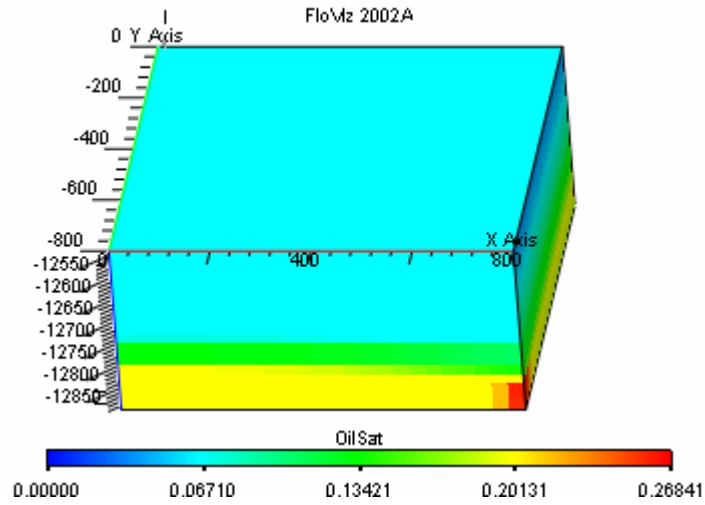


Fig. 4.29a Oil saturation distribution from MBO model for bottom completion at t = 175 days

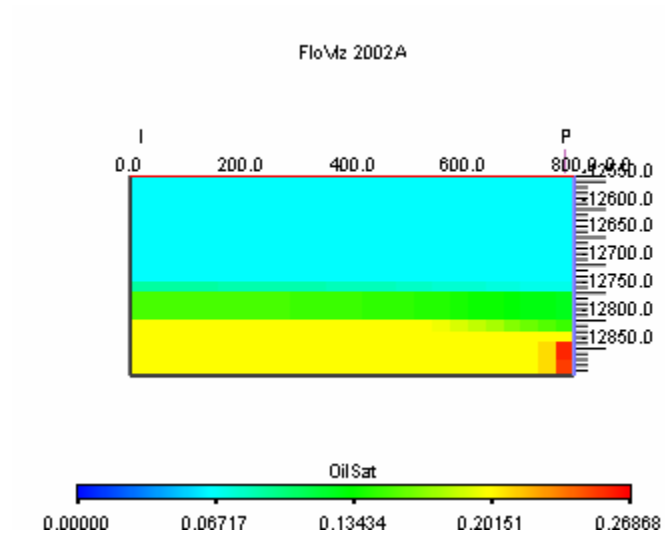


Fig. 4.29b 2-D oil saturation profile from MBO model for bottom completion at t = 175 days

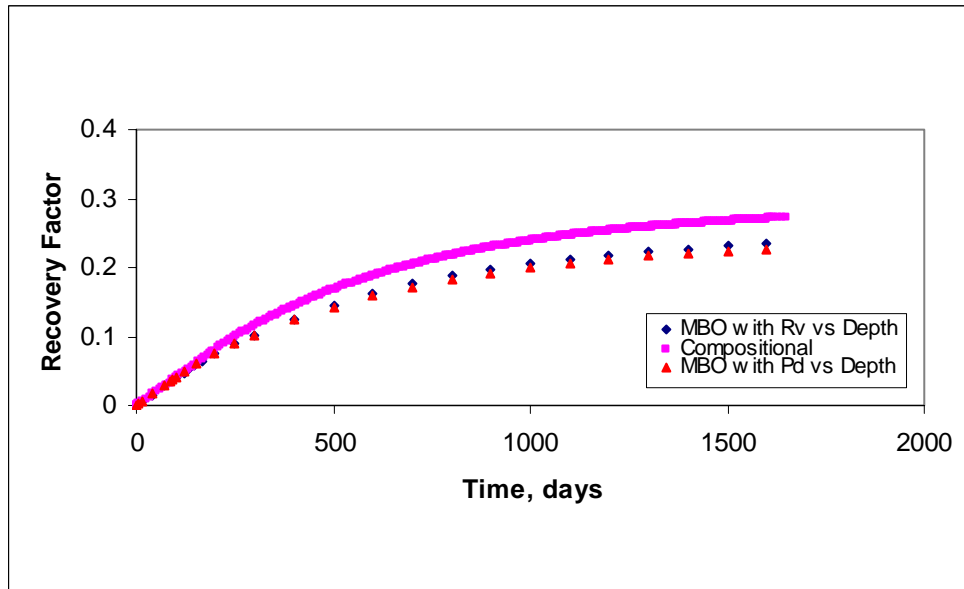


Fig. 4.30 Recovery factor for the well completed in the two upper layers

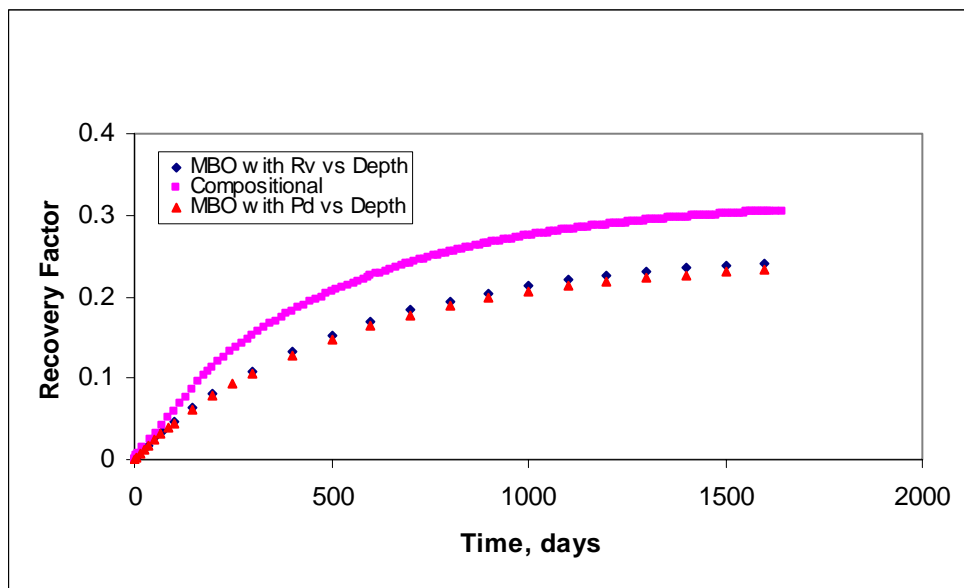


Fig. 4.31 Recovery factor for the well completed in the two bottom layers

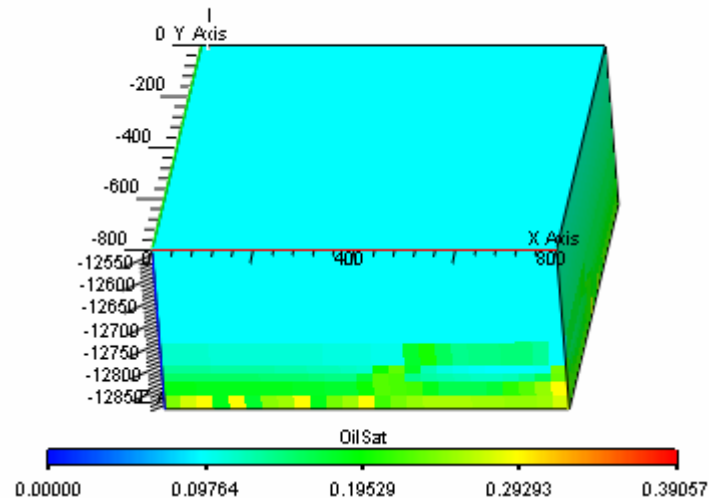


Fig. 4.32a Oil saturation distribution from compositional model for bottom completion at the end of the simulation time

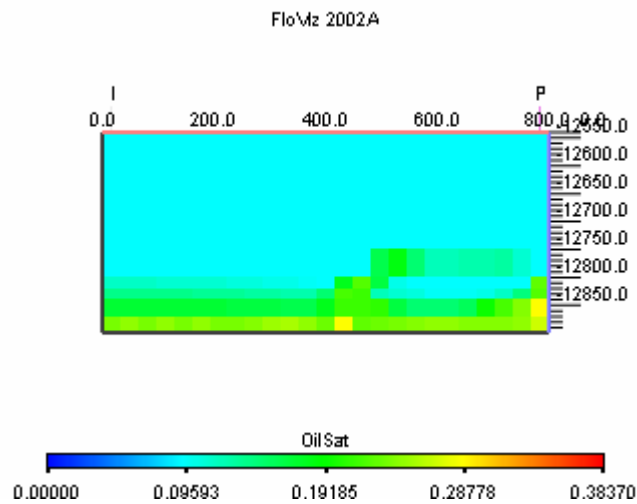


Fig. 4.32b 2-D oil saturation profile from compositional model for bottom completion at the end of the simulation time

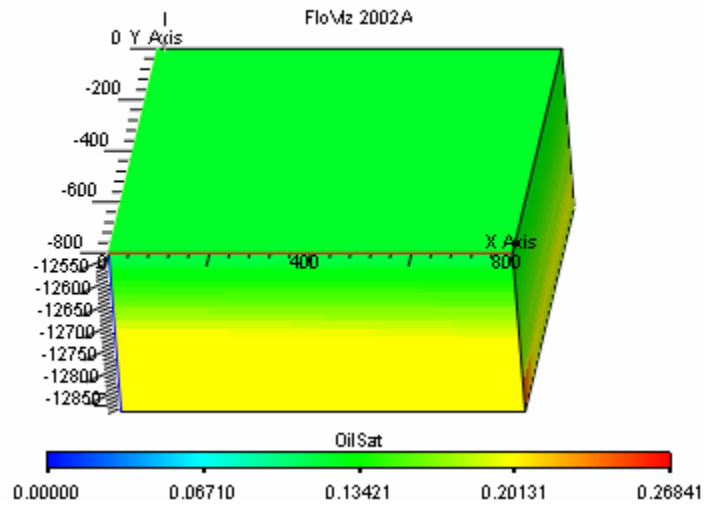


Fig. 4.33a Oil saturation distribution from MBO model for bottom completion at the end of simulation

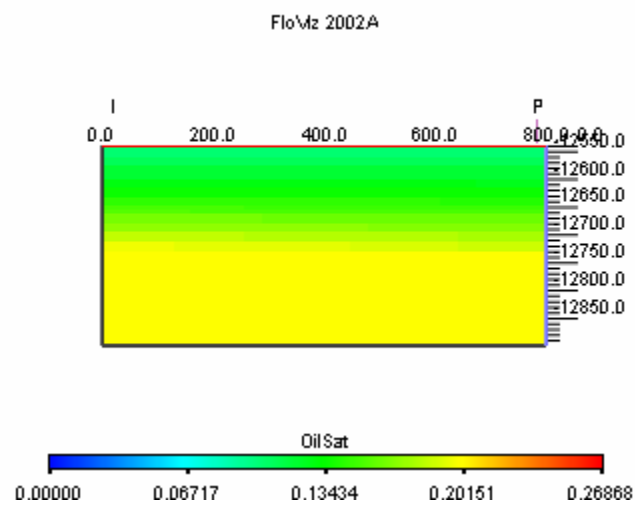
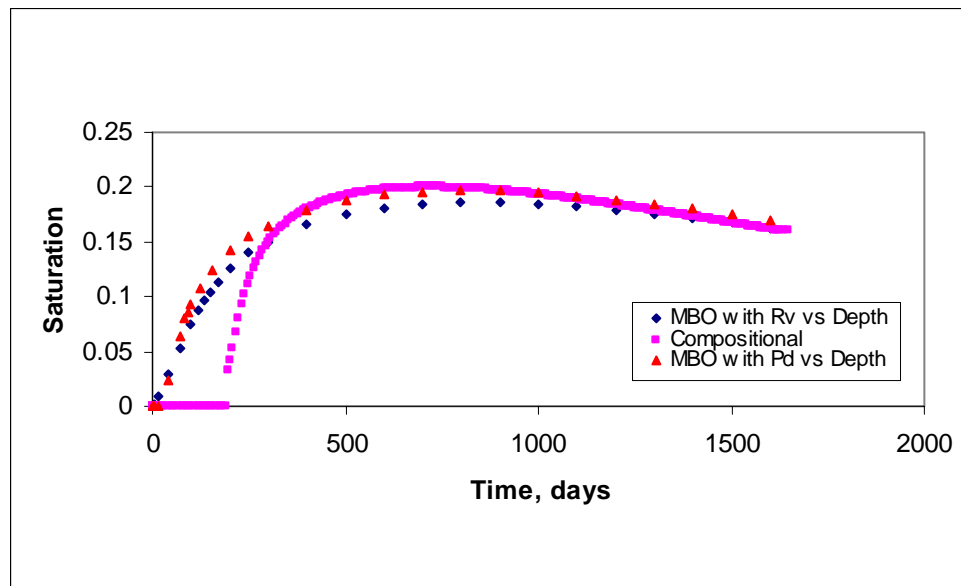


Fig. 4.33b 2-D oil saturation profile from MBO model for bottom completion at the end of simulation

Table 4.5 Oil saturation values for gridblock 25, 25, 18

Time, days	MBO	Compositional	Difference, %
	So	So	
100	0.27	0.00	-100.00
200	0.26	0.31	13.87
400	0.26	0.28	7.47
600	0.26	0.27	4.88
800	0.25	0.25	-0.91
1000	0.25	0.25	0.01
1200	0.25	0.24	-2.79
1400	0.24	0.23	-5.21
1600	0.24	0.22	-11.39

**Fig. 4.34 Average oil saturation for the well completed in the two upper layers**

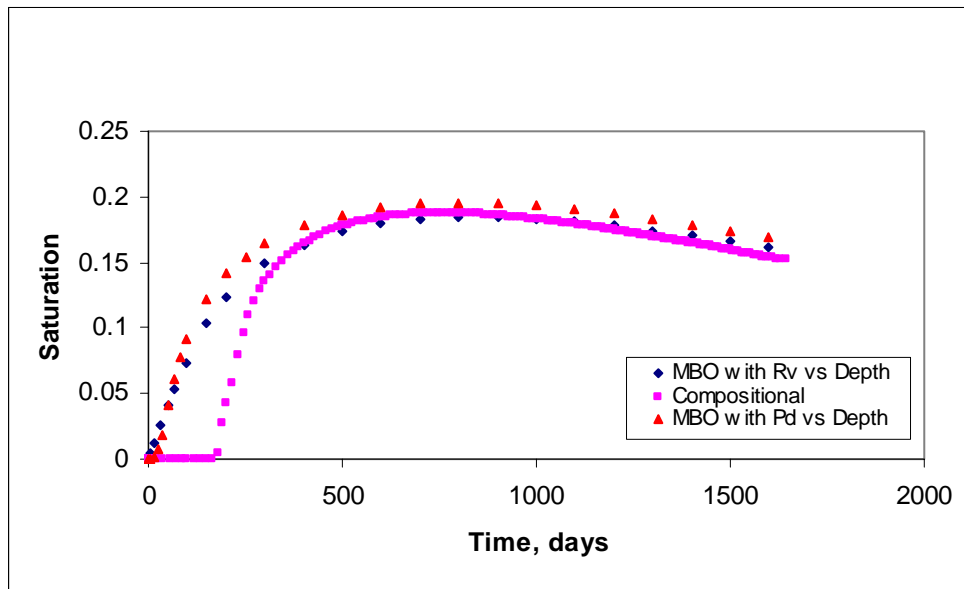


Fig. 4.35 Average oil saturation for the well completed in the two bottom layers

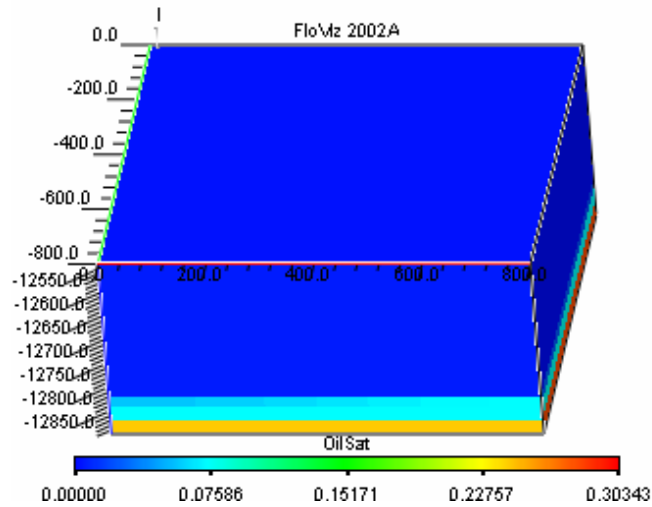


Fig. 4.36a Oil saturation profile at 190 days when the well is completed at the top for the compositional model

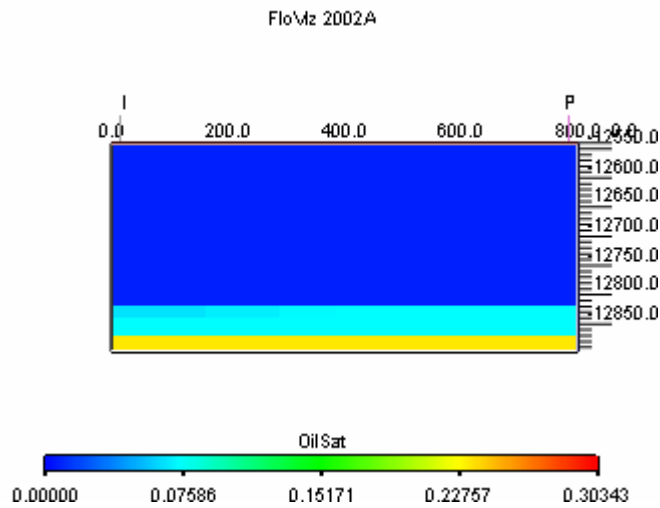


Fig. 4.36b 2-D oil saturation distribution at 190 days when the well is completed at the top for the compositional model

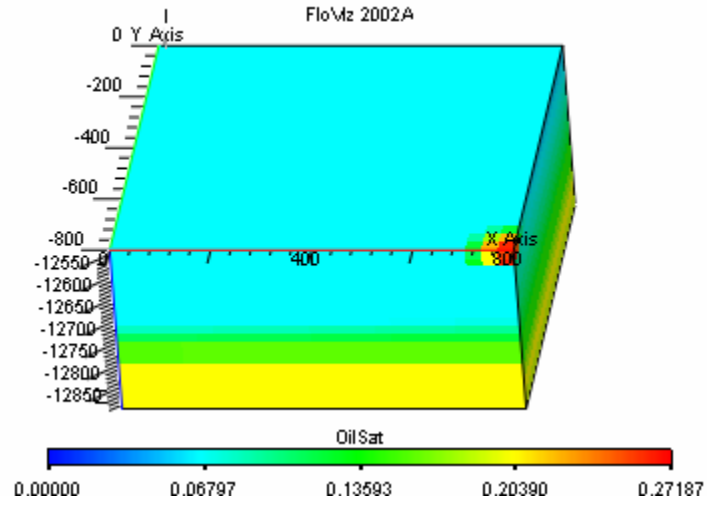


Fig. 4.37a Oil saturation profile at 190 days when the well is completed at the top for the MBO model

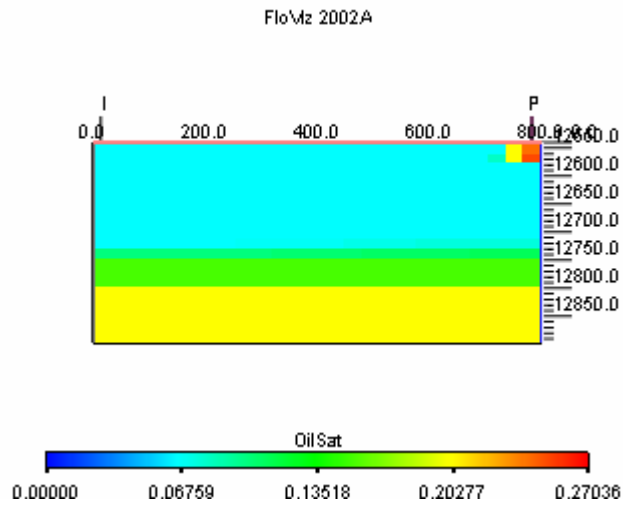


Fig. 4.37b 2-D oil saturation profile at 190 days when the well is completed at the top for the MBO model

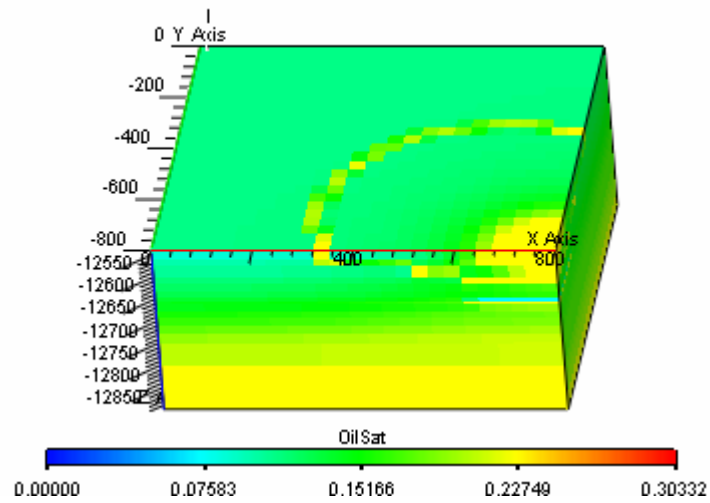


Fig. 4.38a Oil saturation profile at the end of the simulation time when the well is completed at the top for the compositional model

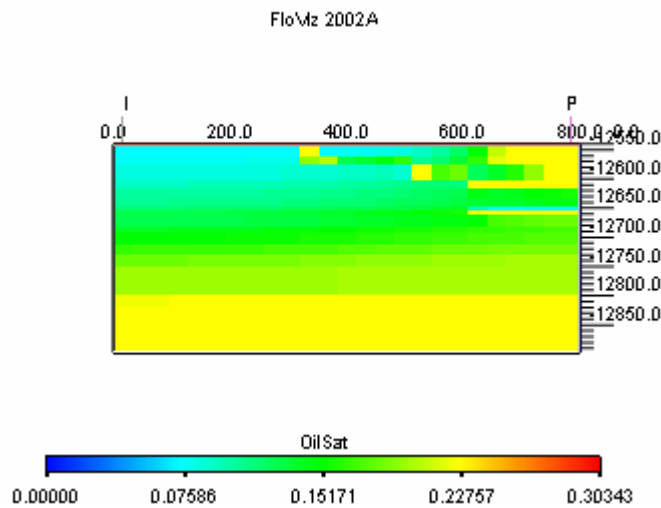


Fig. 4.38b 2-D oil saturation profile at the end of the simulation time when the well is completed at the top for the compositional model

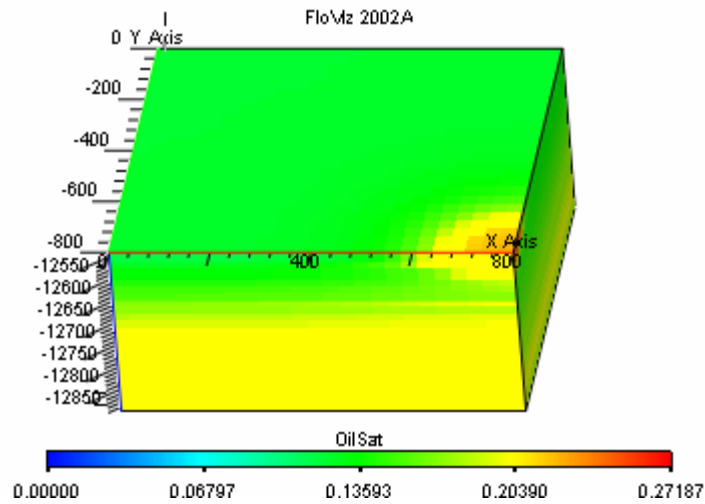


Fig. 4.39a Oil saturation profile at the end of the simulation time when the well is completed at the top for the MBO model

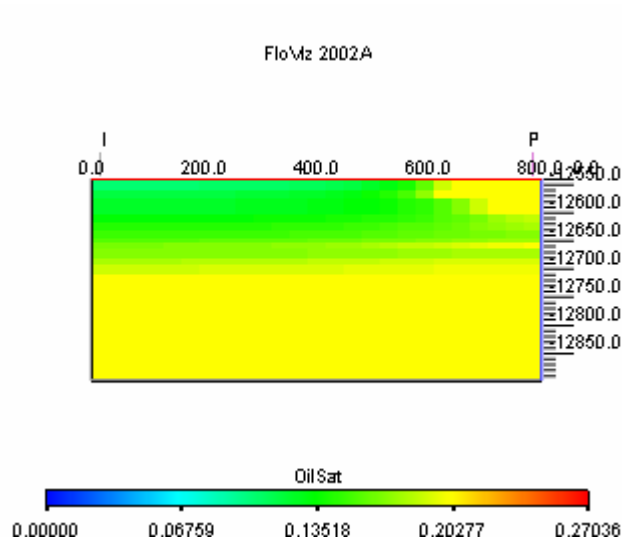


Fig. 4.39a 2-D oil saturation profile at the end of the simulation time when the well is completed at the top for the MBO model

Table 4.6 Oil saturation values for gridblock 25, 25, 1

Time, days	MBO	Compositional	Difference, %
	So	So	
100.00	0.00	0.00	0.00
200.00	0.26	0.00	-100.00
400.00	0.27	0.28	3.12
600.00	0.27	0.26	-2.01
800.00	0.26	0.25	-4.16
1000.00	0.26	0.24	-5.12
1200.00	0.26	0.24	-6.08
1400.00	0.25	0.24	-4.12
1600.00	0.24	0.23	-5.22

4.1.3 Effect of k_v/k_h Ratio

To investigate the effect of reduced communication between layers, k_v/k_h ratio was reduced to an extreme value of 10^{-4} , which almost restricts the mass transfer between layers. The producer well is again completed in the first nine layers. MBO model was initialized with saturation pressure and oil-gas and gas-oil ratios versus depth tables.

Fig. 4.40 and **Fig. 4.41** give the average field pressure and oil production rates from two models.

Average field pressure from both models has the same trend as the previous cases investigated but the decline is less pronounced due to reduced communication between the layers. It takes time for pressure transient to move further into the reservoir for each individual layer. This movement is also restricted by the condensate accumulation around the wellbore.

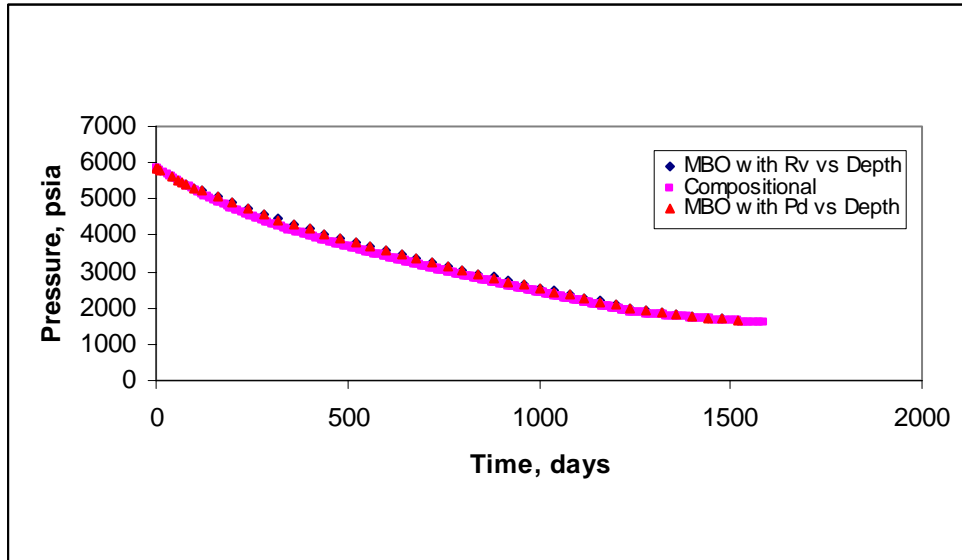


Fig. 4.40 Average field pressure for k_v/k_h ratio of 0.0001

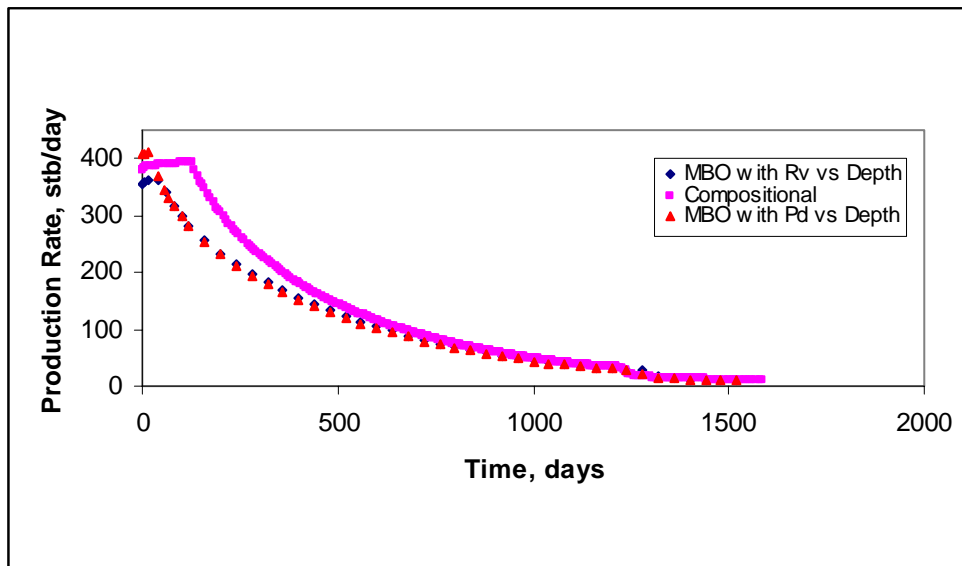


Fig. 4.41 Oil production rate for k_v/k_h ratio of 0.0001

With the reduced communication between layers, it is clearly observed that compositional and MBO models showed closer performances. Liquid content of gas and gas content of oil in MBO model are functions of pressure only. Since the condensation and consequent vaporization processes are controlled by pressure dependent functions, the reduction in pressure drop caused a delay in condensate drop-out for MBO model.

Compositional model also gives early condensation with a low k_v/k_h ratio. From the oil production rate plot it can be seen that the time of constant oil production rate is shorter than the previous cases.

The reduced communication between layers also prevented the mixing of the leaner reservoir gas (relative to initial conditions) with the oil formed after condensation. In the case of good vertical communication; the leaner gas after the first drop-out, tends to go up and at the same time vaporizes the oil on its path during the continuing depletion process. Also the accumulated condensate tends to go down because of gravity effects. Both scenarios are not possible with the restricted vertical communication. Every layer is left with its own ability to vaporize the condensate accumulated. Compositional effects will gain importance at the bottom part of the model because of an isolated richer gas.

When the vertical communication is good between layers after the condensate drops out the reservoir gas becomes leaner and flow of this gas to the wellbore revaporizes the oil bank. In the case of reduced vertical communication, condensate accumulation and vaporization process for each layer is proportional to the layers content of heavy and light component fractions. The bottom layers have higher oil saturation with less vaporization because of their higher content in heavier molecules, while the higher light component fraction in the top layers causes lower oil saturation and higher vaporization. Higher saturations at the bottom of the model also give mobility to oil phase by exceeding the critical saturation value. **Table 4.7** through **Table 4.10** shows the mole

fraction of light (GRP1) and heavy (GRP6) fractions in vapor and liquid phases with time. Notice that at $t=1$ day the reservoir is in single phase.

Table 4.7 Mole fractions of heavy and light components for k_v/k_h ratio of 0.1 in gridblock 25, 25, 18

Time, days	Heavy Component (GRP6)		Light Component (GRP1)	
	In Vapor Phase	In Liquid Phase	In Vapor Phase	In Liquid Phase
1	0.025747	0.025747	0.669263	0.669263
600	0.001882	0.078893	0.744964	0.504738
1200	0.000109	0.123468	0.76311	0.334519
1600	0.0000177	0.170061	0.747434	0.197282

Table 4.8 Mole fractions of heavy and light components for k_v/k_h ratio of 10^{-4} in gridblock 25, 25, 18

Time, days	Heavy Component (GRP6)		Light Component (GRP1)	
	In Vapor Phase	In Liquid Phase	In Vapor Phase	In Liquid Phase
1	0.025747	0.025747	0.669263	0.669263
600	0.007312	0.057486	0.719892	0.582344
1200	0.000662	0.092997	0.756119	0.446069
1600	0.000172	0.113977	0.763	0.364973

Table 4.9 Mole fractions of heavy and light components for k_v/k_h ratio of 0.1 in gridblock 25, 25, 9

Time, days	Heavy Component (GRP6)		Light Component (GRP1)	
	In Vapor Phase	In Liquid Phase	In Vapor Phase	In Liquid Phase
1	0.012728	0.012728	0.709416	0.709416
600	0.000514	0.073698	0.756998	0.449941
1200	1.21E-05	0.100696	0.766412	0.219722
1600	1.00E-05	0.112995	0.767185	0.198768

Table 4.10 Mole fractions of heavy and light components for k_v/k_h ratio of 10^{-4} in gridblock 25, 25, 9

Time, days	Heavy Component (GRP6)		Light Component (GRP1)	
	In Vapor Phase	In Liquid Phase	In Vapor Phase	In Liquid Phase
1	0.012728	0.012728	0.709416	0.709416
600	0.001706	0.073146	0.745531	0.505222
1200	8.86E-05	0.103894	0.764945	0.33641
1600	1.37E-05	0.144964	0.753939	0.194999

In the case of reduced vertical permeability higher amounts of heavier component (GRP6) in vapor phase is observed for gridblock 25, 25, 18, which, means that gas does not get lean compared to the vertical permeability of 0.1 md. Also mole fraction of light component (GRP1) is higher in both liquid and vapor phases, lean gas could not go up and help vaporize the condensate on its way towards producer.

Fig. 4.42 through **Fig. 4.47** and **Table 4.11**, **Table 4.12** provides the details of condensation/vaporization in both models. First condensation is observed at 127 days in compositional model. The first two figures give the comparison of oil saturation distribution at 127 days. Condensation initially takes place in layer nine, which is the lowest completion and progresses upwards then later on downwards. Compared to the above-completed layers, layer nine has a higher permeability and thickness value.

For the third year of simulation, models performances get very close. Then at the fourth year, unrealistic vaporization in MBO model again creates some differences. The unrealistic vaporization results from revaporization of oil at a rate only governed by pressure. This effect is more pronounced for gas injection and will be explained in detail in the following section.

However, the differences in saturations given by the MBO model have little impact on the production performance and ultimate recoveries.

According to **Fig. 4.42** vaporization is less effective for well gridblock (25, 25, 1). From the plots, it can also be inferred that in the case of limited vertical communication, initializing the model with saturation pressure versus depth table in the region of higher lighter component fraction would result in erroneous oil saturations for a rich gas condensate reservoir. Also the size of additional bank forming at the top of the reservoir that cannot be modeled with MBO model becomes smaller with a reduced k_v/k_h ratio. This is the result of lack of flow of gas into the upper layers from the lower layers.

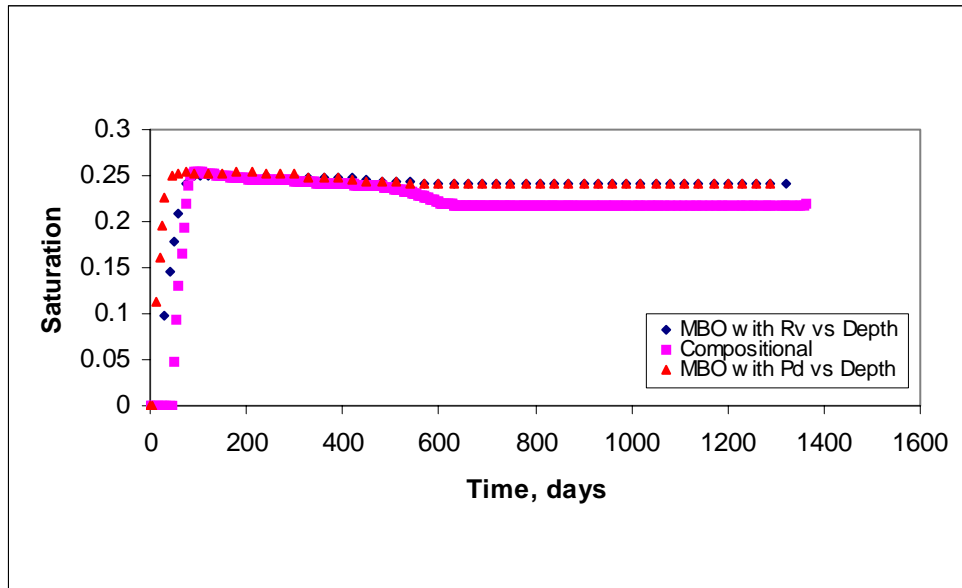


Fig. 4.42 Oil Saturation for well gridblock (25, 25, 1)

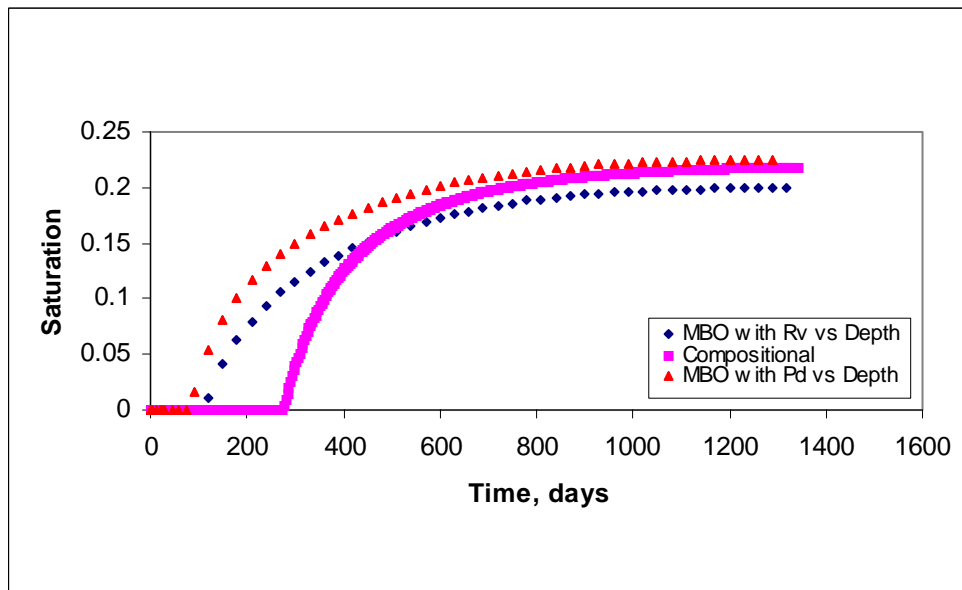


Fig. 4.43 Oil Saturation for well gridblock (25, 25, 9)

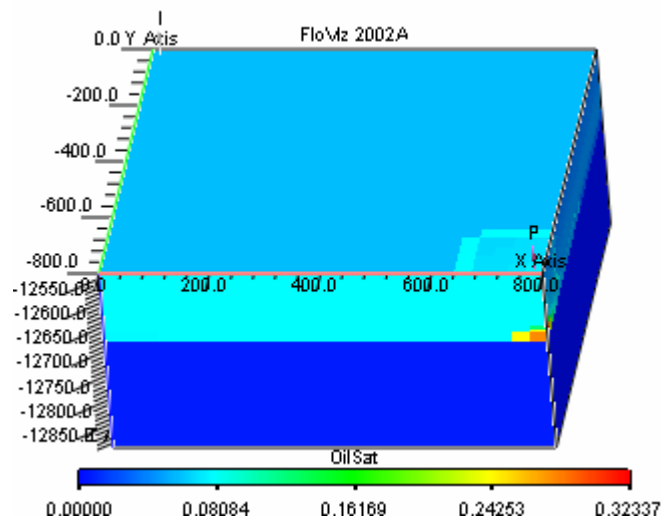


Fig. 4.44a Oil saturation distribution from compositional model for k_v/k_h ratio of 0.0001 at $t = 127$ days

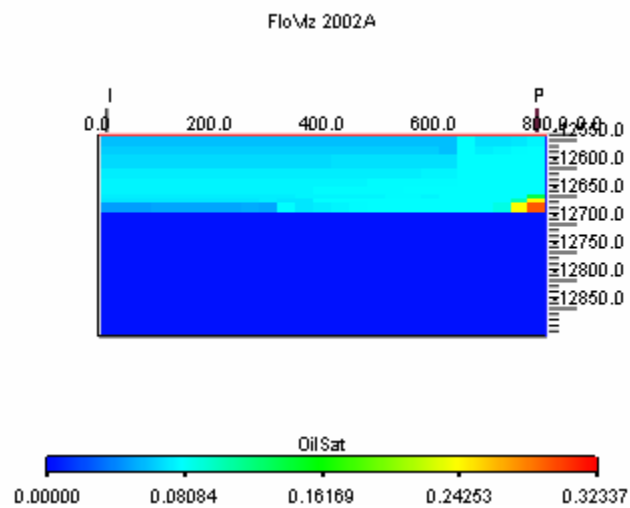


Fig. 4.44b 2-D oil saturation distribution from compositional model for k_v/k_h ratio of 0.0001 at $t = 127$ days

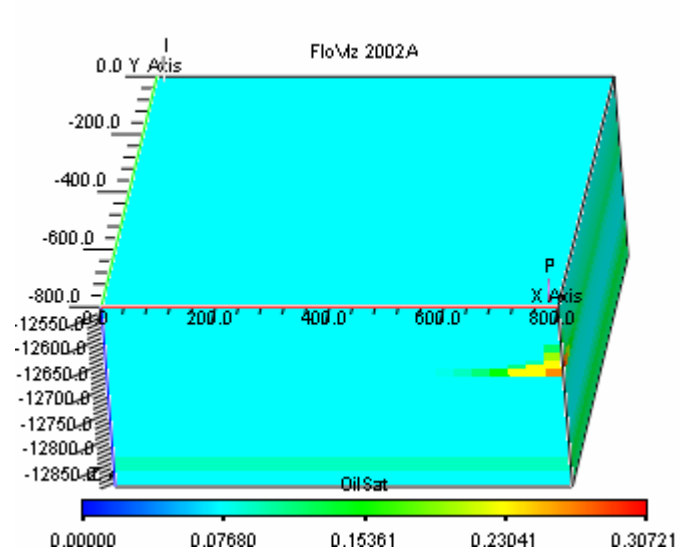


Fig. 4.45a Oil saturation distribution from MBO model for k_v/k_h ratio of 0.0001 at $t = 127$ days

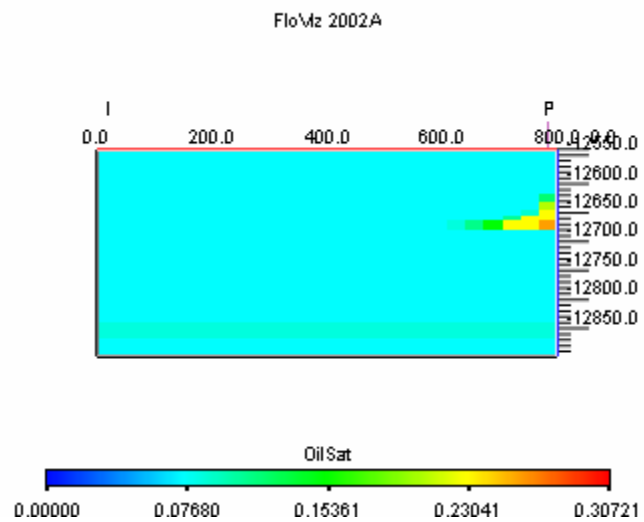


Fig. 4.45b 2-D oil saturation distribution from MBO model for k_v/k_h ratio of 0.0001 at $t = 127$ days

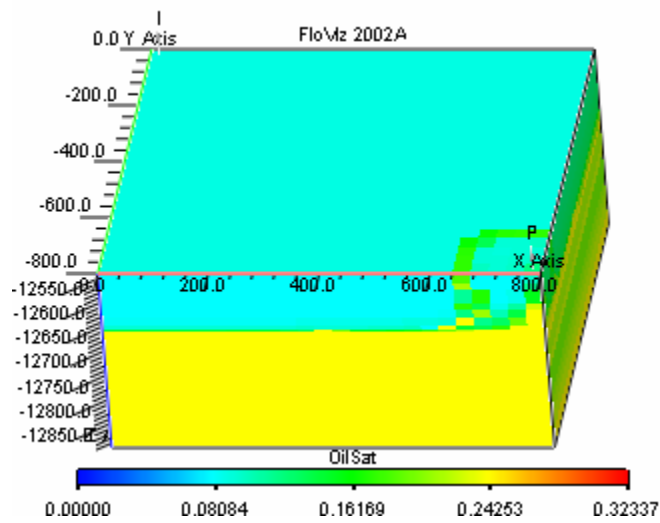


Fig. 4.46a Oil saturation distribution from compositional model for k_v/k_h ratio of 0.0001 after 4 years

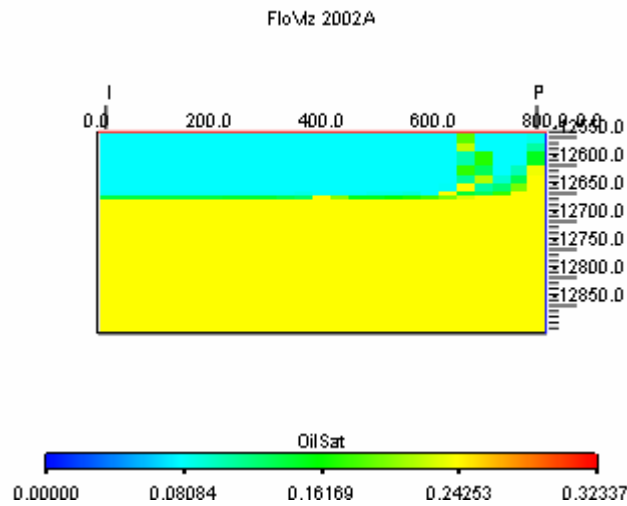


Fig. 4.46b 2-D oil saturation distribution from compositional model for k_v/k_h ratio of 0.0001 after 4 years

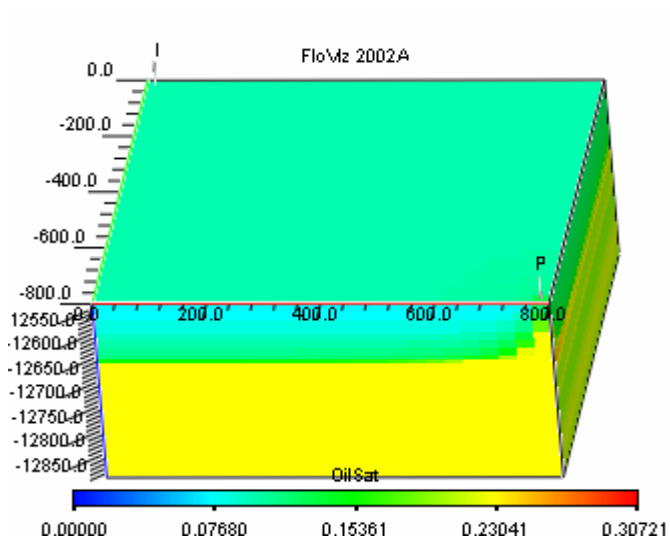


Fig. 4.47a Oil saturation distribution from MBO model for k_v/k_h ratio of 0.0001 after 4 years

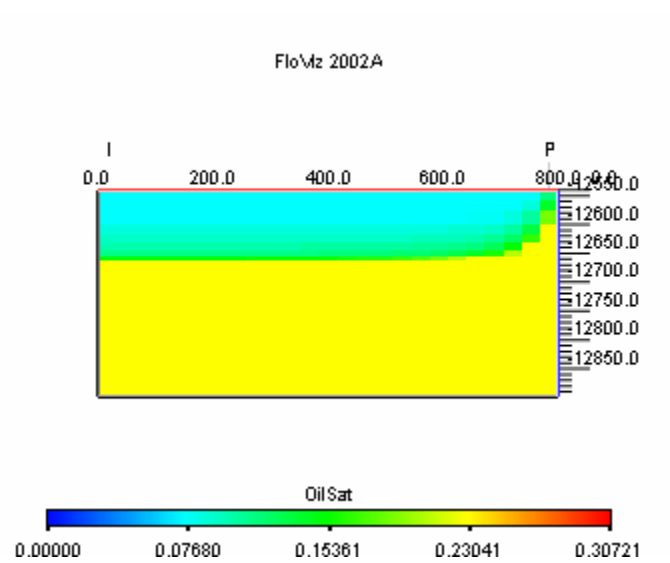


Fig. 4.47b 2-D oil saturation distribution from MBO model for k_v/k_h ratio of 0.0001 after 4 years

Table 4.11 Oil saturation values for gridblock 25, 25, 1

Time, days	MBO	Compositional	Difference, %
	So	So	
100.00	0.05	0.00	-100.00
200.00	0.10	0.08	-26.11
400.00	0.14	0.15	3.48
600.00	0.15	0.16	3.92
800.00	0.26	0.16	-64.81
1000.00	0.15	0.15	-1.77
1200.00	0.14	0.14	-4.96
1400.00	0.14	0.14	-3.50
1520.00	0.14	0.14	-3.50

Table 4.12 Oil saturation values for gridblock 25, 25, 9

Time, days	MBO	Compositional	Difference, %
	So	So	
100.00	0.28	0.00	-100.00
200.00	0.29	0.32	8.81
400.00	0.30	0.31	1.74
600.00	0.30	0.30	-2.91
800.00	0.30	0.28	-5.71
1000.00	0.28	0.26	-8.73
1200.00	0.26	0.24	-9.04
1400.00	0.25	0.23	-7.39
1520.00	0.25	0.23	-7.00

Fig. 4.48 shows the producing gas-oil ratio with 22 % difference in gas-oil ratios at the end of the simulation. The difference in gas-oil ratios at the end of the simulation is due to richer gas produced from compositional model. At the time gas-oil ratios become almost stable around 1,100 days, compositional model gives a lower value of GOR. Because of a slow ongoing revaporization process this oil is being added to the gas phase and carried to the producer well.

Revaporization of remaining oil in the reservoir cannot be handled in MBO model especially in the thin layers with low permeability in the absence of good vertical

communication. Thin layers with low permeability give higher amounts of condensate saturation, and then as soon as the gas gets leaner in this area due to liquid drop-out, it exhibits an unrealistic revaporization due to pressure owned higher vaporization ability of gas in MBO model. When the produced gas gets leaner with time, its ability to vaporize disappears. The vaporization in MBO is still effective at the end of the simulation time. The injected gas in MBO model does not get lean with time and has the same properties as before whereas in the compositional model the recycled gas becomes leaner every time it passes through the surface separators and injected back into the reservoir.

Fig 4.49 gives 17.5 % and 20 % recovery factors for MBO and compositional models.

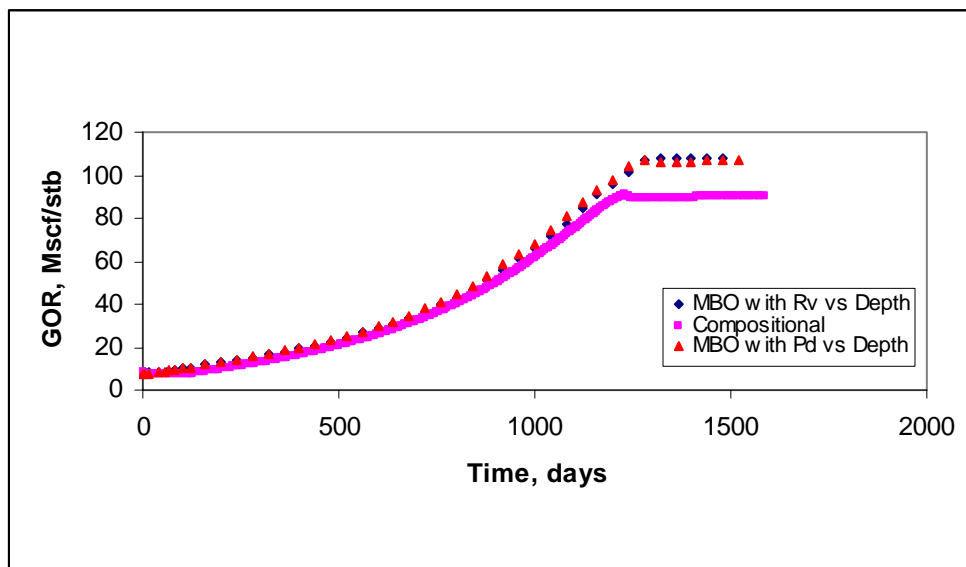


Fig. 4.48 Gas-oil ratio for k_v/k_h ratio of 0.0001

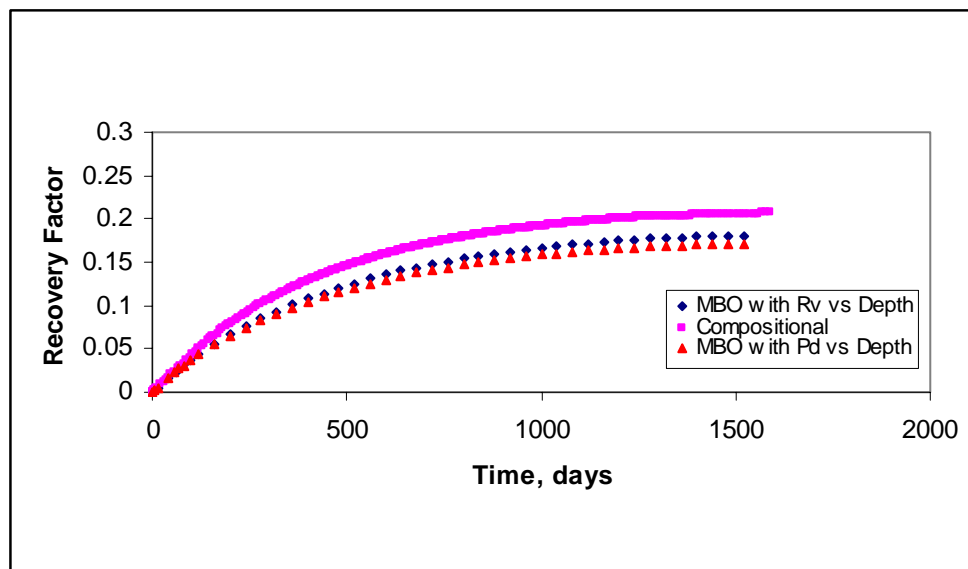


Fig. 4.49 Recovery factor for k_v/k_h ratio of 0.0001

Fig 4.50 and **Table 4.13** give the performance comparison of the models for different completion scenarios in the case of reduced vertical communication.

When the bottom layers are completed higher recovery factors are obtained. If the well is completed closer to the top of the reservoir most of the oil coming out from gas phase cannot be carried to the upper completions and is left in the reservoir.

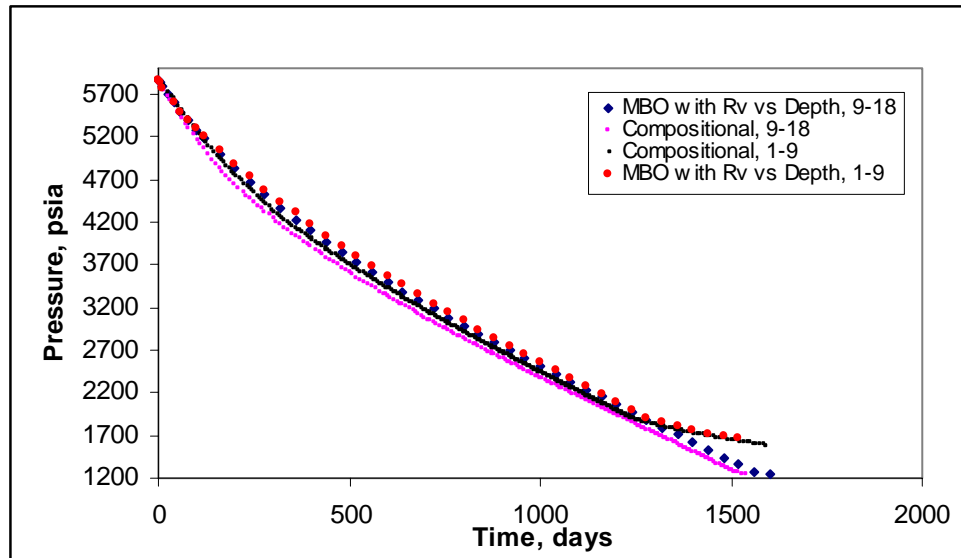


Fig. 4.50 Average reservoir pressure for different completion of layers for k_v/k_h ratio of 0.0001

Table 4.13 Performance of different completions for reduced vertical communication

Completion	MBO		Compositional	
	1 To 9	1 To 9	9 To 18	9 To 18
$S_{o_{max}}$	0.19	0.21	0.18	0.19
P_{min}	1659.91	1583.66	1242.31	1248.46
RF	0.18	0.21	0.23	0.27
GOR_{end}	108.38	90.45	111.86	95.83

4.2 Gas Cycling Case

The MBO model was initialized with R_s/R_v and saturation pressure versus depth tables. To investigate the effect of different parameters on revaporization process, the producer is completed in the top nine layers and the injector is completed in the bottom nine layers for all the cases except, the cases including the investigation of effects of completion locations. By doing so the bottom layers with high permeability and higher heavy fractions are open to flow and also consequent channeling with revaporization is expected to take place. Production and injection rates are 3,000 and 2,500 Mscf/day.

Compositional model will have the produced gas as injection gas, which gets leaner with time by passing through the three-stage separator system and MBO model has the regular gas phase option as an injection gas. The injected gas behavior in MBO will follow the gas PVT table characteristics obtained by Whitson and Torp⁶ method.

4.2.1 Effect of Initialization

Figs. 4.51 through **4.54** gives the performance of compositional and MBO models for the gas cycling case. The average reservoir pressure in both models is represented similarly. Because of early liquid drop-out the MBO model begins with lower oil production rate. If MBO is initialized with saturation pressure versus depth table the early condensation effects does not lower the oil production rate at the beginning of the simulation. The model begins with higher amounts of oil saturation in the reservoir and higher oil rates initially.

As the reservoir is depleted, the reservoir gas becomes leaner and both models begin to provide similar results.

At the end of 5000 days of simulation time, oil production rate obtained from the compositional model is slightly lower than the MBO model. This is the result of excess

amount of revaporization process in the MBO model by ignoring the compositional effects. By doing so, the oil uptake of the injected gas becomes only a function of pressure. However, stripping of the liquid components should be in inverse proportion to their molecular weight. Higher, pressure dependent vaporization leaves less oil in the reservoir giving higher oil production and two models slightly depart from each other again towards the end of the simulation. This can be clearly observed from **Fig. 4.58** and **Fig. 4.59**.

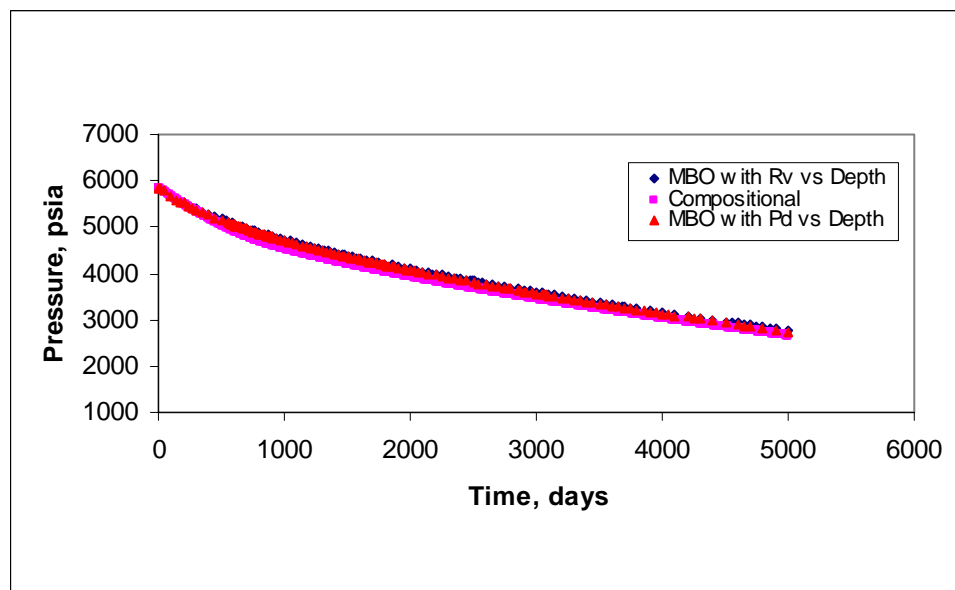


Fig. 4.51 Average field pressure for gas cycling case

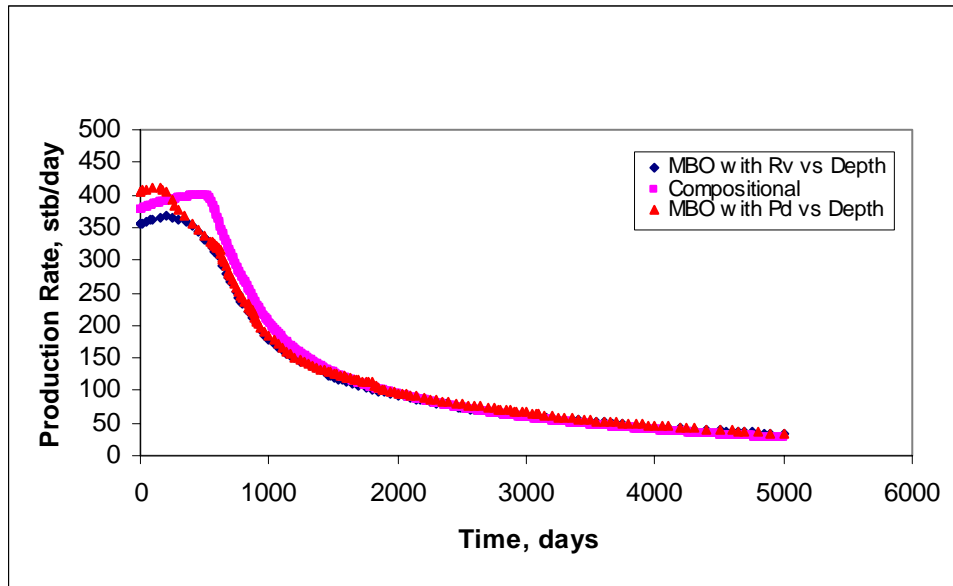


Fig. 4.52 Oil production rate for gas cycling case

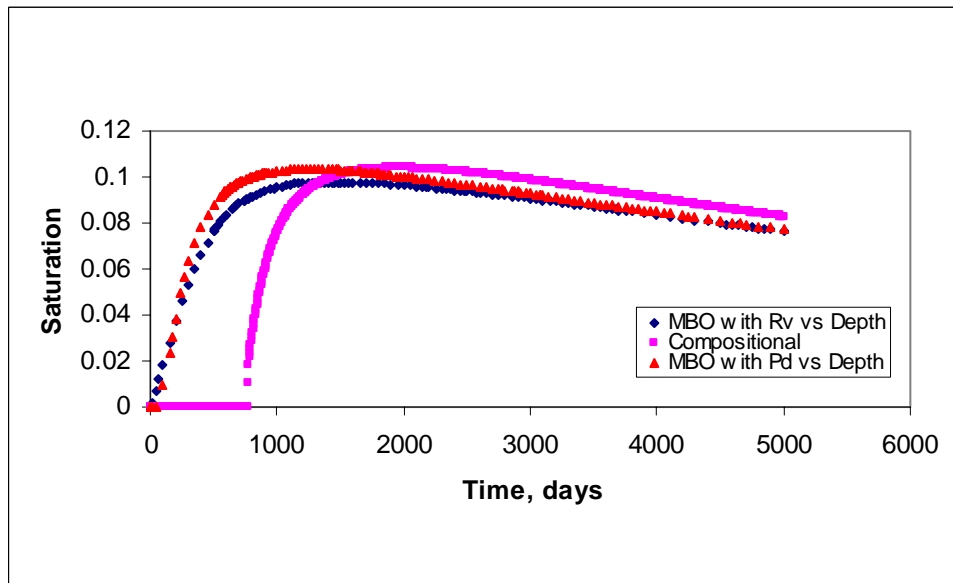


Fig. 4.53 Average oil saturation for gas cycling case

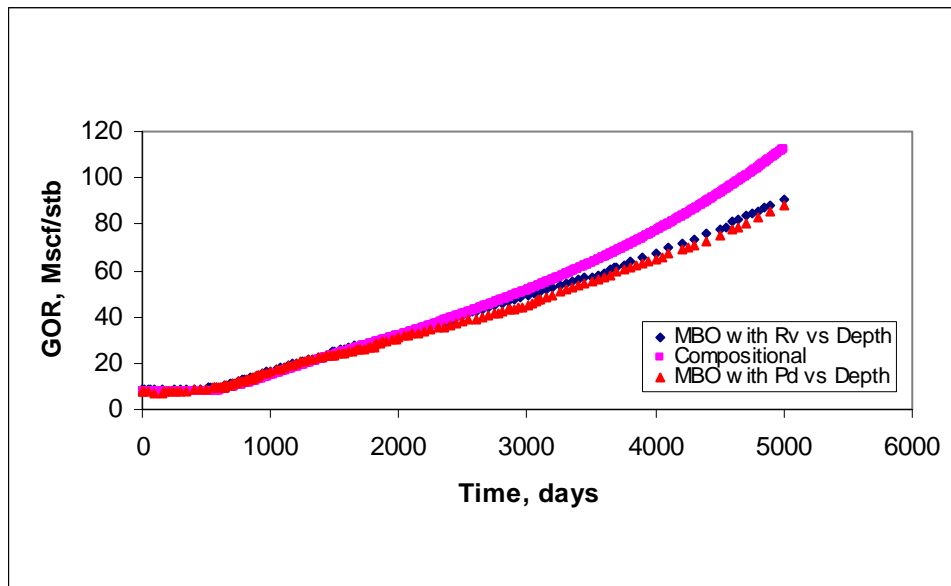


Fig. 4.54 Gas-oil ratio for gas cycling case

The extent of vaporization occurring in both models can be quantified from **Fig. 4.55** through **Fig. 4.57**. The figures represent the condensate distribution around the producer well at different times. From these plots conclusions about the vaporization process and the arrival of displacement front in the whole reservoir could be obtained since the location of the gridblocks give the last point for the displacement front. The third gridblock from the producer for layer nine (23, 23, 9), gives zero condensate saturation at the end of simulation, which is not the case with compositional model. This means excess amount of vaporization takes place up to this point for the whole reservoir in MBO model. Vaporization process in compositional model, around the producer takes place earlier compared to MBO model. The beginning of vaporization for compositional and MBO models are 2,000 and 4,000 days respectively. Since miscibility cannot be represented in MBO, the arrival time of displacement front is longer, which is also different for different initialization methods in MBO model. Also condensate drop-out around the injector well is observed for longer periods of time in compositional model. However, at the end of the total simulation time condensate saturation around the injector well is zero in both models.

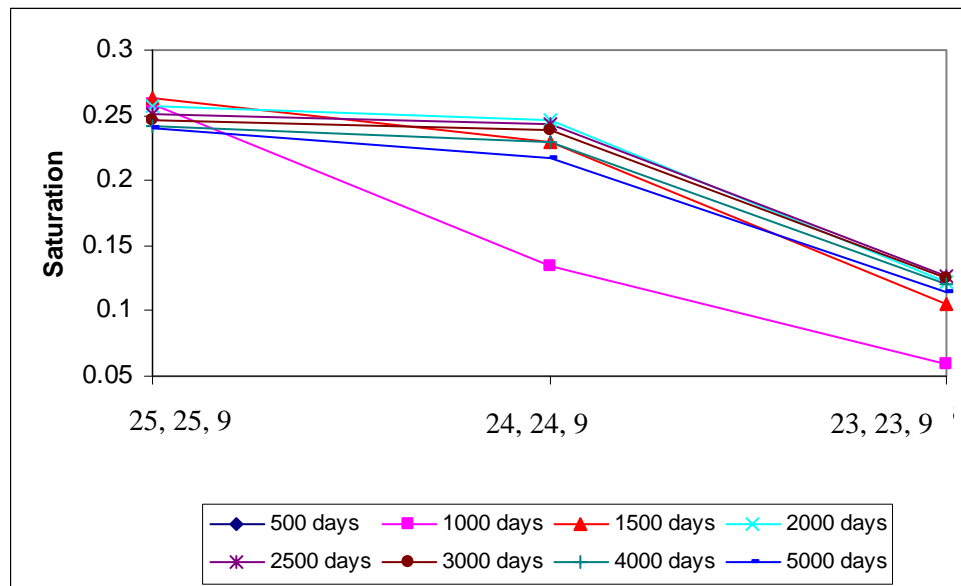


Fig. 4.55 Saturation distribution for compositional model for layer 9, 3 gridblocks from the producer

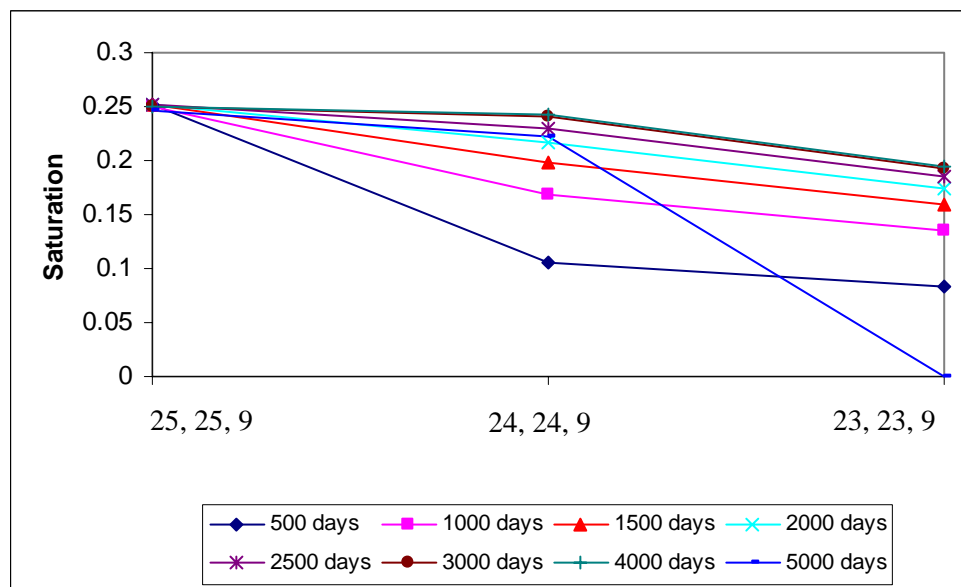


Fig. 4.56 Saturation distribution for MBO model for layer 9, 3 gridblocks from the producer

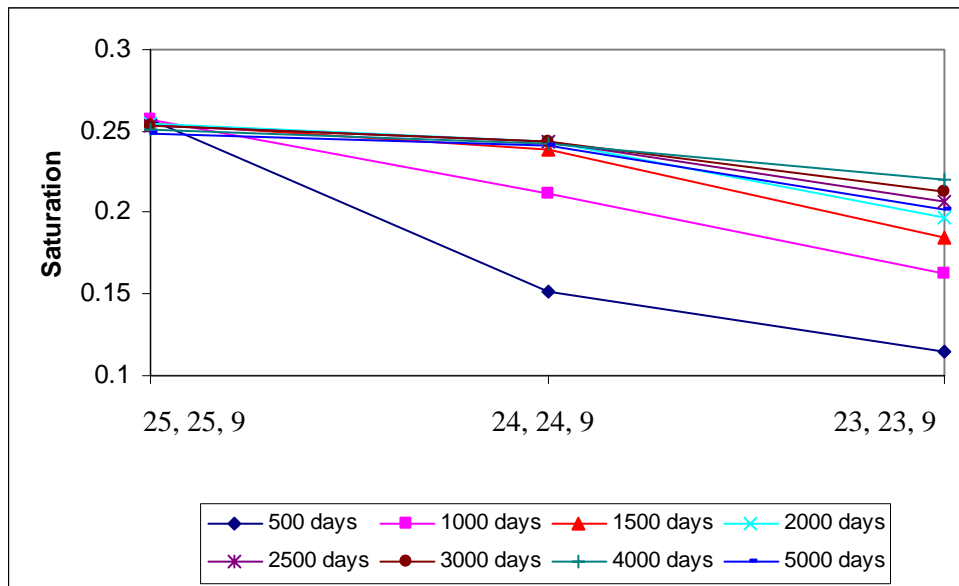


Fig. 4.57 Saturation distribution for MBO model (Pd versus depth initialization) for layer 9, 3 gridblocks from the producer

Fig. 4.58 and **Fig. 4.59** are examples of unrealistic vaporization for gridblocks at the end of layer four and five. The same pattern is observed for the other layers also; more oil saturation is obtained from MBO model but when the displacement front arrives all the oil is vaporized if the communication between the layers are good. The arrival time for the displacement front will be dependent on the distance between the injector and producer and the heterogeneities between them. Also grid orientation effects with different types of grids (rectangular, hexagonal, or irregular) can be observed.

As we can see from the plots this quick revaporization is not observed in compositional model. In compositional model the revaporization process begins with the lighter ends of the oil and proceeds with time slowly.

Fig. 4.60 gives the recovery factors for 5000 days.

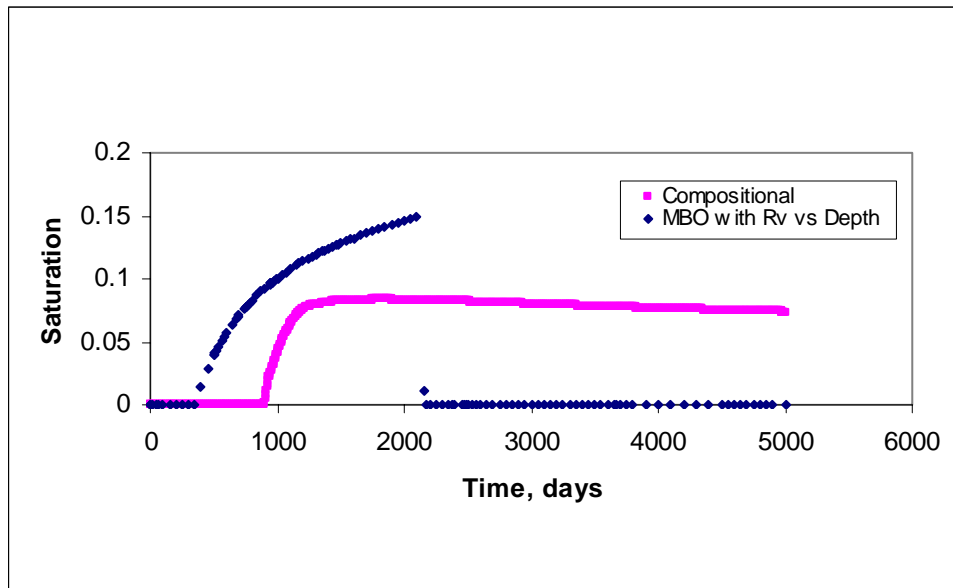


Fig. 4.58 Saturation distribution for MBO model gridblock (25, 25, 4)

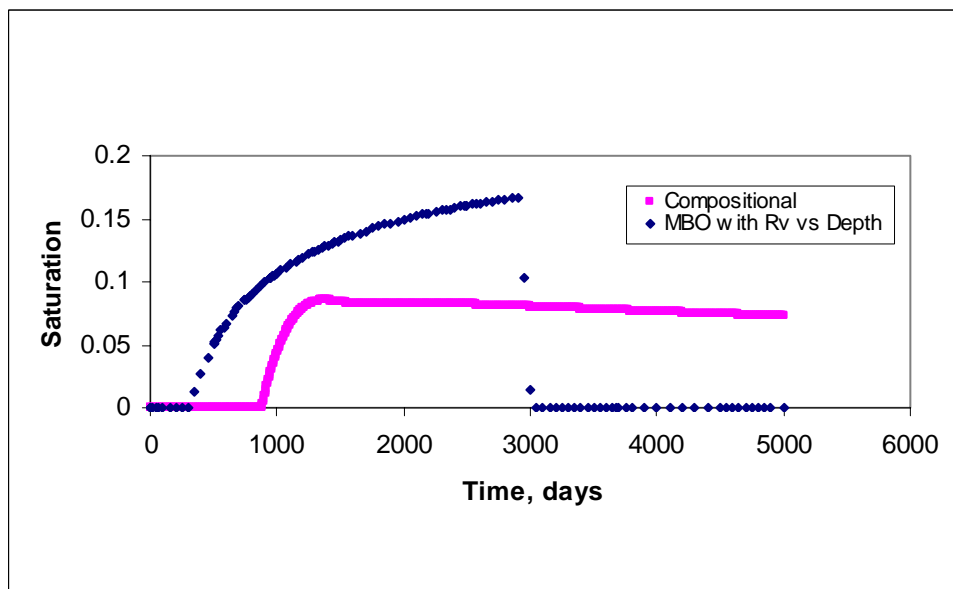


Fig. 4.59 Saturation distribution for MBO model gridblock (25, 25, 5)

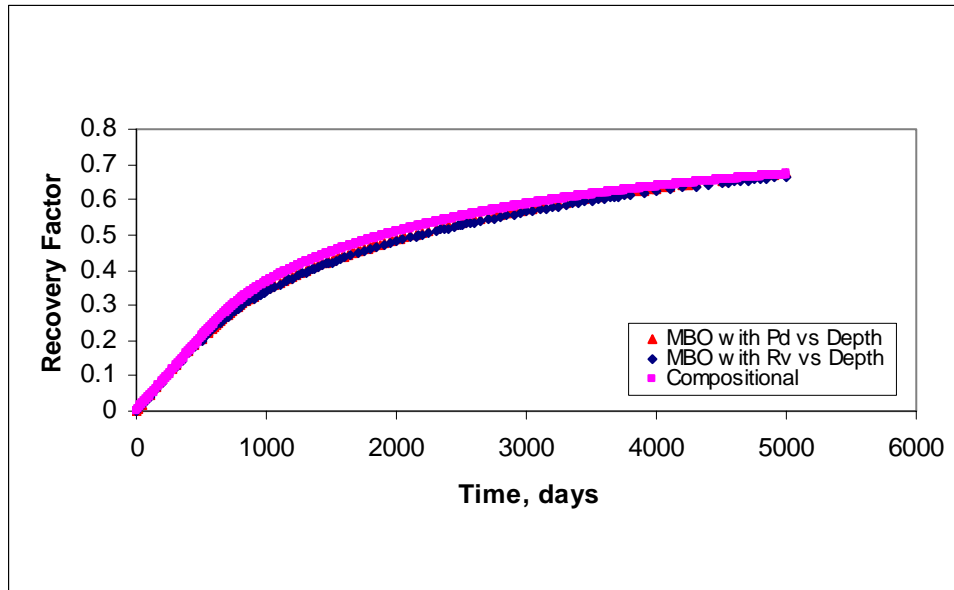


Fig. 4.60 Recovery factor for cycling case

4.2.2 Effect of k_v/k_h Ratio for Gas Cycling

Ratio of 0.0001 was used for k_v/k_h value to minimize the communication between layers. Layer nine; the bottom part of the completion in producer gives zero oil saturation for both models. Along the highly permeable bottom layers, in MBO model, vaporization process is higher than the compositional model.

Production performance of the models is presented in **Fig. 4.61** through **Fig. 4.64**.

Fig. 4.65 and **4.66** show the condensate saturation distribution at the end of the simulation time. For both models layer one and the low permeability thin layers were modeled similarly. The bottom layer in compositional model has higher oil saturation due to differences in vaporization process in two models.

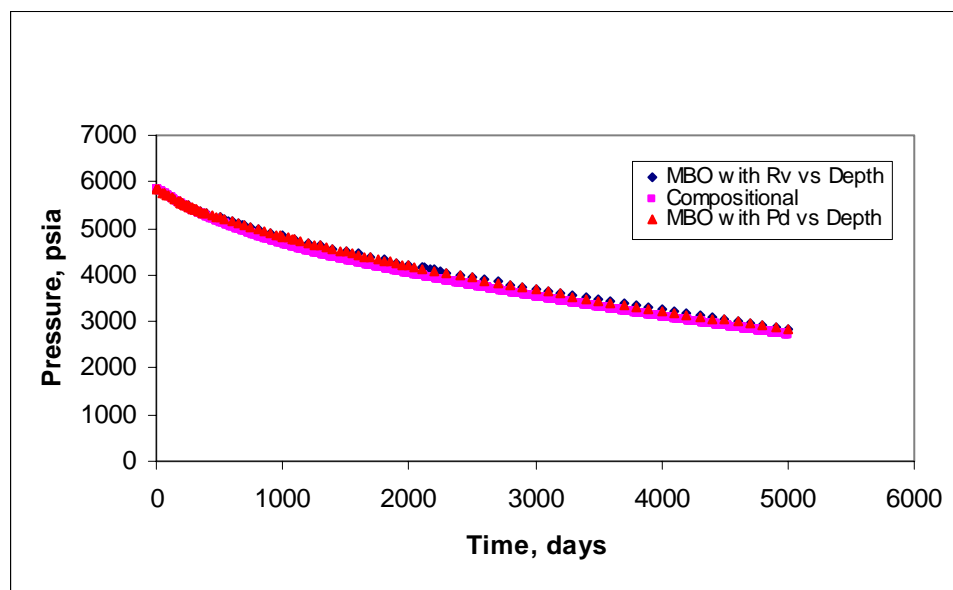


Fig. 4.61 Average field pressure for k_v/k_h ratio of 0.0001

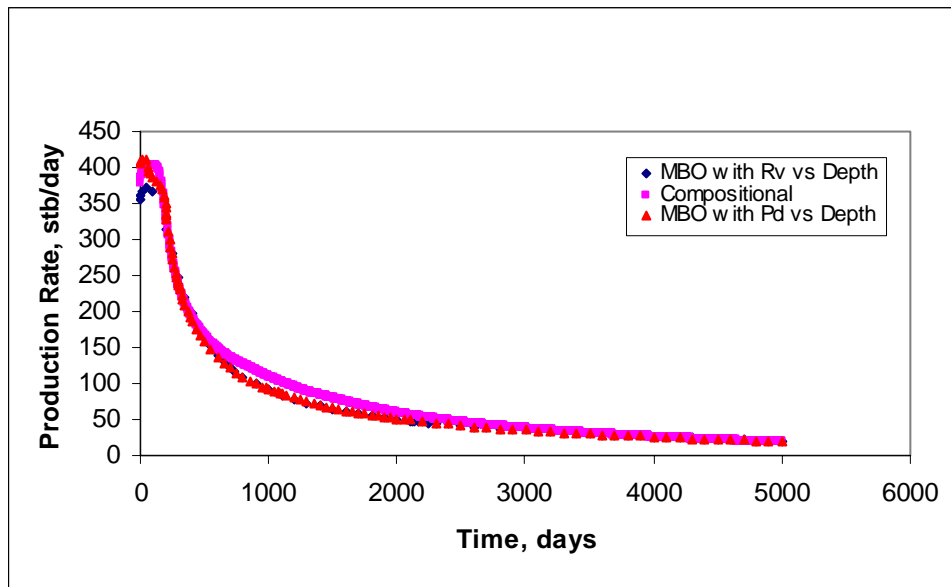


Fig. 4.62 Oil production rate for k_v/k_h ratio of 0.0001

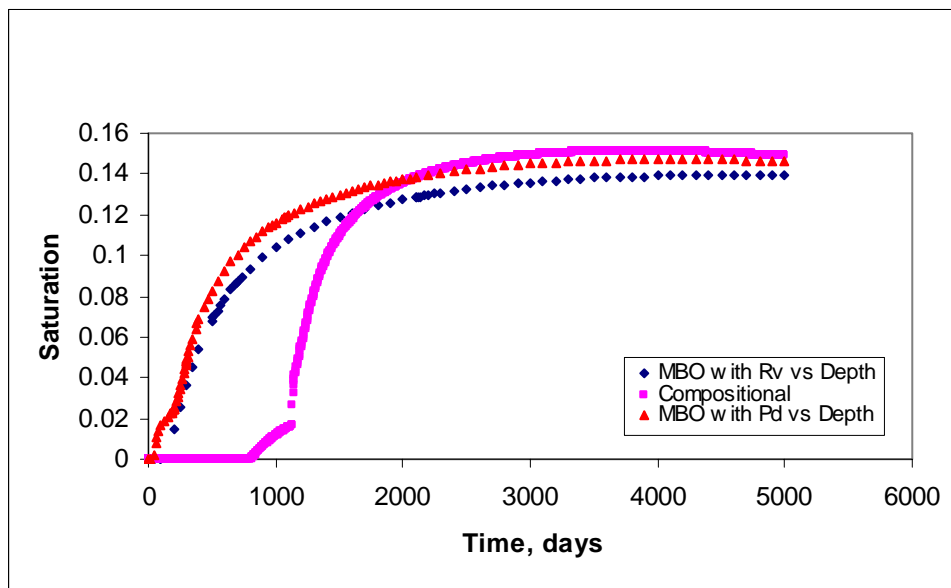


Fig. 4.63 Average field oil saturation for k_v/k_h ratio of 0.0001

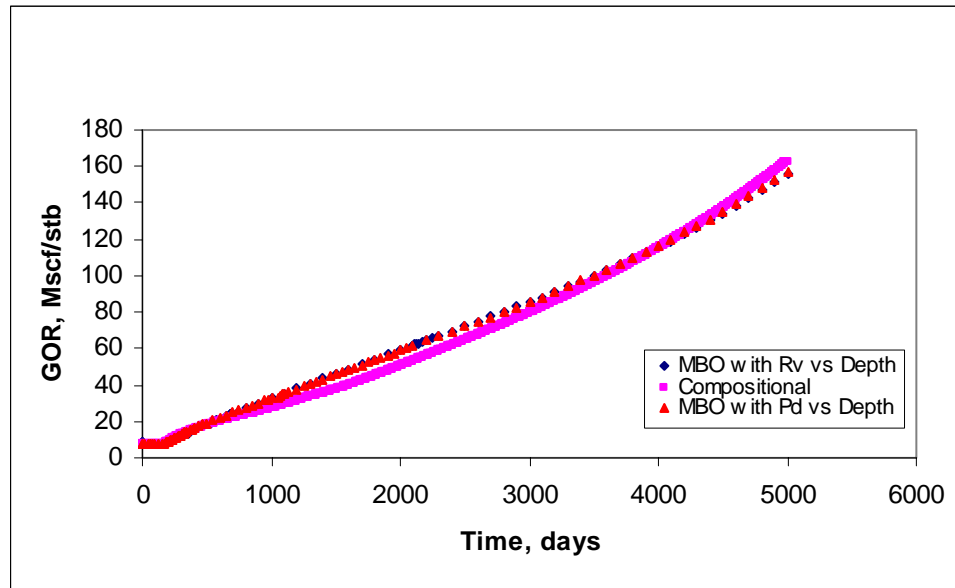


Fig. 4.64 Gas-oil ratio for k_v/k_h ratio of 0.0001

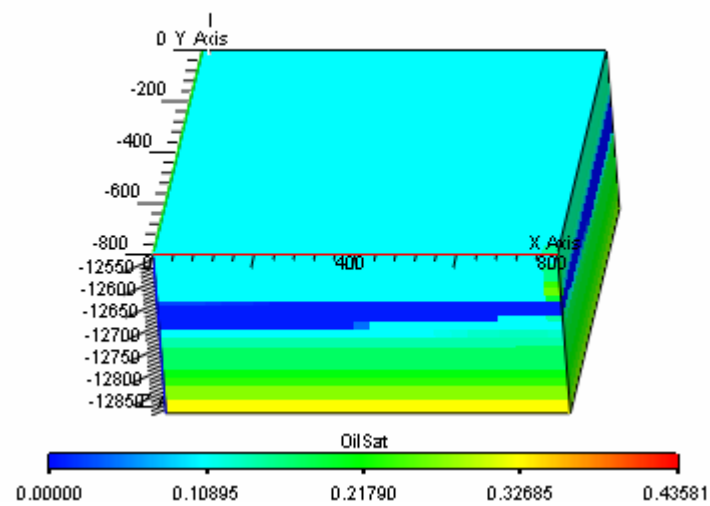


Fig. 4.65 Saturation distribution from compositional model for k_v/k_h ratio of 0.0001 at the end of the simulation

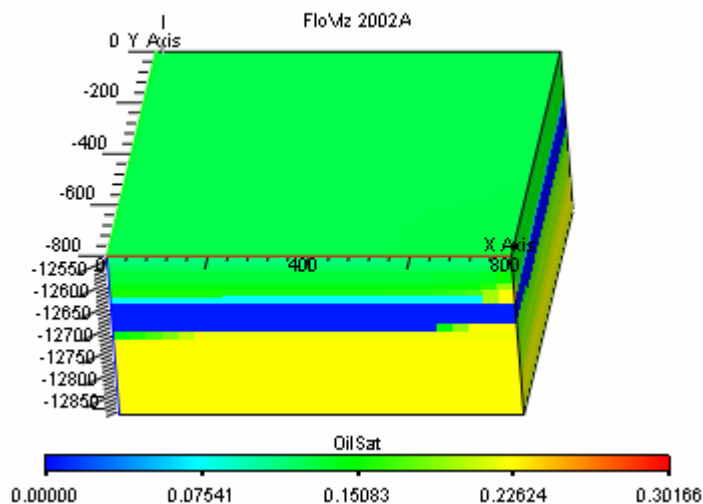


Fig. 4.66 Saturation distribution from MBO model for k_v/k_h ratio of 0.0001 at the end of the simulation

The basic assumption for the MBO system is that dry gas holds hydrocarbon liquid as a single valued-function of pressure. This assumption is essential to the characterization of a gas-condensate reservoir as a two-component system and based on the facts that; liquid condenses from a condensate gas by retrograde condensation when the pressure is reduced isothermally from the dew point, retrograde liquid is picked up or vaporized by dry gas.

The MBO formulation allows dry gas to pick up oil until the gas becomes saturated. This is an optimistic approximation to the actual reservoir behavior.

The liquid content of the gas is designated in **Fig 4.67**.

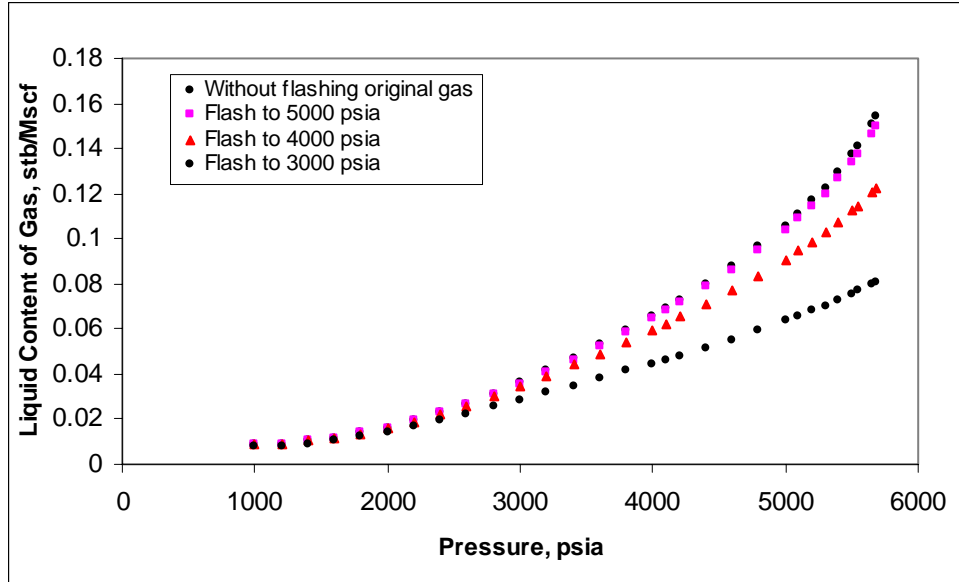


Fig. 4.67 Oil-gas ratio versus pressure generated from different compositions

This plot shows the oil gas ratio, in other words liquid holding tendency for the original gas and for different gas compositions obtained by flashing the original gas. The figure was generated by flashing the original gas to 5,000, 4,000 and 3,000 psia and generating black oil tables for each pressure. In fact, this process represents the changes in oil-gas ratio of the injected gas during the cycling. The oil-gas ratio of injected gas changes continuously. However MBO uses just one set of PVT table, which in turn gives a unique R_v versus pressure values throughout the cycling process.

In the reservoir the first gas injected will vaporize liquid according to the equilibrium liquid content curve. As this gas flows through the reservoir, it will come into contact with either wetter or dryer gas and its liquid content should change accordingly.

At a given pressure if the liquid content of the gas is equal to the value indicated by the equilibrium liquid content curve, it will not be able to vaporize liquid anymore. Without the additional lean gas coming from the bottom layers, the gas in layer one is not able to vaporize condensate accumulated.

Lean gas injected into a saturated reservoir fluid causes the stripping of the light and intermediate components from the reservoir fluid, resulting in an enriched gas phase and a depleted liquid phase.

At a given time and position in the swept zone, the pressure is either above or below its original dew point when the injection gas front arrives. If it is above the dew point a gas-gas miscible displacement will yield 100 % recovery of the current condensate in place. A miscible displacement is guaranteed, independent of the injection gas used, even though the injected gas may be first contact immiscible with the original reservoir gas. Miscibility develops by a simple vaporizing mechanism.

If reservoir pressure is below the dew point when the displacement front arrives, ultimate recovery of condensate is dictated by two processes; gas-gas miscible displacement of the reservoir gas, and partial vaporization of the retrograde condensate. The recovery efficiency of retrograde condensate by vaporization increases gradually as increasing volumes of injection gas sweep this point (**Fig. 4.68**).

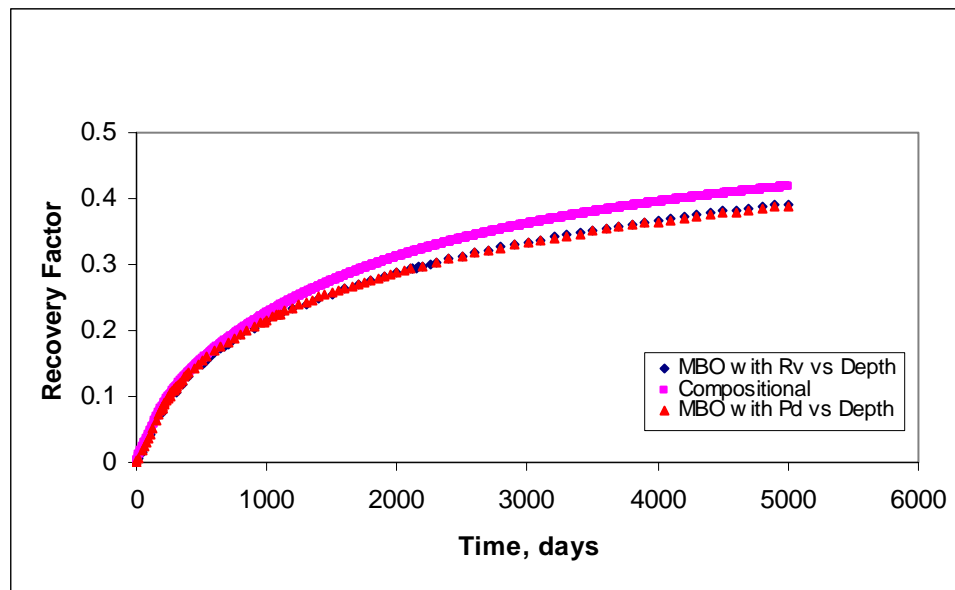


Fig. 4.68 Recovery factor for k_v/k_h ratio of 0.0001

4.2.3 Effect of Production and Injection Rates

This section will mainly focus on the investigation of low rate effects on both models. Since the injected gas amount is the fraction of the produced gas, injection rate will go down with a reduction in production rate. Production and injection rates of 1,000 and 750 Mscf/day were used. With the low rates, compositional effects will become more important since more condensate drops out before the gas-gas miscible displacement takes place. Consequently revaporization of retrograde condensate will also come into play as a recovery process with lower production as injection rates.

The difference between MBO and compositional models vanish as the reservoir is depleted with higher gas rates. However it is observed that there exists a maximum rate above which the performance of models does not get any closer.

For a gas condensate reservoir, with high production and injection rates, rich reservoir gas can be produced by a gas-gas miscible displacement before a significant liquid drop-out takes place and even if these rates are increased, the gas-gas miscible displacement will not improve any further and the amount of condensate in the reservoir will not change. So the match between the models will remain the same after that limit production and injection rates are reached.

MBO model gives a better representation of oil production rate and gas-oil ratio when it is initialized with R_v versus depth table. Oil production rate plot exhibits different performances for both models especially between 1,800 and 3,000 days.

This difference has also been reflected in gas-oil ratio values. Around 1800 days average condensate saturation in MBO model is about to reach its maximum value. This makes the oil production rates go down.

At 2400 days in MBO model, condensate saturation around the wellbore exceeds critical saturation, becomes mobile and flows. This changes the trend in decline for oil production rate. The first liquid drop-out in compositional model is observed around 1,900 days in the bottom layer. For the compositional model the condensate around the wellbore begins to flow around 3,000 days. After 3,000 days the models begin to produce the same amount of oil. The mobility of the condensate around the wellbore makes the differences get smaller. At 4,000 days condensate saturation in compositional model reaches its maximum value and the performance of the models depart slightly again.

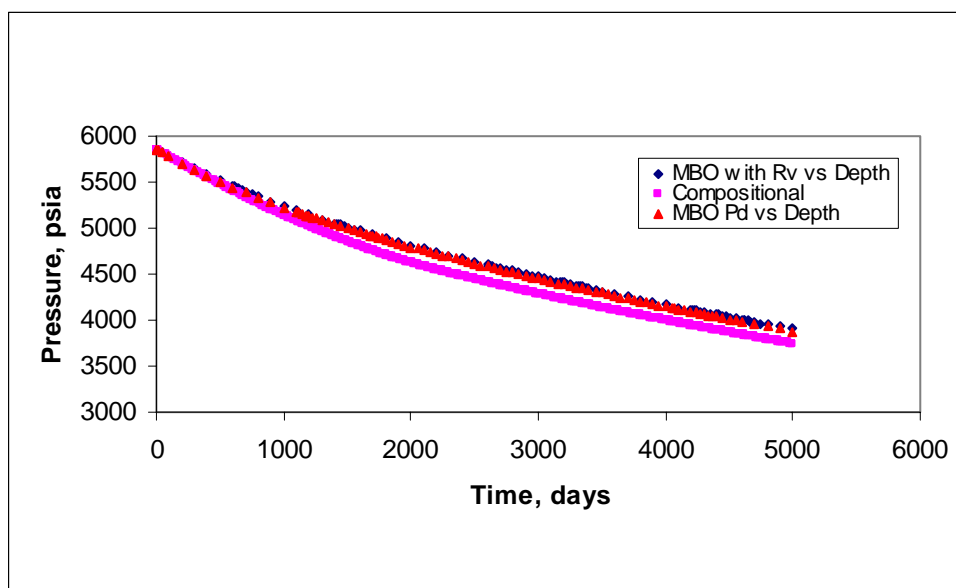


Fig. 4.69 Average reservoir pressure for low production and injection rates

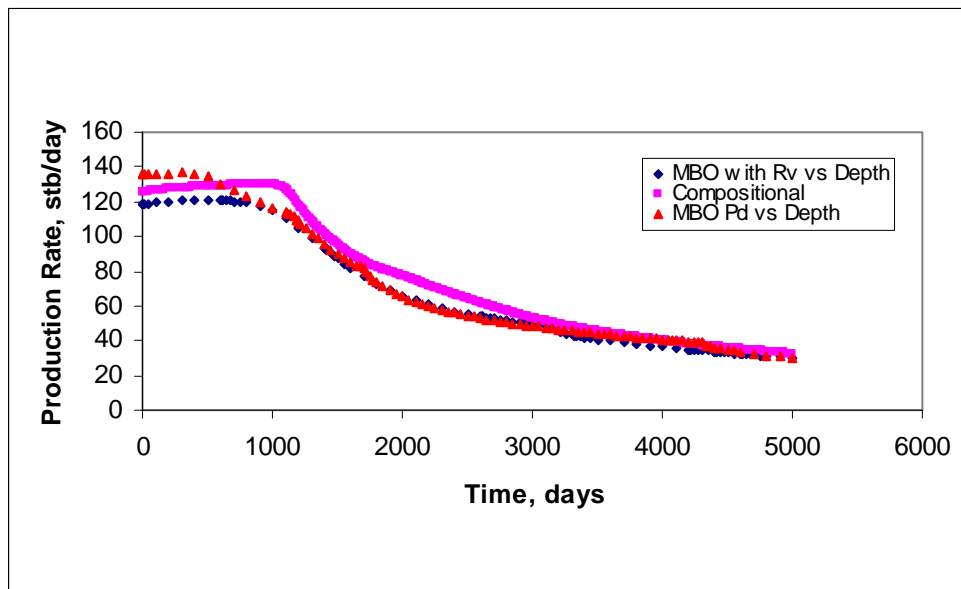


Fig. 4.70 Oil production rate for low production and injection rates

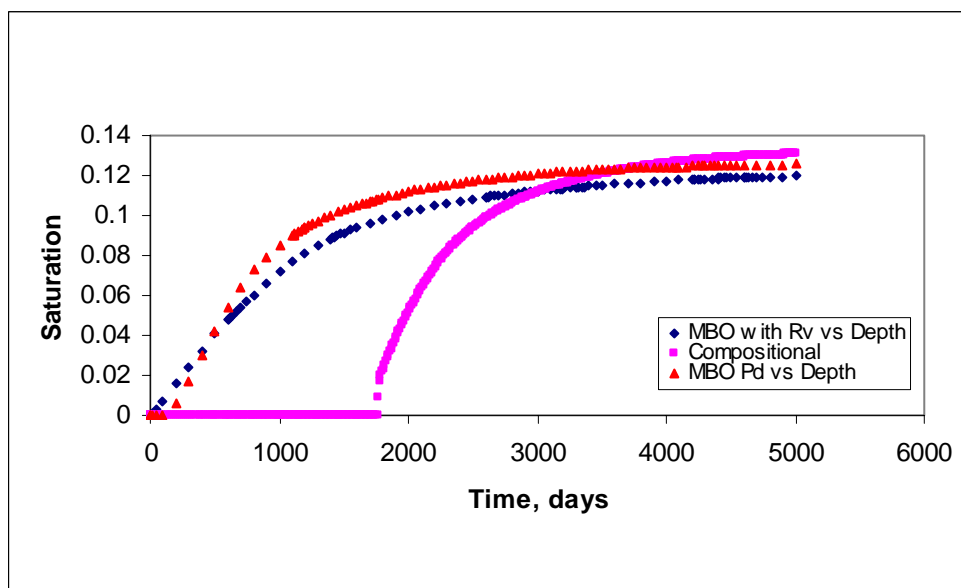


Fig. 4.71 Average oil saturation for low production and injection rates

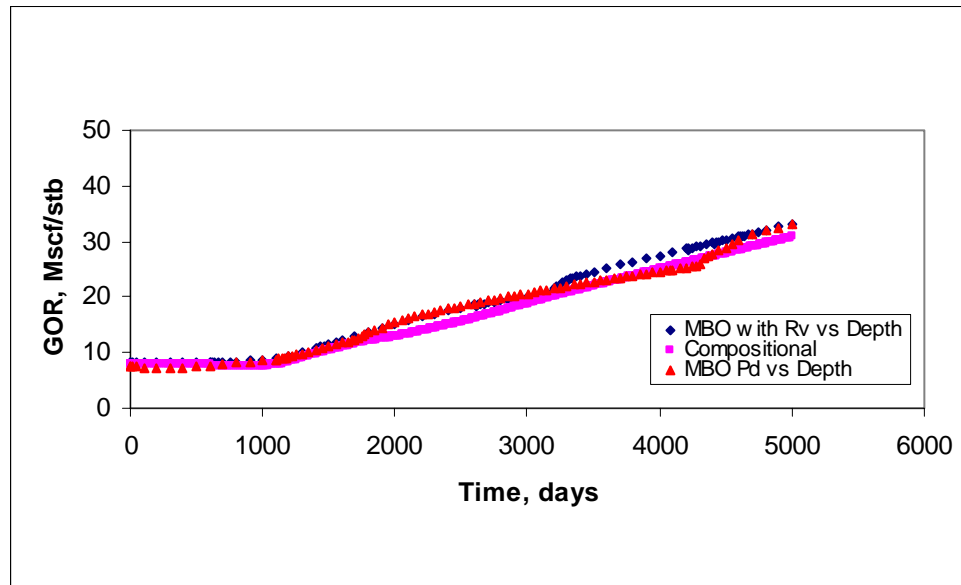


Fig. 4.72 Gas-oil ratio for low production and injection rates

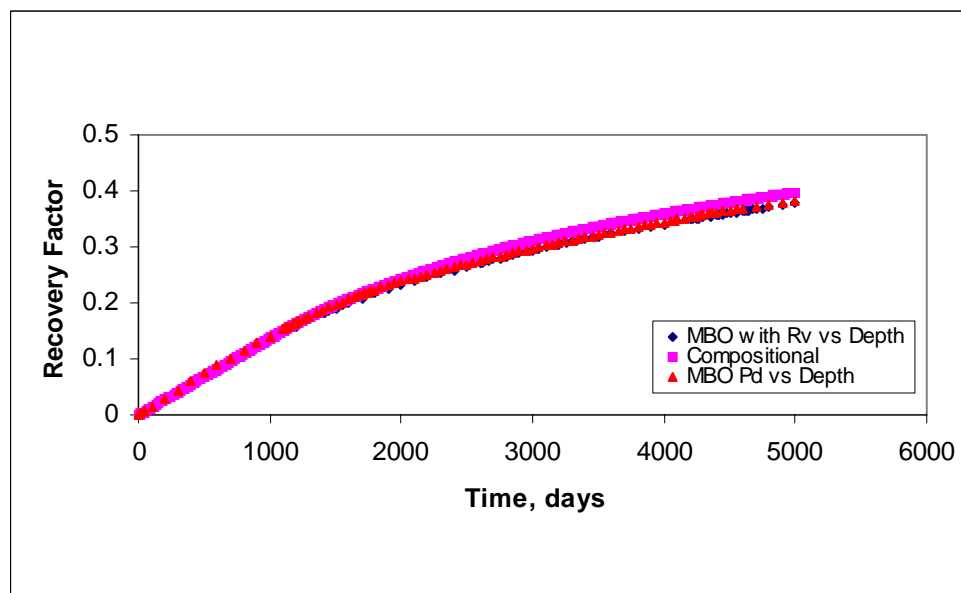


Fig. 4.73 Recovery factor for low production and injection rates

4.2.4 Effect of Completion

To investigate the effects of completion interval on the performance of models, initially the producer and injector were completed at the bottom part of the reservoir, which is layers 10 to 18, and later on the wells were completed at the top of the reservoir from layer 1 to 9.

The pressure distribution for compositional and black-oil models for the two cases mentioned above is very similar as can be seen in **Figs. 4.74** and **4.75**.

The mole fraction of the lighter components decreases with depth, while the mole fraction of the heavy components increases from the top to the bottom of the reservoir.

If the wells are completed at the bottom part of the reservoir, the production performance of the models differs from each other (**Fig. 4.76**, **Fig. 4.80**, **Fig. 4.82**) and if the completion location is in the region of lighter components the models exhibit similar production performances (**Fig. 4.77**, **Fig. 4.81**, **Fig. 4.83**).

In other words richest part of the gas is located at the bottom of the reservoir due to gravitational forces. When considering gas injection, one must be aware that the compositional effects, such as development of miscibility changes with depth. Also miscibility cannot be represented with black-oil models. More discrepancies are expected in the regions where highly miscible processes take place i.e. around the bottom completions.

In MBO model liquid content of the gas at the bottom of the reservoir is higher and this liquid holding capacity is a function of pressure.

Figs. 4.78 and **4.79** give field wide oil saturation distribution for two different completion strategies. When the bottom layers are completed initialization method can

make a big difference in results. For the particular fluid used in this study bottom layer completion resulted in high amounts of condensate accumulation initially in MBO and an unrealistic vaporization of all the condensed oil until the saturation becomes to the level given by compositional model.

The larger vaporization forms a richer gas phase flowing towards wellbore in black-oil model compared to the compositional model. This process is represented by higher gas-oil ratios in compositional model and higher oil production rates in modified black-oil model.

Higher recovery factors are obtained with the bottom completions. The deviation in the recovery of models starting from 1000 days with the bottom completions disappear as the excess condensate drop-out is vaporized.

Only 2 % deviation between compositional and MBO models is observed in recovery factors with the model completed in the upper layers. No difference observed for the bottom completion since less condensate is left in the bottom layers compared to the upper completion case in both models.

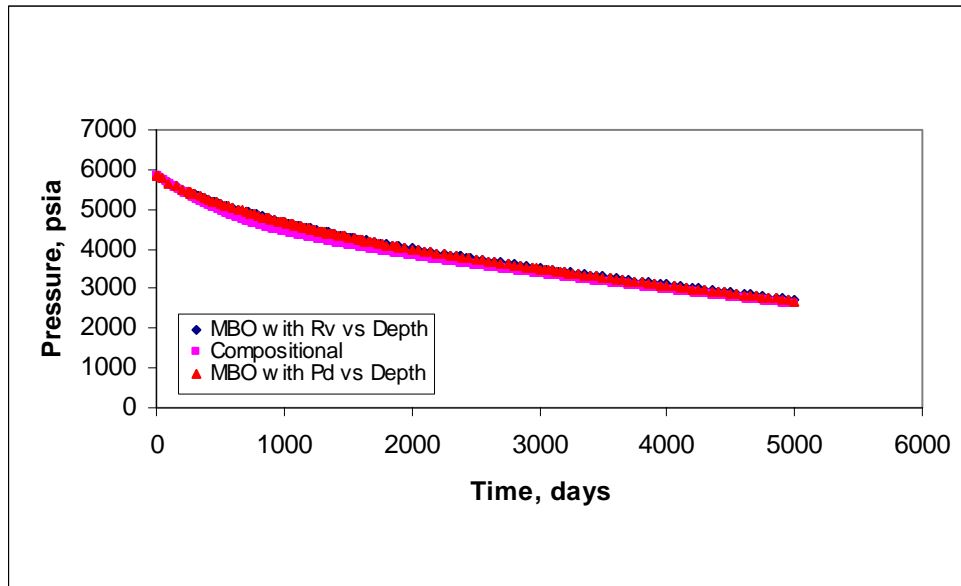


Fig. 4.74 Average field pressure with wells completed at the bottom of the model

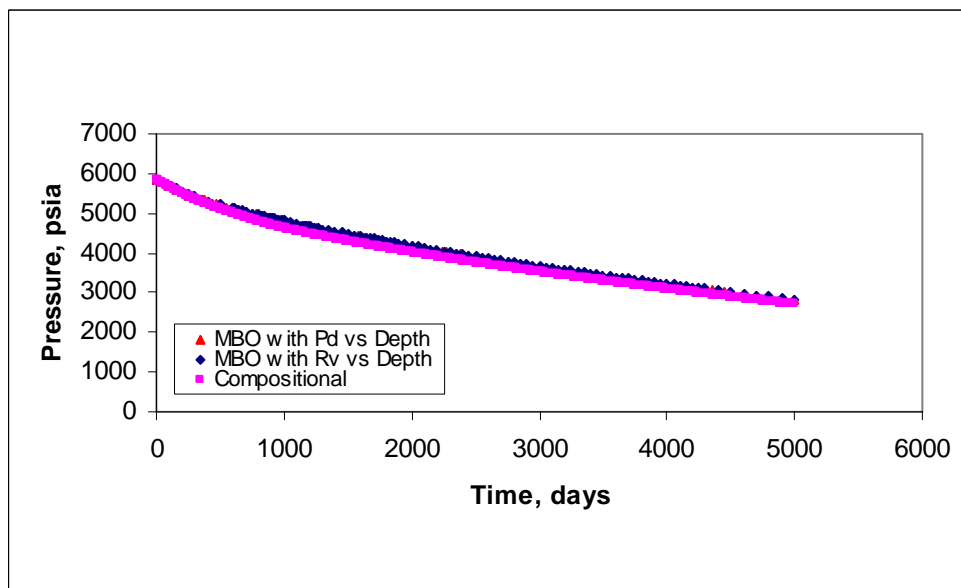


Fig. 4.75 Average field pressure with wells completed at the top of the model

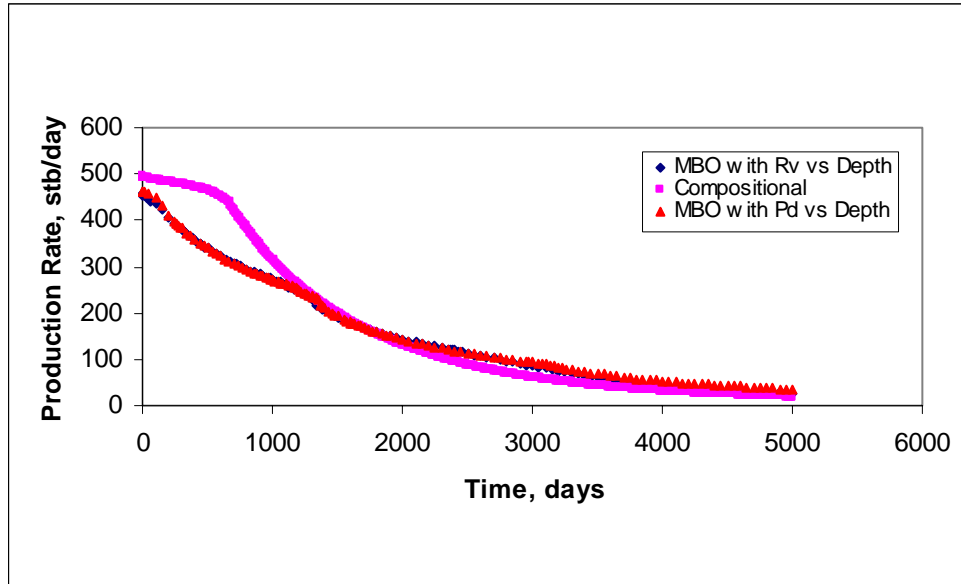


Fig. 4.76 Oil production rate with wells completed at the bottom of the model

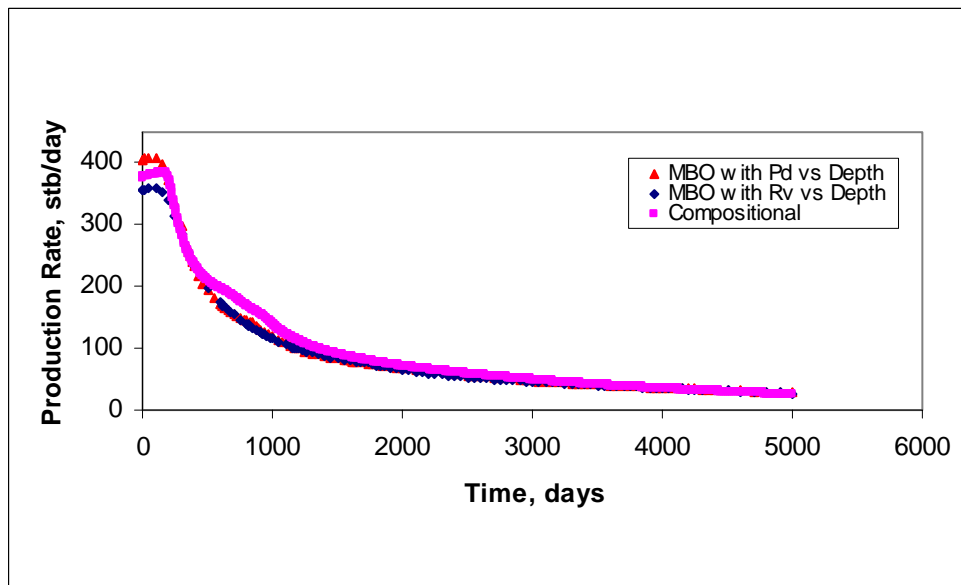


Fig. 4.77 Oil production rate with wells completed at the top of the

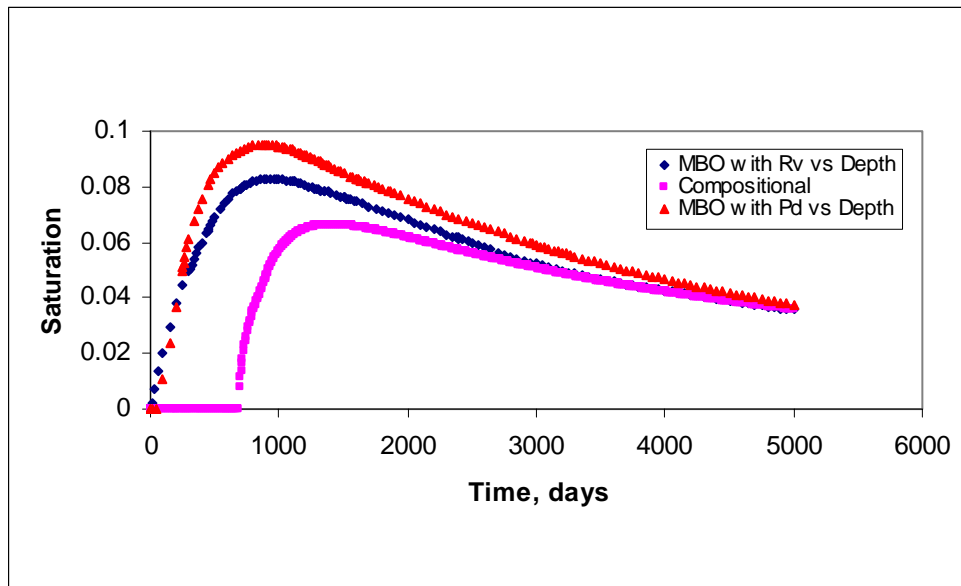


Fig. 4.78 Average oil saturation with wells completed at the bottom of the model

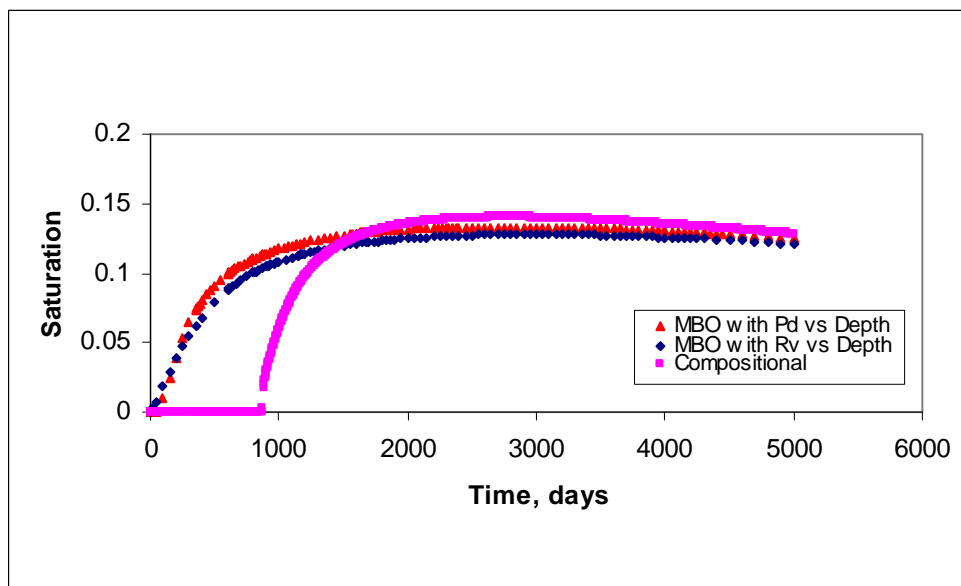


Fig. 4.79 Average oil saturation with wells completed at the top of the model

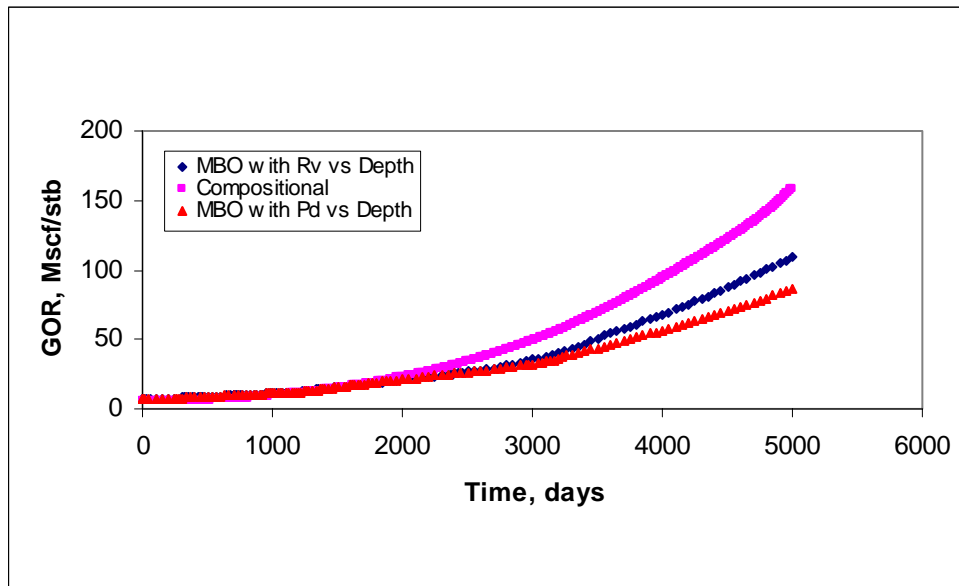


Fig. 4.80 Gas-oil ratio with wells completed at the bottom of the model

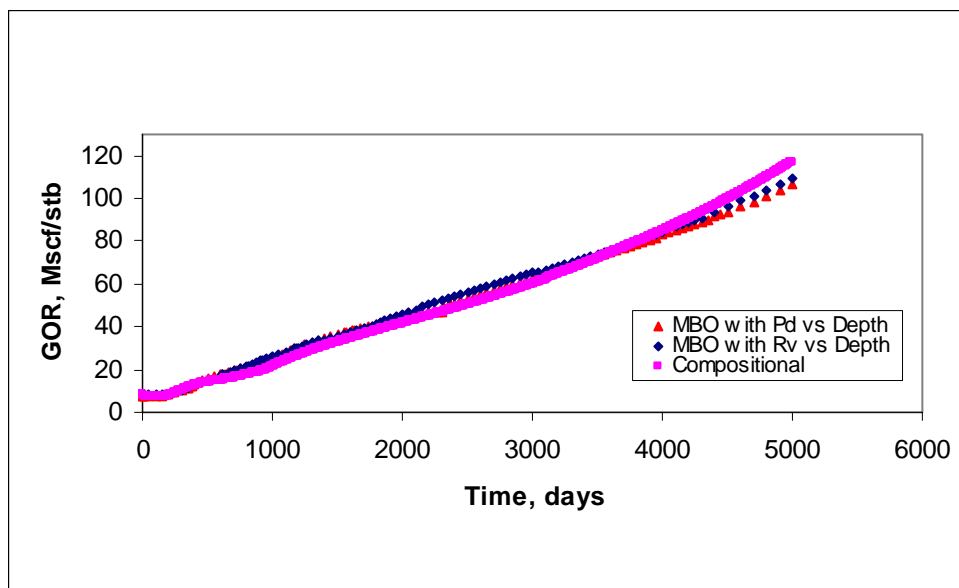


Fig. 4.81 Gas-oil ratio with wells completed at the top of the model

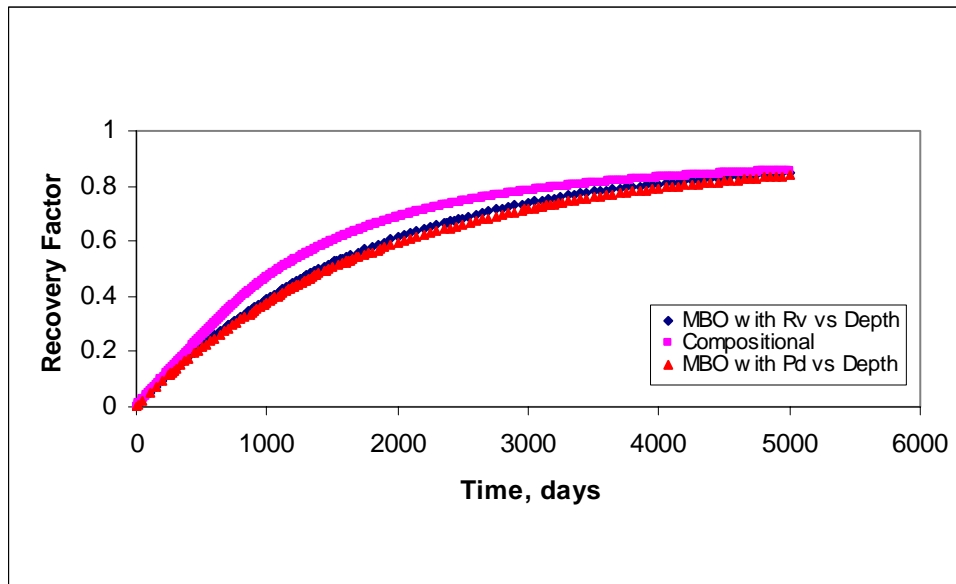


Fig. 4.82 Recovery factor with wells completed at the bottom of the model

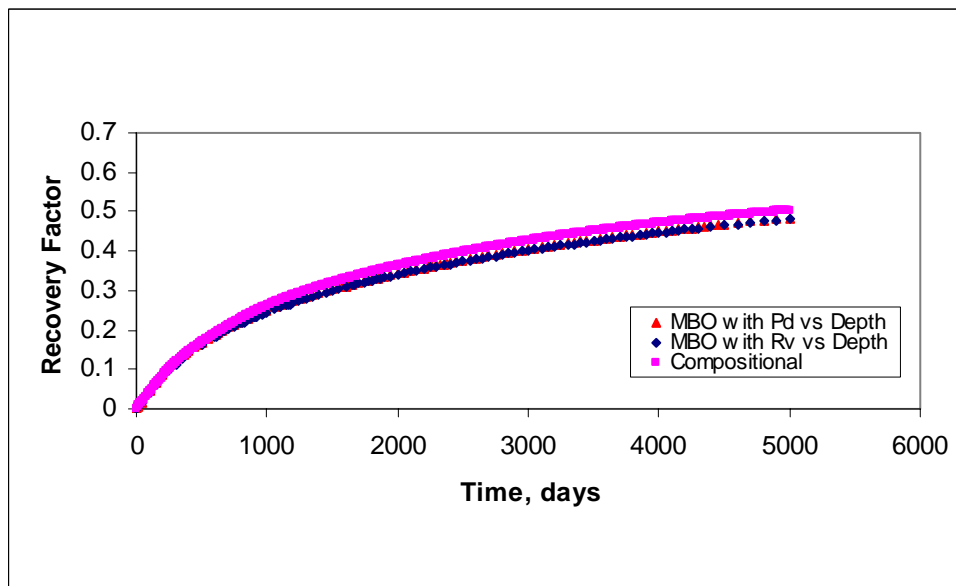


Fig. 4.83 Recovery factor with wells completed at the top of the model

4.3 Horizontal Wells

4.3.1 Natural Depletion

In this part of the study, the effects of horizontal wells on the performance of MBO model for the rich gas condensate reservoir have been investigated. The lower drawdown pressure for horizontal well, compared to the vertical well, for the same flow rate, considerably reduces retrograde condensation.³¹ Therefore, there is less condensate deposited near the horizontal wellbore. This means lesser liquid drop-out and smaller amounts of vaporization for MBO model, which in turn makes the models give similar performances.

Layers with higher kh values contain the higher amounts liquid accumulations. To study the effect of kh values, more heterogeneous reservoir model with lower permeability values was used. **Table 4.14** gives the permeability values.

Table 4.14 Layer thickness, porosity and permeability values for model with horizontal well

Layer	Thickness	Porosity	Permeability (md)
1	20	0.087	0.1
2	15	0.097	0.2
3	26	0.111	0.3
4	15	0.16	0.2
5	16	0.13	7
6	14	0.17	0.1
7	8	0.17	14
8	8	0.08	2
9	18	0.14	12
10	12	0.13	3
11	19	0.12	10
12	18	0.105	9
13	20	0.12	0.1
14	50	0.116	0.3
15	20	0.157	0.2
16	20	0.157	0.2
17	30	0.157	0.2
18	30	0.157	0.2

Horizontal well was placed in layer 9, which has the highest kh value to maximize the differences between two models. To observe the effects of different well placements in relation to increasing heavy component fraction with depth, runs with horizontal well placed in layer 3 and 16 was also simulated. In natural depletion case production rate was selected as 3000 Mscf/day. Models were run with two different drain hole lengths, 352 and 640 ft. Dehane and Tiab³¹ compared the productivity of the horizontal and vertical wells for a gas condensate reservoir. According to their results the productivity of the horizontal well outperforms the productivity of the vertical well and drain hole length is the most important criteria for the productivity of a horizontal well. Longer drain hole causes a lower drawdown and less condensation around the wellbore, which may be an important factor in duplicating the fully compositional model performance with MBO model. The MBO model was initialized with solution oil-gas ratio versus depth tables. When the well was completed in layer 9 with and without compositional gradient, two models exhibited exactly the same performance as vertical wells regardless of the drain hole length used. Also the reduction in vertical communication had the same effect as vertical wells and the match between two models improved in the same way.

In comparison with the runs that had horizontal well completed in upper and bottom layers, it can be concluded that MBO model performance with horizontal well approaches to the compositional model performance if the well is placed closer to the area where fluid sample is coming from, even if the sample is coming from the bottom part of the reservoir. If the well is placed in the upper layers also a good match can be obtained since the gas becomes heavier with increasing depth.

The short-lived error in saturation pressure versus depth was also observed with horizontal wells. However, it was seen that the error in change of dew point pressure with depth is less effective if the well is completed in the bottom or top of the reservoir with horizontal wells because of above-mentioned effects.

Figs. 4.84 through 4.86 shows the performance of models when the horizontal well is placed in the upper layer (layer 3).

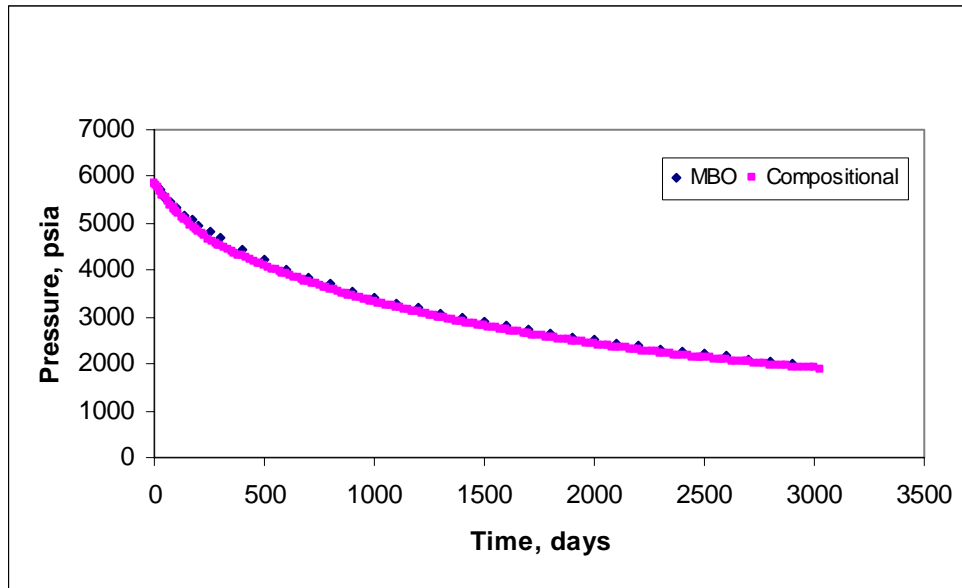


Fig. 4.84 Average field pressure with horizontal well in layer 3

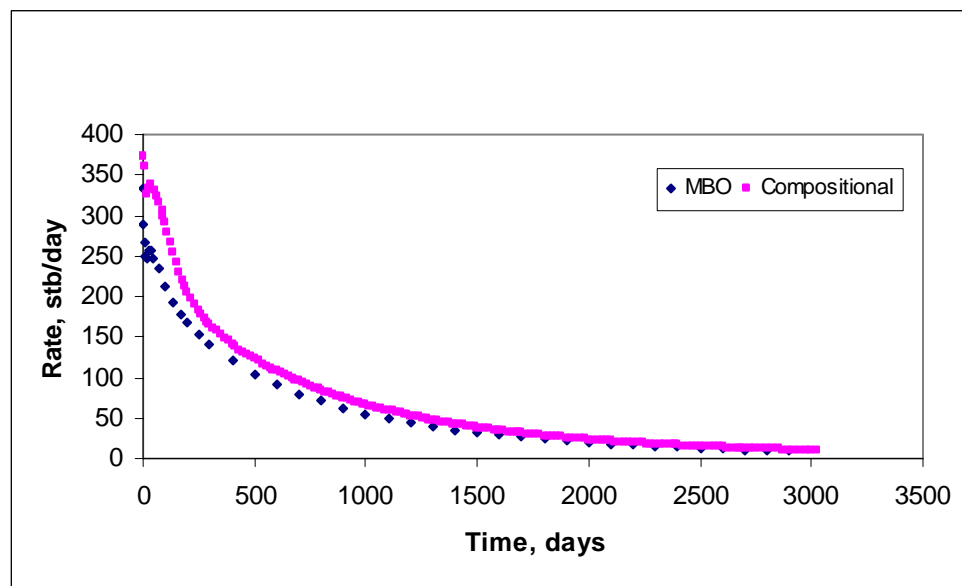


Fig. 4.85 Oil production rate with horizontal well in layer 3

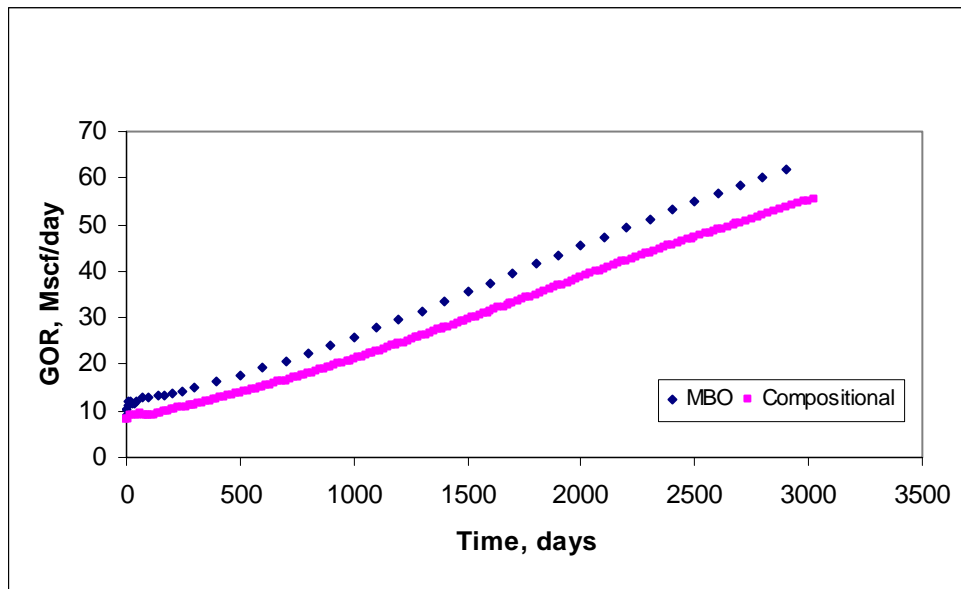


Fig. 4.86 Gas-oil ratio with horizontal well in layer 3

Figs. 4.87 and **4.88** represent oil production rate and gas-oil ratios for the horizontal well placed closer to the bottom layer (layer 16). Notice that for both bottom and upper layer well placements, gas-oil ratios can be represented better with vertical wells compared to horizontal wells in MBO model.

Fig. 4.89 shows the oil production rate for the same layer completed with a longer drain hole length of 640 ft. This plot shows that with a longer horizontal well, the initial effect of error in saturation pressure with depth can be reduced. This behavior can be attributed to the reduced drawdown when the longer drain hole is used. The condensate accumulation around the well bore is reduced and a better representation of fully compositional model was obtained. Notice that the comparison with gas-oil ratios could not be improved with length of the horizontal well. **Fig. 4.90** and **Fig. 4.91** show the average oil saturation and recovery factors.

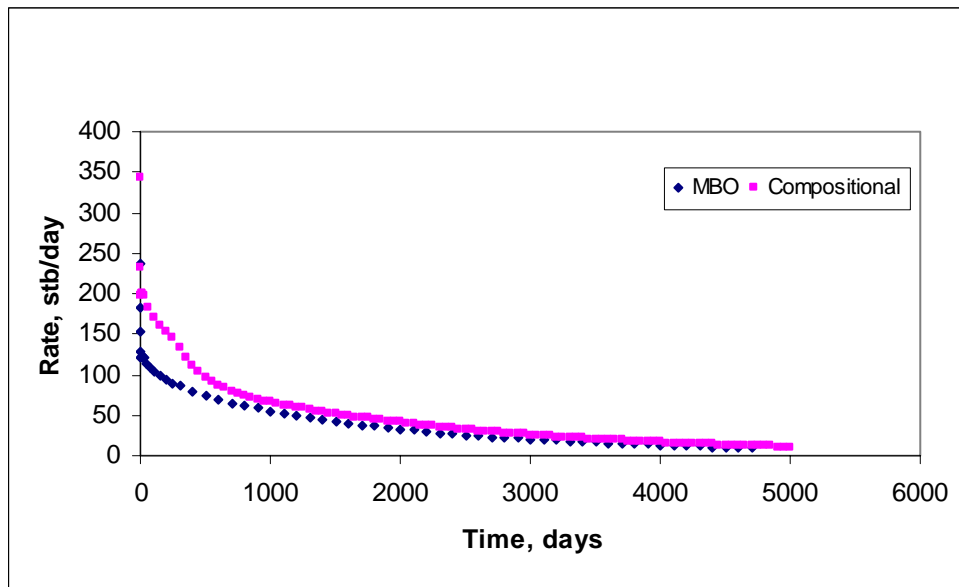


Fig. 4.87 Oil production rate with horizontal well in layer 16

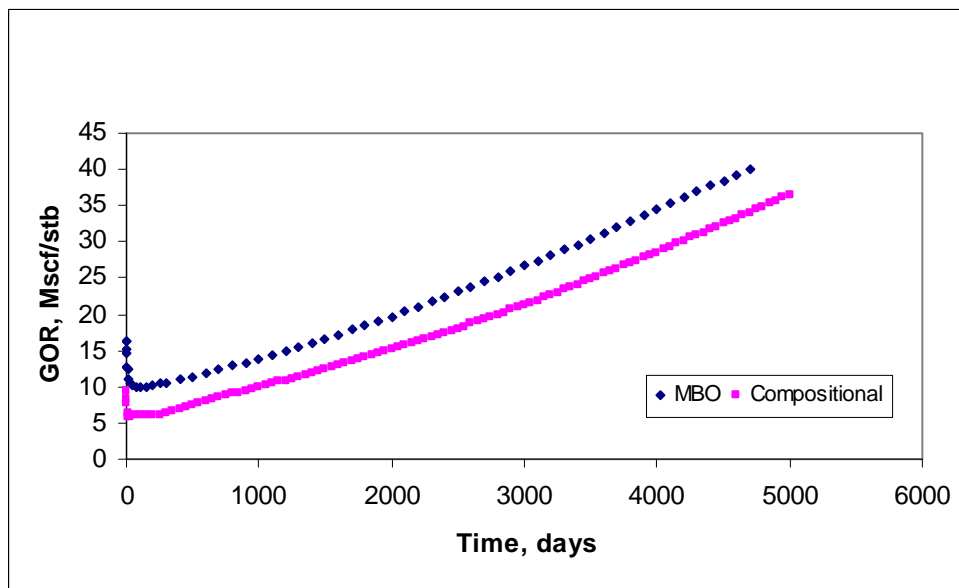


Fig. 4.88 Gas-oil ratio with horizontal well in layer 16

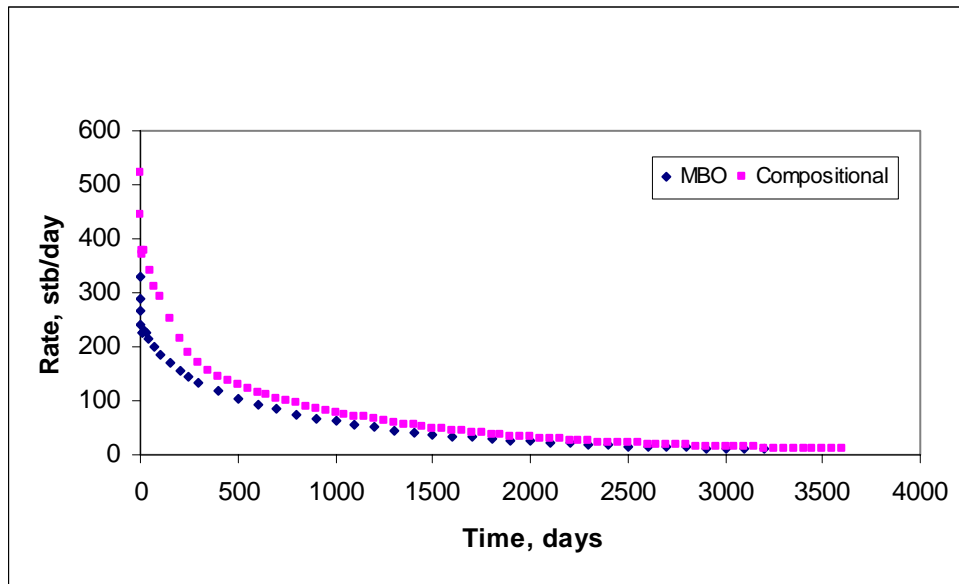


Fig. 4.89 Oil production rate with horizontal well in layer 16 with longer drain hole

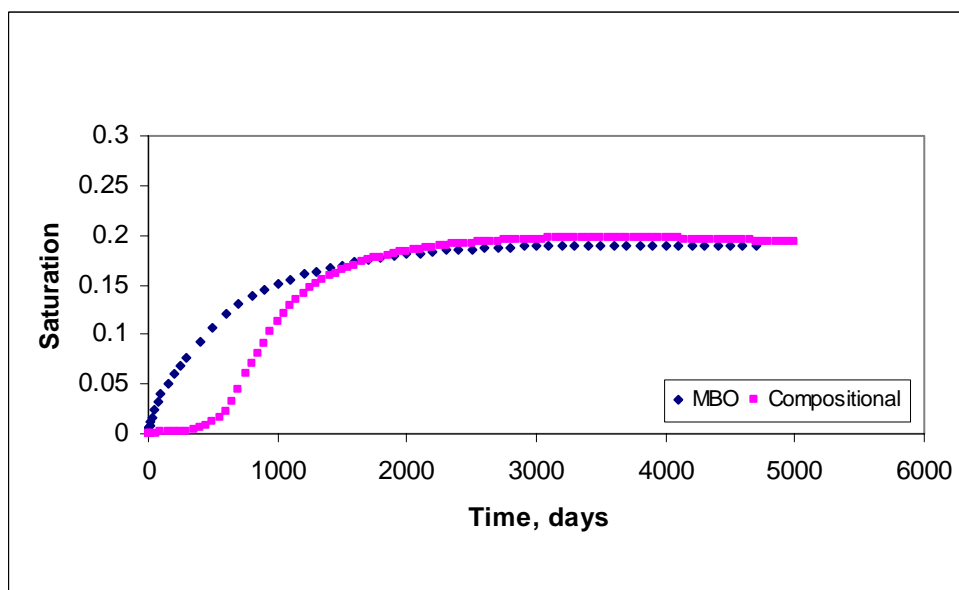


Fig. 4.90 Average oil saturation for horizontal well in layer 16

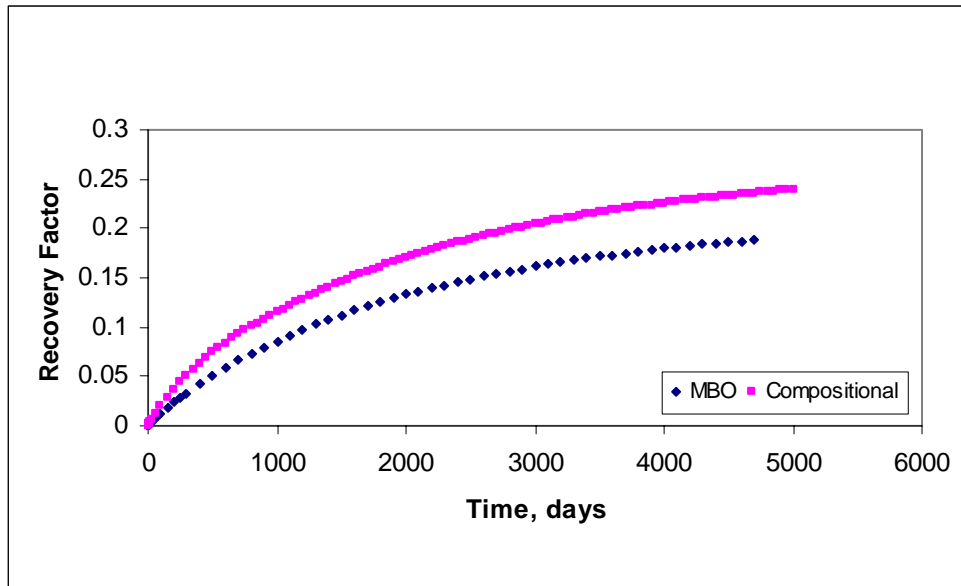


Fig. 4.91 Recovery factor for horizontal well in layer 16

4.3.2 Gas Cycling

Figs. 4.92 through **4.94** give the performance comparison of compositional and MBO models for the gas cycling. Horizontal well was placed in layer 9 and the drain hole length was chosen as 352 ft. Injection was accomplished by using a vertical well completed from layer 10 to 18. With the horizontal well, error in dew point pressure versus depth is almost eliminated for the gas cycling case and a good agreement between the models has been obtained compared to the vertical wells.

The CPU times for MBO model and compositional model are 188 and 2469 seconds respectively. **Figs. 4.95** through **4.97** represent the performances without the full pressure maintenance. The production and injection rates were 1000 and 750 Mscf/day for these plots. The small rates were chosen to minimize gas-gas miscible displacement and consequently, maximize the differences that may occur between the models.

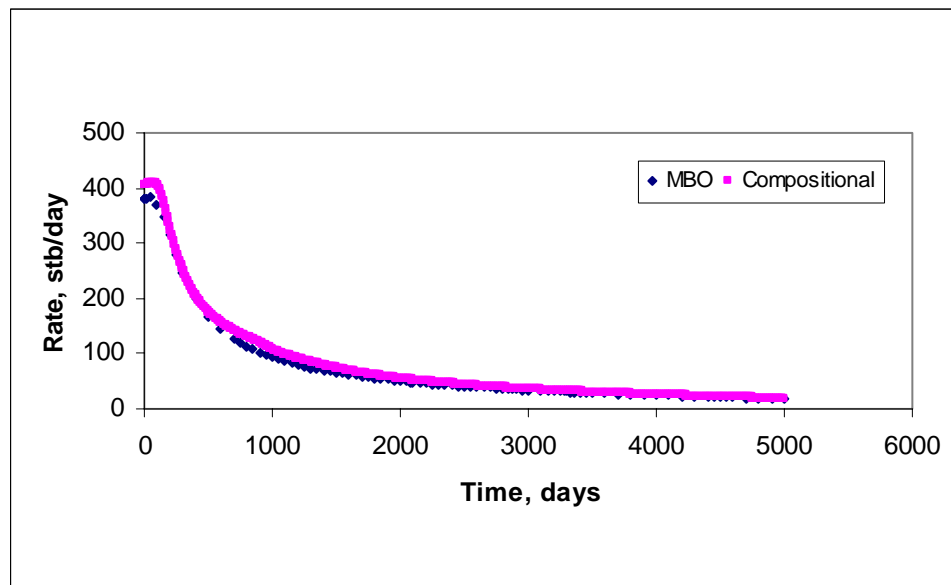


Fig. 4.92 Oil production rate for gas cycling with horizontal well

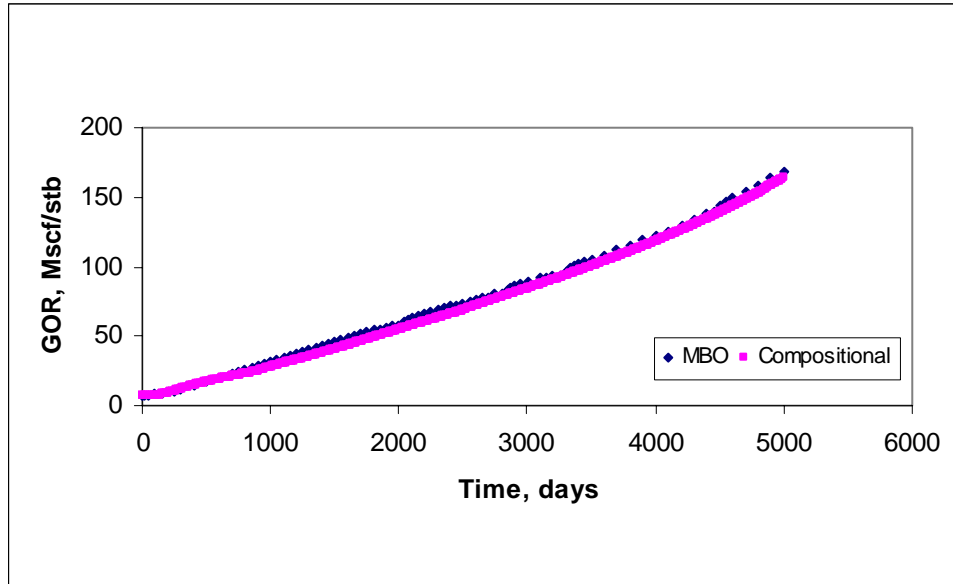


Fig. 4.93 Gas-oil ratio for gas cycling with horizontal well

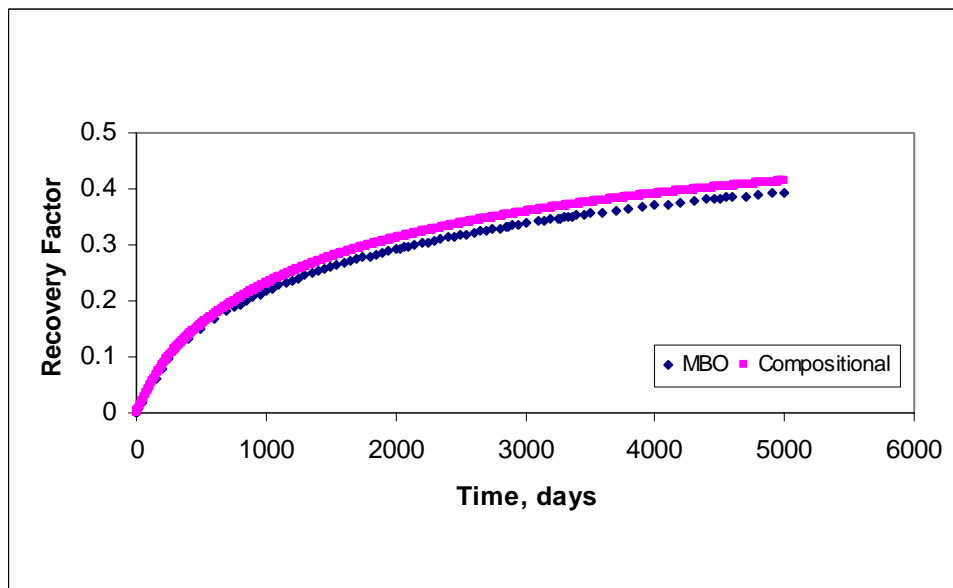


Fig. 4.94 Recovery factor for gas cycling with horizontal well

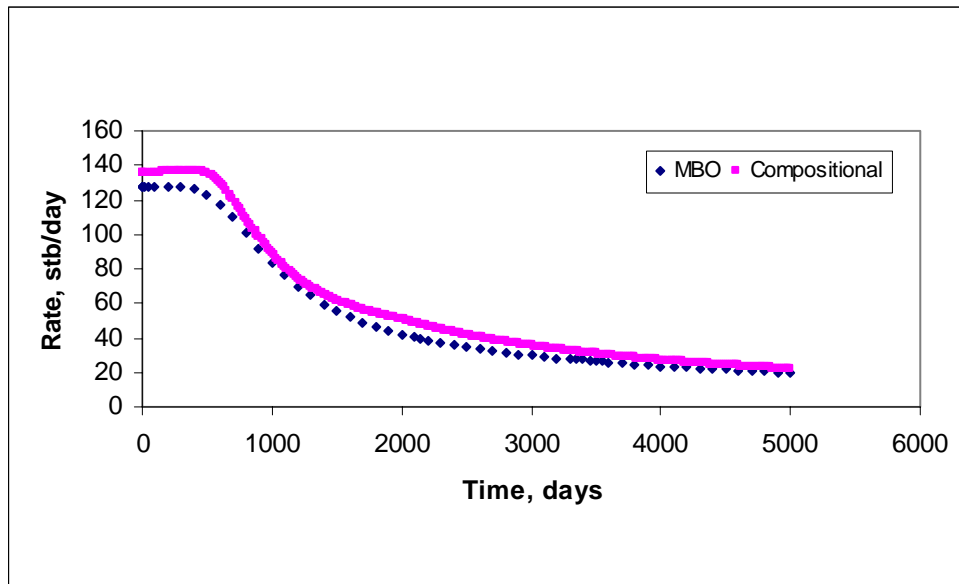


Fig. 4.95 Oil production rate for low production and injection rates for horizontal well

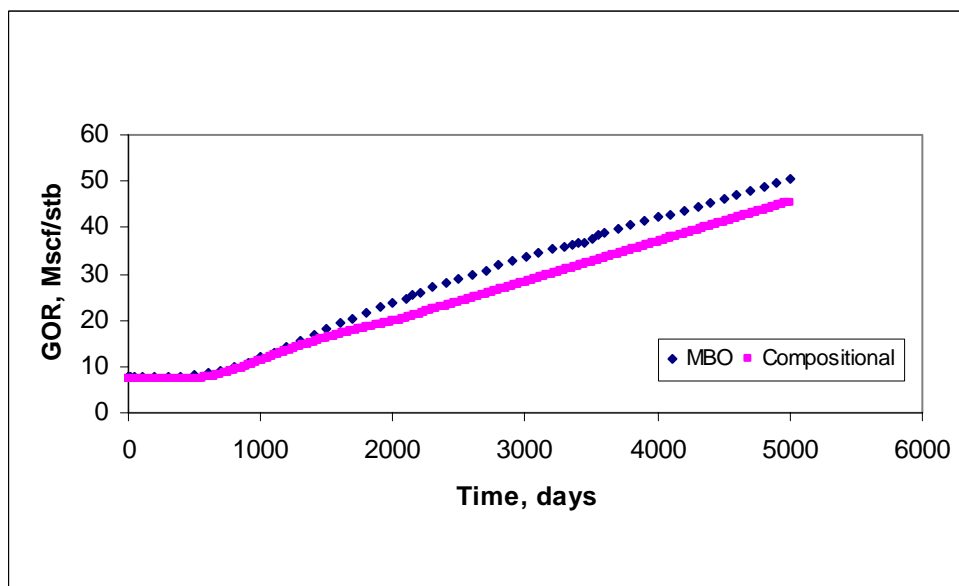


Fig. 4.96 Gas-oil ratio for low production and injection rates for horizontal well

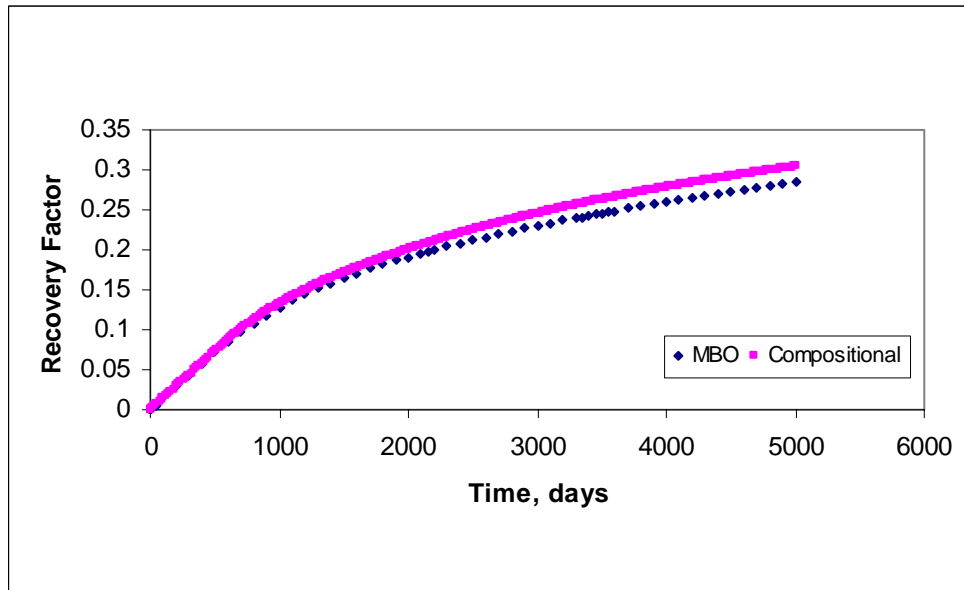


Fig. 4.97 Recovery factor for low production and injection rates for horizontal well

CHAPTER V

SUMMARY AND CONCLUSIONS

A gas condensate fluid was characterized using the PVTi fluid characterization package with the four-parameter Peng-Robinson equation of state, and experimental PVT data.

This fluid was characterized with six pseudocomponents and CO₂. An excellent match between the experimental and the simulated data was achieved by regressing the binary interaction coefficients and shift factors of the selected pseudocomponents.

Using the tuned equation of state, black-oil PVT properties have been generated using Whitson and Torp and Coats methods. However, the gas formation volume factors (B_g) generated by two methods showed differences especially at lower pressures. Also negative oil and gas compressibilities were obtained during the simulation. Consequently the MBO run, which uses black-oil tables generated by Coats' method, was cancelled due to number of errors encountered in the simulation.

In Whitson and Torps's approach, a depletion type experiment was simulated (CVD). At each step in the depletion test, the equilibrium oil and equilibrium gas were taken separately through a surface separation process (the compositional models surface separators). The surface oil and surface gas products from the reservoir oil phase were used to define the oil FVF and solution GOR. The surface oil and surface gas products from the reservoir gas phase were used to define the dry gas FVF and solution OGR. The equilibrium calculations in MBO model were made using the solution gas-oil and oil-gas ratios using the tables generated.

Also a single set of constant surface gas and surface oil densities were calculated to determine the reservoir densities together with pressure dependent properties.

In Coats' calculation, the basic idea is to set the solution oil-gas ratio to the measured values from the CVD experiment accounting for separator conditions and calculate the rest of the PVT parameters by using mass conservation equations. Mass conservation error is unavoidable in the conventional black-oil treatment that assumes constant densities of separator oil and gas while they are not constant.³² The methodology used by Coats' amplifies the errors included in mass conservation equations, leading to differences in gas formation volume factors calculated by two methods.

Also the dew point values for oil properties are not well defined, as no liquid is present. Extrapolation of sub-dew point properties to the dew point can lead to situations where oil has non-physical negative compressibility, which was one of the problems in our simulation. It was reported that a better agreement between compositional and MBO models could be obtained if surface oil, gas molecular weights and densities are obtained from the separation of the mixture at each CVD pressure step to calculate R_v at each pressure step instead of using the properties obtained from the separation of the "original fluid" for Coats' method.

A 3D synthetic reservoir model was built with one producer and one injector well located at the opposite corners of the quarter five spot model. Later on vertical producer was replaced with a horizontal well for the final step of the study.

The initial reservoir fluid composition was either constant with depth or exhibited a vertical compositional gradient. MBO model was initialized with solution gas-oil and oil-gas ratio and saturation pressure versus depth tables to represent the vertical compositional gradient.

Contrary to the common belief that oil-gas ratio versus depth initialization method gives better representation of original fluids in place, initializations with saturation pressure versus depth gave closer original fluids in place values. For the case of uniform

composition with depth both initialization methods gave the same initial fluids in place and no difference in their production performance was observed.

Saturation pressure versus depth initialization makes the model give earlier condensate drop-out and higher oil rates initially. Especially in the region of higher heavier fractions, initialization with saturation pressure versus depth resulted in high oil saturations for the particular fluid used in this study.

After the pressure throughout the reservoir decreases below the dew point, condensate is formed throughout the reservoir and, the gas flowing into the condensate bank becomes leaner causing some vaporization on its way to the producer. This means that unrealistic vaporization in MBO model is not just limited to the gas cycling case, it can also be encountered in natural depletion case to some degree depending on the depletion scenario i.e. production rate, vertical communication, completion strategies and the type of well used.

In natural depletion case the gas present in MBO has a lower capacity to hold liquid and more oil is left in the reservoir. In gas cycling case, the injected gas in MBO can pick up oil as a function of pressure and the oil left in the reservoir is always lower than compositional model.

Initially a discrepancy in saturation pressure versus depth was observed in MBO model. However, it was observed that the error in saturation pressure versus depth had a little impact on the production performance and ultimate recoveries and it diminished as the reservoir was depleted. In the cases of full pressure maintenance, reduced vertical communication and horizontal well set as producer, this error was reduced significantly and a better match was obtained between two models.

For the full pressure maintenance, gas-gas miscible displacement is improved with higher injection and production rates. This resulted in reduced amount of condensate drop-out and a condensate reservoir becoming leaner very quickly that can be represented easily with the MBO model.

Reduced vertical communication prevents the mixing of leaner reservoir gas (relative to initial conditions) with oil formed after condensation. Also the accumulated condensate was not able to go down under the effect of gravity forces. So, each individual layers condensation and vaporization process becomes proportional to that layers content of heavy and light component fractions.

These two phenomena encountered in the reduced vertical communication case limited the amount of condensation and vaporization.

The lower drawdown pressure for horizontal well, compared to the vertical well, for the same flow rate, considerably reduces retrograde condensation, giving less condensate deposited near the horizontal wellbore. Lesser liquid drop-out and smaller amounts of vaporization for MBO model makes the models give similar performances. Also, it was observed that longer drain hole causes a lower drawdown and less condensation around the wellbore.

If the perforations are placed in the upper part of the reservoir, when the compositional gradient takes part, the performance of two models get closer since leaner gas drops less condensate in this part of the reservoir.

No effect of production rate was observed for natural depletion cases.

Also vaporization characteristics of both models affected the performance of the models. In MBO model compositional dependence in the fluid PVT properties are disregarded

and consequently when the gas is injected into the reservoir, revaporization of the liquid is governed only by pressure. With this approach, the primary compositional effect, stripping of the liquid components in inverse proportion to their molecular weights is ignored.

During the gas cycling a miscible displacement is guaranteed in compositional model, independent of the injection gas used, even though the injected gas may be first contact immiscible with the original reservoir gas. Miscibility develops by a simple vaporizing mechanism. However miscibility cannot be represented by MBO model resulting in late arrival of displacement fronts. The arrival time can also change in relation to the initialization method used.

For the gas cycling cases the models were in good agreement as long as the reservoir was produced fast enough to minimize condensation. Lower production and injection rates and bottom completions created differences between the performances of the models.

The changes in oil-gas ratio of the cycling gas showed that, it is not possible to accurately represent the changing PVT properties of recycled gas with single PVT table in MBO model since every time the produced gas passes through the separators and injected back into the reservoir its oil-gas ratio and accordingly vaporization characteristics changes.

The oil saturation profiles illustrated how the condensation and vaporization processes advanced for two models. Almost all the cases showed differences in condensate saturation distribution around the wellbore area and the entire reservoir. The cases with the horizontal wells exhibited better agreement with compositional model compared to the vertical wells. When the horizontal well is completed closer to the depth where the sample fluid is coming from, MBO model exhibited a closer performance to the

compositional model. The MBO model performance with the horizontal well approaches to the model with vertical well as the completion depth moves away from the depth of the fluid sample, but at some point again the performance begins to approach the compositional model due to reduction in heavy fraction amount.

An additional bank away from to producer closer to the upper boundary of the producing formation was observed which is important in locating the injector to enhance productivity of the producer well. The extent of this bank gets larger if the reservoir has no compositional gradient. MBO model was not able to produce the same banking.

Care should be taken with the studies sensitive to saturations and fluid movement, i.e. pressure transient analysis to determine the size of the condensate bank or history matching with acoustic impedance since oil saturation distributions around the well and throughout the reservoir may be quite different in two models regardless of a match with the production performance.

Analysis of the performance of fully compositional model and MBO model under different natural depletion and gas cycling scenarios allowed us to summarize the following conclusions:

Natural Depletion with a Vertical Well

- For constant composition case initialization methods does not make difference on the performance of the MBO model. Also OOIP is the same with both methods if no compositional gradient is used.
- Changes in dew point with depth are difficult to represent with MBO model. Most of the time error in saturation pressure versus time has a short-lived effect on recoveries. However, studies that are sensitive to saturations may require fully compositional models.

- MBO and compositional models get closer as the reservoir is depleted independent of the initialization method.
- For some gas condensates liquid drop-out is very slow, sometimes several thousand psia below the dew point. It is more difficult to represent this type of behavior with MBO models since the so-called “short-lived” effect will be more effective.
- Any effect that reduces the amount condensation and revaporization process in the reservoir makes MBO and compositional models exhibit closer performances
- For a rich gas condensate reservoir OOIP is represented better if the model is initialized with saturation pressure versus depth table
- If the layers are completed closer to the top of the reservoir, a closer performance with the compositional model can be obtained
- For the bottom layer completion case with compositional grading, initializing method does not affect the oil production rate
- When layers are completed at closer to the top of the reservoir, actual behavior is represented better in MBO model and initialization with saturation pressure versus depth table improves the performance
- The match between MBO and compositional model is not affected by the production rate for natural depletion case
- In the case of poor vertical communication between layers, a better match between two models can be obtained in terms of oil production rates and recoveries
- Reduced vertical communication gives less pressure drop for both models. This causes higher oil saturations in compositional model and lower oil saturations in MBO model. Revaporization in compositional model creates differences in gas oil ratio values

Gas Cycling

- Models get closer as the reservoir is depleted. If the reservoir is depleted faster the performance of compositional and MBO models get closer. This is due to gas-gas miscible displacement above dew point independent of the type of the injection gas. At the time dew point is reached because of the previous quick displacement and production, reservoir gas is already leaner and drops less condensate. As the reservoir gets leaner it gets easier to represent it with black-oil simulation.
- Early pressure dependent liquid drop-out gives lower oil production rates for MBO at the beginning of the simulation
- Higher amounts of revaporization gives higher oil production rates in MBO after the gas gets leaner and more oil is left in the reservoir in compositional model. Consequently this creates a difference in gas –oil ratios
- Revaporization begins earlier in compositional model because of earlier arrival of displacement front compared to MBO model due to a better representation of miscibility.
- Since miscibility can not be represented in MBO models the displacement front arrives later than in compositional model
- MBO model gives higher amounts of vaporization around injector wells
- Lower production and injection rates make the model performances depart from each other
- For lower rates the difference between first condensation times get larger
- Upper completions make the performance of models get closer. Also OGR versus depth table for initialization has a positive impact on upper completions
- If the layers are completed at the bottom, initialization methods do not create any difference in performances and the models depart from each other since very high oil saturations are encountered in MBO in the bottom layers

- In the case of poor vertical communication, if the model is initialized with saturation pressure versus depth table, bottom layers tend to give higher oil saturations for gas cycling

REFERENCES

1. Coats, K.H.: "Simulation of Gas Condensate Reservoir Performance," *JPT* (October 1985), **5**, 1870.
2. Fevang, O., and Whitson, C.H.: "Modeling Gas Condensate Deliverability," paper SPE 30714 presented at the 1995 SPE Annual Technical Conference and Exhibition, Dallas, Texas, 22-25 October.
3. Fevang, O., Singh, K., Whitson, C.H.: "Guidelines for Choosing Compositional and Black-Oil Models for Volatile Oil and Gas-Condensate Reservoirs," paper SPE 63087 presented at the 2000 SPE International Conference and Exhibition, Dallas, Texas, 1-4 October.
4. El-Banbi, A.H., and McCain, W.D.: "Investigation of Well Productivity in Gas-Condensate Reservoirs," paper SPE 59773 presented at the 2000 SPE/CERI Gas Technology Symposium, Calgary, Alberta, Canada, 3-5 April.
5. El-Banbi, A.H., McCain, W.D, Forrest, J.K., Fan, L.: "Producing Rich Gas-Condensate Reservoirs-Case History and Comparison Between Compositional and Modified Black-Oil Approaches," paper SPE 58988 presented at the 2000 SPE International Conference and Exhibition, Villahermosa, Mexico, 1-3 February.
6. Whitson, C.H., Torp, S.B.: "Evaluating Constant Volume Depletion Data," paper SPE 10067 presented at the 1981 Annual Fall Technical SPE Conference and Exhibition, San Antonio, Texas, 5-7 October.

7. Crichlow, H. B.; *Modern Reservoir Engineering - A Simulation Approach*, Prentice-Hall, Englewood Cliffs, New Jersey (1977).
8. Peaceman, D. W.; *Fundamentals of Numerical Reservoir Simulation*, Elsevier, NY, (1977).
9. Wattenbarger, R.A.: "Practical Aspects of Compositional Simulation," paper SPE 2800 presented at the 1970 SPE Symposium on Numerical Simulation of Reservoir Performance, Dallas, Texas, 5-6 February.
10. Zudkevitch, D., and Joffe, J.: "Correlation and Prediction of Vapor-Liquid Equilibrium with the Redlich Kwong Equation of State," *AIChE J.* (May 1970), **2**, 112.
11. Joffe, J., Schroeder, G.M., and Zudkevitch, D.: "Vapor Liquid Equilibria with the Redlich Kwong Equation of State," *AIChE J.* (May 1970) **2**, 496.
12. McCain, W.D. Jr.: *The Properties of Petroleum Fluids*, Pennwell Books, Tulsa, Oklahoma (1990).
13. Jhaveri, B. S. and Youngren, G.K.: "Three Parameter Modification of the Peng Robinson Equation of State to Improve Volumetric Predictions," *SPERE* (August 1988) 1033.
14. Li, Y.K., Nghiem, L.X., and Siu, A.: "Phase Behavior Computation for Reservoir Fluid: Effects of Pseudo Component on Phase Diagrams and Simulation Results," paper CIM 84-35-19 presented at the 1984 Petroleum Soc. of CIM Annual Meeting, Calgary, Alberta, Canada, 10-13 June.

15. Whitson, C.H.: "Characterizing Hydrocarbon Plus Fractions," *SPEJ* (August 1983) 683; *Trans.*, AIME, **275**, 42.
16. Lee, S.T., Jacoby, R.H., Chen, W.H., and Culham W.E.: "Experiments and Theoretical Simulation on the Fluid Properties Required for Simulation of Thermal Process," *SPEJ* (October 1982) 535.
17. Behrens, R.A., and Sandler, S.I.: "The Use of Semicontinuous Description to Model the C_7^+ Fraction in Equation of State Calculations," paper SPE 14925 presented at the 1986 SPE/DOE Symposium on Enhanced Oil Recovery, Tulsa, Oklahoma, 23-23 April.
18. Kuenen, J.P.: "On Retrograde Condensation and the Critical Phenomena of Two Substances," *Commun. Phys. Lab U. Leiden* (1892) **4**, 7.
19. Coats, K.H., and Thomas, L.K.: "Compositional and Black-Oil Reservoir Simulation," paper SPE 29111 presented at the 1995 SPE Symposium on Reservoir Simulation, San Antonio, Texas, 12-15 February.
20. Whitson, C.H., and Thomas, L.K.: "Simplified Compositional Formulation for Modified Black-Oil Simulators," paper SPE 18315 presented at the 1988 SPE Annual Technical Conference and Exhibition, Houston, Texas, 2-5 October.
21. Nolen, J.S.: "Numerical Simulation of Compositional Phenomena in Petroleum Reservoirs," paper SPE 4274 presented at the 1973 SPE Symposium on Numerical Simulation of Reservoir Performance, Houston, Texas, 11-12 January.

22. Spivak, A., Dixon, T.N.: "Simulation of Gas-Condensate Reservoirs," paper SPE 4271 presented at the 1973 SPE Symposium on Numerical Simulation of Reservoir Performance, Houston, Texas, 11-12 January.
23. Cook, A.B., Walker, C.J.: "Realistic K Values of C₇₊ Hydrocarbons for Calculating Oil Vaporization During Gas Cycling at High Pressures," *JPT* (July 1969), **2**, 901.
24. Geoquest, *PVTi Reference Manual 2001a*, Geoquest, Houston (2001).
25. Schulte, A.M.: "Compositional Variations within a Hydrocarbon Column due to Gravity," paper SPE 9235 presented at the 1980 SPE Fall Technical Conference and Exhibition, Dallas, Texas, 21-24 September.
26. Hirschberg, A.: "Role of Asphaltenes in Compositional Grading of a Reservoir's Fluid Column," *JPT* (January 1988), **5**, 89.
27. Whitson, C.H., and Thomas, L.K.: "Compositional Gradients in Petroleum Reservoirs," paper SPE 28000 presented at the 1994 SPE Annual Technical Conference and Exhibition, Houston, Texas, 29-31 August.
28. Fevang, O., and Whitson, C.H.: "Accurate *in situ* Compositions in Petroleum Reservoirs," paper SPE 28829 presented at the 1994 SPE European Petroleum Conference, London, U.K, 25-27 October.
29. Jaramillo, J.M.: "Vertical Composition Gradient Effects on Original Hydrocarbon in Place Volumes and Liquid Recovery for Volatile Oil and Gas Condensate Reservoirs," MS thesis, Texas A&M University, College Station, Texas (2000).

30. Kenyon, D. E. and Behie, G.A.: "Third SPE Comparative Solution Project: Gas Cycling of Retrograde Condensate Reservoirs," paper SPE 12278 presented at the 1983 Reservoir Simulation Symposium, San Francisco, 15-18 November.
31. Dehane, A., Tiab, D.: "Comparison of Performance of Vertical and Horizontal Wells in Gas-Condensate Reservoirs," paper SPE 63164 presented at the 2000 SPE Annual Technical Conference and Exhibition, Dallas, Texas, 1-4 October.
32. McVay, D.A.: "Generation of PVT Properties for Modified Black-Oil Simulation of Volatile Oil and Gas Condensate Reservoirs," PhD dissertation, Texas A&M University, College Station, Texas (1994).

APPENDIX A

CPU TIMES IN SECONDS FOR SIMULATIONS CONDUCTED WITH VERTICAL WELLS

	Compositional	MBO	MBO
		R_v vs Depth	P_d vs Depth
Natural Depletion			
Constant Composition	785.91	64.47	65
Compositional Gradient	745.56	72.22	64.28
Bottom Completion	539.12	82.58	81.32
Top Completion	820.37	80.35	79.01
Reduced k_v	985.45	106.35	103.2
Gas Cycling			
Compositional Gradient	3021.78	597.77	582.49
Bottom Completion	3068.71	458.86	479.42
Top Completion	3296.56	531	603.04
Reduced k_v	4743.82	363	453.81
Low Rates	1957.74	401.39	626.68

APPENDIX B

DATA FILE FOR COMPOSITIONAL MODEL

```

MEMORY
200 50 /
=====
--RESEARCH BULENT IZGEC
--Compositional Model for Gas Condensate Reservoirs
--Working File Data Spring-03
--Texas A&M University
--Dr. Maria Barrufet
=====

-----
RUNSPEC This section is mandatory and it is used to set up the
--      specification for the simulation run.
-----

DIMENS
--Grid dimensions
--Nx Ny Nz
25 25 18 /

FIELD
--Request the unit convention to be used

WELLDIMS
2 40 2 2 /

COMPS
7 /

TABDIMS
--Determines the # of pressure and saturation tables and the maximum # of rows
1 1 40 40 /

WATER
--Water is present

AIM
--AIM solution method, avoids time step restrictions
EOS
--Peng-Robinson equation of state to be used
PR /

ISGAS
--States the run is a gas condensate

NSTACK
200 /
  MULTSAVE
--Overwrite the save at each state
0 /

-----
GRID   This section is mandatory and it is used to input the grid
--     or cells to be used into the simulation model.
-----
-- MODEL 25*25*18 EACH BLOK 32FT (PERMEABILITY AND POROSITY DISTRIBUTION)

```

EQUALS

```
--      VALUE  X    X    Y    Y    Z    Z
DX      32    1  25  1  25  1  18 /
DY      32    1  25  1  25  1  18 /
DZ      20    1  25  1  25  1   1 /
DZ      15    1  25  1  25  2   2 /
DZ      26    1  25  1  25  3   3 /
DZ      15    1  25  1  25  4   4 /
DZ      16    1  25  1  25  5   5 /
DZ      14    1  25  1  25  6   6 /
DZ       8    1  25  1  25  7   7 /
DZ       8    1  25  1  25  8   8 /
DZ      18    1  25  1  25  9   9 /
DZ      12    1  25  1  25 10  10 /
DZ      19    1  25  1  25 11  11 /
DZ      18    1  25  1  25 12  12 /
DZ      20    1  25  1  25 13  13 /
DZ      50    1  25  1  25 14  14 /
DZ      20    1  25  1  25 15  15 /
DZ      20    1  25  1  25 15  16 /
DZ      30    1  25  1  25 15  17 /
DZ      30    1  25  1  25 15  18 /
/
```

TOPS

```
625*12540
/
```

PORO

```
625*0.087 625*0.097 625*0.111 625*0.16 625*0.13
625*0.17 625*0.17 625*0.08 625*0.14 625*0.13
625*0.12 625*0.105 625*0.12 625*0.116 625*0.157
625*0.157 625*0.157 625*0.157
/
```

PERMX

```
625*180 625*180 625*100 625*100 625*50
625*50 625*50 625*50 625*80 625*80
625*80 625*150 625*150 625*180 625*180
625*180 625*180 625*180
/
```

PERMY

```
625*180 625*180 625*100 625*100 625*50
625*50 625*50 625*50 625*80 625*80
625*80 625*150 625*150 625*180 625*180
625*180 625*180 625*180
/
```

PERMZ

```
625*18 625*18 625*10 625*10 625*5
625*5 625*5 625*5 625*8 625*8
625*8 625*15 625*15 625*18 625*18
625*18 625*18 625*18
/
```

```
-----
PROPS  This section is mandatory and it is used to incorporate the
--      fluid and reservoir properties
-----
```

INCLUDE

```
TESTCON.PVO /
```

```
-- Reservoir temperature in Deg F
```

RTEMP
254 /

SWFN
--Water saturation functions
-- SWAT KRW PCOW
0.16 0 50
0.18 0 41
0.20 0.002 32
0.24 0.010 21
0.28 0.020 15.5
0.32 0.033 12.0
0.36 0.049 9.2
0.40 0.066 7.0
0.44 0.090 5.3
0.48 0.119 4.2
0.52 0.150 3.4
0.56 0.186 2.7
0.60 0.227 2.1
0.64 0.277 1.7
0.68 0.330 1.3
0.72 0.390 1.0
0.76 0.462 0.7
0.8 0.540 0.5
0.84 0.620 0.4
0.88 0.710 0.3
0.92 0.800 0.2
0.96 0.900 0.1
1.00 1.000 0.0 /

SGFN
--Gas saturation functions
-- SGAS KRG PCOG
0.00 0.000 0.0
0.04 0.005 0.1
0.08 0.013 0.2
0.12 0.026 0.3
0.16 0.040 0.4
0.20 0.058 0.5
0.24 0.078 0.6
0.28 0.100 0.7
0.32 0.126 0.8
0.36 0.156 0.9
0.40 0.187 1.0
0.44 0.222 1.1
0.48 0.260 1.2
0.56 0.349 1.4
0.60 0.400 1.5
0.64 0.450 1.6
0.68 0.505 1.7
0.72 0.562 1.8
0.76 0.620 1.9
0.80 0.680 2.0
0.84 0.740 2.1
/

SOF3
--Oil saturation functions
-- SOIL KRO PC
0.00 0.000 0.000
0.04 0.000 0.000
0.08 0.000 0.000
0.12 0.000 0.000
0.16 0.000 0.000
0.20 0.000 0.000
0.24 0.000 0.000

```

0.28 0.005 0.005
0.32 0.012 0.012
0.36 0.024 0.024
0.40 0.040 0.040
0.44 0.060 0.060
0.48 0.082 0.082
0.52 0.112 0.112
0.56 0.150 0.150
0.60 0.196 0.196
0.68 0.315 0.315
0.72 0.400 0.400
0.76 0.513 0.513
0.80 0.650 0.650
0.84 0.800 0.800
/

ROCK
--Reference Pressure and Rock compressibility
5868 4e-6/

PVTW
--Pref, Bw, Cw, Uw
5868 1.0 0.000003 0.31 0.0 /

DENSITY
--Surface density of water
48.0917039246529 63.0 0.0606568949955782 /

=====
SOLUTION This section is mandatory
=====
--Defines the initial solution into the reservoir

EQUIL
-- FT PRES WGC pc
12800 5868 12950 0 1* 0 1 1 0 /

OUTSOL
--Solution output for GRAF
PRESSURE SOIL PSAT/

RPTSOL
--Output to the initial solution to the print files
PRESSURE SOIL SWAT SGAS /

FIELDSEP
1 180 500 /
2 150 30 /
3 80 14.7 /
/

=====
SUMMARY This optional section specifies quantities to be written to
-- the summary file to be read by GRAF
=====

RUNSUM
--Field oil production rate and total, GOR and field pressure
FPR
FOPR
FOPT
FGPR
FGIR
FGOR
FOSAT

```

FGSAT
 FWPR
 FGPT
 FWPT
 FWIR
 WBHP
 /

 SCHEDULE Specifies the production system

RPTSCHED
 PRESSURE SOIL PSAT /

SEPCOND
 SEP FIELD 1 180 500 /
 SEP FIELD 2 150 30 /
 SEP FIELD 3 80 14.7 /
 /

WELSPECS
 P FIELD 25 25 12540 GAS 6* 1 /
 I FIELD 1 1 12680 GAS 2* SHUT 3* 1 /
 /

WSEPCOND
 P SEP /
 /

COMPDAT
 P 25 25 1 9 1* 1 1* 0.3 /
 I 1 1 10 18 1* 1 1* 0.3 /
 /

WELTARG
 P BHP 1000 /
 /

WCONINJE
 I GAS SHUT RATE 1500 1* 5995 /
 /

WINJGAS
 I GV FIELD /
 /

WECON
 P 10 5* YES /
 /

TUNING
 2* 0.0001 /
 /
 15 1 200 /

TSTEP
 50*100 /

SAVE

END

DATA FILE FOR MODIFIED BLACK-OIL MODEL

```

MEMORY
200 50 /
=====
--RESEARCH BULENT IZGEC
--Modified Black-Oil Model for Gas Condensate Reservoirs
--Working File Data Spring-03
--Texas A&M University
--Dr. Maria Barrufet
=====

-----
RUNSPEC This section is mandatory and it is used to set up the
--      specification for the simulation run.
=====

DIMENS
--Grid dimensions
--Nx Ny Nz
25 25 18 /

FIELD
--Request the unit convention to be used

WELLDIMS
4 40 2 2 /

TABDIMS
--Determines the # of pressure and saturation tables and the maximum # of rows
1 1 40 40 1* 100 /

--Water, gas, oil, vaporized oil and dissolved gas are present
GAS
WATER
OIL
VAPOIL
DISGAS

NSTACK
200 /

MULTSAVE
--Overwrite the save at each state
0 /

START
1 'JAN' 2003 /

EQLDIMS
2* 100 /

-----
GRID      This section is mandatory and it is used to input the grid
--      or cells to be used into the simulation model.
=====
-- MODEL 25*25*15 EACH BLOK 32FT (PERMEABILITY AND POROSITY DISTRIBUTION)

EQUALS
--      VALUE   X     X     Y     Y     Z     Z
DX      32     1    25    1    25    1    18 /
DY      32     1    25    1    25    1    18 /
DZ      20     1    25    1    25    1     1 /
DZ      15     1    25    1    25    2     2 /
DZ      26     1    25    1    25    3     3 /

```

```

DZ      15      1      25      1      25      4      4      /
DZ      16      1      25      1      25      5      5      /
DZ      14      1      25      1      25      6      6      /
DZ       8      1      25      1      25      7      7      /
DZ       8      1      25      1      25      8      8      /
DZ      18      1      25      1      25      9      9      /
DZ      12      1      25      1      25     10     10     /
DZ      19      1      25      1      25     11     11     /
DZ      18      1      25      1      25     12     12     /
DZ      20      1      25      1      25     13     13     /
DZ      50      1      25      1      25     14     14     /
DZ      20      1      25      1      25     15     15     /
DZ      20      1      25      1      25     15     16     /
DZ      30      1      25      1      25     15     17     /
DZ      30      1      25      1      25     15     18     /
/

```

```

TOPS
625*12540
/

```

```

PORO
625*0.087 625*0.097 625*0.111 625*0.16 625*0.13
625*0.17 625*0.17 625*0.08 625*0.14 625*0.13
625*0.12 625*0.105 625*0.12 625*0.116 625*0.157
625*0.157 625*0.157 625*0.157
/

```

```

PERMX
625*180 625*180 625*100 625*100 625*50
625*50 625*50 625*50 625*80 625*80
625*80 625*150 625*150 625*180 625*180
625*180 625*180 625*180
/

```

```

PERMY
625*180 625*180 625*100 625*100 625*50
625*50 625*50 625*50 625*80 625*80
625*80 625*150 625*150 625*180 625*180
625*180 625*180 625*180
/

```

```

PERMZ
625*18 625*18 625*10 625*10 625*5
625*5 625*5 625*5 625*8 625*8
625*8 625*15 625*15 625*18 625*18
625*18 625*18 625*18
/

```

```

-----
PROPS  This section is mandatory and it is used to incorporate the
--      fluid and reservoir properties
-----
--This file provides the PVT tables generated by Whitson and Torp method
INCLUDE
PVT.PVO /

-- Reservoir temperature in Deg F
RTEMP
254 /

SWFN
--Water saturation functions
--  SWAT  KRW  PCOW
   0.16  0    50
   0.18  0    41

```

0.20	0.002	32
0.24	0.010	21
0.28	0.020	15.5
0.32	0.033	12.0
0.36	0.049	9.2
0.40	0.066	7.0
0.44	0.090	5.3
0.48	0.119	4.2
0.52	0.150	3.4
0.56	0.186	2.7
0.60	0.227	2.1
0.64	0.277	1.7
0.68	0.330	1.3
0.72	0.390	1.0
0.76	0.462	0.7
0.8	0.540	0.5
0.84	0.620	0.4
0.88	0.710	0.3
0.92	0.800	0.2
0.96	0.900	0.1
1.00	1.000	0.0 /

SGFN

--Gas saturation functions

--	SGAS	KRG	PCOG
	0.00	0.000	0.0
	0.04	0.005	0.1
	0.08	0.013	0.2
	0.12	0.026	0.3
	0.16	0.040	0.4
	0.20	0.058	0.5
	0.24	0.078	0.6
	0.28	0.100	0.7
	0.32	0.126	0.8
	0.36	0.156	0.9
	0.40	0.187	1.0
	0.44	0.222	1.1
	0.48	0.260	1.2
	0.56	0.349	1.4
	0.60	0.400	1.5
	0.64	0.450	1.6
	0.68	0.505	1.7
	0.72	0.562	1.8
	0.76	0.620	1.9
	0.80	0.680	2.0
	0.84	0.740	2.1

/

SOF3

--Oil saturation functions

--	SOIL	KRO	PC
	0.00	0.000	0.000
	0.04	0.000	0.000
	0.08	0.000	0.000
	0.12	0.000	0.000
	0.16	0.000	0.000
	0.20	0.000	0.000
	0.24	0.000	0.000
	0.28	0.005	0.005
	0.32	0.012	0.012
	0.36	0.024	0.024
	0.40	0.040	0.040
	0.44	0.060	0.060
	0.48	0.082	0.082
	0.52	0.112	0.112
	0.56	0.150	0.150
	0.60	0.196	0.196


```

0.68 0.315 0.315
0.72 0.400 0.400
0.76 0.513 0.513
0.80 0.650 0.650
0.84 0.800 0.800 /

```

ROCK

```

--Reference Pressure and Rock compressibility
5868 4e-6/

```

PVTW

```

--Pref, Bw, Cw, Uw
5868 1.0 0.000003 0.31 0.0 /

```

DENSITY

```

--Surface density of water
1* 63.0 1* /

```

```

=====
SOLUTION This section is mandatory
=====

```

```

--Defines the initial solution into the reservoir

```

RPTRST

```

PRESSURE SOIL /

```

EQUIL

```

-- FT PRES WGC pc
12800 5868 12950 0 12950 0 1 1 0 /

```

RSVD

```

12540 2.83
12950 2.83
/

```

RVVD

```

--

```

```

-- Rv v Depth

```

```

--

```

```

12539.99999872 0.11161894807196
12545 0.112104318955872
12550 0.112596042104918
12555 0.113094290559185
12560 0.113599244608021
12565 0.114111092345918
12570 0.114630030137485
12575 0.115156263117926
12580 0.115690005732376
12585 0.116231482317793
12590 0.116780927720094
12600 0.117904721195717
12610 0.119063502709017
12620 0.120259607059715
12630 0.121495618948745
12640 0.122774410666841
12650 0.124099187255617
12660 0.12547354100803
12670 0.126901517886589
12675 0.127637022861561
12680 0.128387698094832
12690 0.129937298053075
12700 0.131556294683257
12710 0.133251584912151
12720 0.135031188588174
12730 0.136904511606289
12740 0.138882691963682
12750 0.140979062517524
12760 0.143209783834266
12770 0.145594716495373
12780 0.148158678927883

```

```

12790 0.150933287133691
12799.9995904 0.153959616660158
12800 0.153959740777501
12810 0.15729324910968
12820 0.161010353700329
12830 0.165221858511965
12840 0.170097440583076
12850 0.175917703430637
12860 0.183200814972792
12870 0.193083766775274
12880 0.208926371240204
12890 0.241932463428651
12900 0.272327083435377
12910 0.289987650704482
12920 0.302808389464073
12930 0.313177863957058
12940 0.322043942496393
12950 0.329881285934716

```

/

--PDVD

--

-- Dew Point v Depth

--

```

-- 12539.99999872 5422.6752737675
-- 12550 5430.98786409969
-- 12560 5439.39144048838
-- 12570 5447.88957783948
-- 12580 5456.48610647143
-- 12590 5465.18514034066
-- 12600 5473.9911080606
-- 12610 5482.90878840716
-- 12620 5491.9433511291
-- 12630 5501.10039796623
-- 12650 5519.80692662585
-- 12670 5539.08530369287
-- 12680 5548.95914670044
-- 12690 5559.00238632849
-- 12700 5569.22601090308
-- 12710 5579.64233616844
-- 12720 5590.26524714437
-- 12730 5601.11050017343
-- 12740 5612.1961048124
-- 12750 5623.54281154624
-- 12760 5635.17475516019
-- 12770 5647.12025362148
-- 12780 5659.41293275391
-- 12790 5672.09463205455
-- 12799.9995904 5685.21313451731
-- 12800 5685.21365752185
-- 12810 5698.83282546448
-- 12820 5713.03152713762
-- 12830 5727.91369790957
-- 12840 5743.61909177113
-- 12850 5760.34862422994
-- 12860 5778.38279985318
-- 12865 5788.01250441451
-- 12870 5798.12421435996
-- 12875 5808.74340907733
-- 12880 5819.6805799533
-- 12885 5829.57122937151
-- 12890 5832.16696518874
-- 12895 5824.69311493555
-- 12900 5814.43962137929
-- 12910 5794.4766759914
-- 12915 5785.22618068948

```

```

--          12920 5776.42553987767
--          12925 5768.01241606138
--          12930 5759.9387030852
--          12935 5752.16237242486
--          12940 5744.65205801844
--          12945 5737.37619431062
--          12950 5730.31226530939
--/

```

```

=====
SUMMARY This optional section specifies quantities to be written to
-- the summary file to be read by GRAF
=====

```

```

RUNSUM
SEPARATE
EXCEL
--Field oil production rate and total, GOR and field pressure
FPR
FOPR
FOPT
FGPR
FGIR
FGOR
FOSAT
FGSAT
FWPR
FGPT
FWPT
FWIR
WBHP
/

```

```

=====
SCHEDULE Specifies the production system
=====

```

```

WELSPECS
P P1 25 25 12540 GAS 6* 1 /
I I1 1 1 12680 GAS 6* 1 /
/

```

```

COMPDAT
P 25 25 1 9 1* 1 1* 0.3 /
I 1 1 10 18 1* 1 1* 0.3 /
/

```

```

WCONPROD
--Well P set to target gas rate of 3000, with min bhp of 1000 psi
P OPEN GRAT 1* 1* 3000 1* 1* 1000/
/

```

```

WCONINJE
I GAS SHUT RATE 3000 1* 5995 /
/

```

```

GECON
FIELD 10 5* YES /
/

```

```

TUNING
2* 0.0001 /
/
15 1 200 /

```

MESSAGES
3* 1000 1000 4* 1000 /

TSTEP
50*100 /

SAVE

END

TESTCON.PVO FILE

This file contains the PVI properties of the gas condensate analyzed. Data files in the PROPS section require it.

```

EOS
--
-- Equation of State (Reservoir EoS)
--
  PR3
/

NCOMPS
--
-- Number of Components
--
  7
/

CNAMES
--
-- Component Names
--
  'CO2'
  'GRP1'
  'GRP2'
  'GRP3'
  'GRP4'
  'GRP5'
  'GRP6'
/

MW
--
-- Molecular Weights (Reservoir EoS)
--
  44.01
  16.1325726
  34.55606427
  67.96383608
  112.5175
  178.788
  303.6435714
/

OMEGAA
--
-- EoS Omega-a Coefficient (Reservoir EoS)
--
  0.477635
  0.477635
  0.477635
  0.457236
  0.457236
  0.380486
  0.380486
/

OMEGAB
--
-- EoS Omega-b Coefficient (Reservoir EoS)
--
  0.070049
  0.070049
  0.070049

```

```

    0.077796
    0.077796
    0.07256
    0.07256
/
TCRIT
--
-- Critical Temperatures (Reservoir EoS)
--
    548.45998547
    342.212551
    586.8298284
    809.9493175
    1051.5824721
    1241.5823671
    1460.809749
/
PCRIT
--
-- Critical Pressures (Reservoir EoS)
--
    1056.6352099669
    651.772745079581
    664.036546479197
    490.468298884635
    384.191974487964
    269.516340491557
    180.198300994355
/
VCRIT
--
-- Critical Volumes (Reservoir EoS)
--
    1.50573518513559
    1.56885008183587
    2.63712620491114
    4.67964434648799
    7.26188848439886
    11.0953460957193
    17.6736680960253
/
ZCRIT
--
-- Critical Z-Factors (Reservoir EoS)
--
    0.2740777974
    0.2847159002
    0.2842260192
    0.2719781757
    0.256686814
    0.2366761979
    0.2197244778
/
SSHIFT
--
-- EoS Volume Shift (Reservoir EoS)
--
    -0.04579201311
    -0.1441688522
    -0.0950276543
    -0.04100635693
    0.003672142675

```

```
0.008934047066
0.01156164308
/
ACF
--
-- Acentric Factors (Reservoir EoS)
--
0.327911086
0.01320204346
0.1158061209
0.2285995736
0.3309925
0.490667998
1.124565237
/
BIC
--
-- Binary Interaction Coefficients (Reservoir EoS)
--
0
0.06571622708 0
0.06571622708 0 0
0.06571622708 0.0657162261 0 0
0.06571622708 0.02477685516 0.006571622463 0 0
0.06571622708 0.1051586553 0.02264839242 0 0 0
0.06571622708 0.12313464 0.022648392 0 0 0 0
/
PARACHOR
--
-- Component Parachors
--
78
76.73060872
121.5282336
215.8816613
358.2117489
490.0019888
781.5087913
/
PEDERSEN
--
-- Use Pedersen et al Viscosity Calculation
--
INCLUDE
COMPOSGRAD.PVO /
```

COMPOSGRAD.PVO FILE

This file contains the compositional gradient of the analyzed gas condensate. It is required by TESTCON.PVO file.

```

ZMFVD
--
-- Total Composition vs Depth
--
    12540 0.0453828233890574
          0.718750388016166
          0.127686631506782
          0.0433243126768361
          0.0344592976265433
          0.0199207483957635
          0.0104757983888517
12548.7234042553 0.0453939571894633
          0.718218829691822
          0.127763704324963
          0.0434087722624619
          0.0345861636827282
          0.0200321080869612
          0.0105964647616007
12557.4468085106 0.0454050844924257
          0.717677472597476
          0.127841719098703
          0.0434945676529872
          0.0347152337786119
          0.0201456380456286
          0.0107202843341676
12566.170212766 0.0454162042389383
          0.717125867808932
          0.127920714762212
          0.0435817573828981
          0.0348466054383341
          0.0202614365677828
          0.0108474138009026
12574.8936170213 0.0454273152627938
          0.71656353301861
          0.128000732970994
          0.0436704042350048
          0.0349803833148193
          0.0203796092208471
          0.010978021976932
12583.6170212766 0.0454384162773797
          0.715989949049276
          0.128081818373747
          0.0437605756767574
          0.0351166799258287
          0.0205002696005677
          0.0111122910964431
12592.3404255319 0.0454495058604687
          0.715404555893121
          0.128164018920022
          0.0438523443552174
          0.03525561648938
          0.0206235401907489
          0.0112504182910418
12601.0638297872 0.0454605824366381
          0.714806748195572
          0.128247386209543
          0.0439457886605403
          0.0353973238752863

```


0.0207495533432256
0.0113926172791949
12609.7872340426 0.0454716442568684
0.714195870086787
0.128331975890262
0.044040993369826
0.035541943692985
0.0208784523990654
0.0115391203042066
12618.5106382979 0.0454826893747715
0.713571209243235
0.128417848113693
0.0441380503856713
0.035689629540046
0.0210103929764013
0.011690180366182
12627.2340425532 0.0454937156187719
0.712931990035963
0.128505068057879
0.0442370595868884
0.0358405484410968
0.0211455444558833
0.0118460738035172
12635.9574468085 0.0455047205594013
0.712277365589973
0.12859370653063
0.0443381298127246
0.035994882513511
0.0212840917016666
0.0120071032920936
12644.6808510638 0.0455157014706599
0.711606408537945
0.128683840668546
0.044441380006892
0.0361528309047058
0.0214262370647433
0.0121736013465072
12653.4042553191 0.0455266552841271
0.710918100199246
0.128775554751011
0.0445469405540002
0.0363146120566384
0.0215722027266972
0.0123459344282805
12662.1276595745 0.0455375785341574
0.710211317847608
0.128868941153002
0.0446549548490986
0.0364804663669726
0.0217222334565199
0.0125245077926418
12670.8510638298 0.0455484672920355
0.709484819643341
0.12896410146665
0.0447655811515238
0.0366506593343456
0.021876599871992
0.0127097712401123
12679.5744680851 0.0455593170863552
0.708737226690874
0.129061147829354
0.0448789947880186
0.0368254852987517
0.0220356023219129
0.0129022259847335
12688.2978723404 0.0455701228060746
0.70796700153056

0.129160204506662
0.0449953907882211
0.037005271919139
0.0221995755381679
0.0131024329111749
12697.0212765957 0.0455808785815884
0.707172422170257
0.129261409791941
0.0451149870598603
0.0371903855719053
0.0223688942504134
0.0133110225740348
12705.7446808511 0.045591577637652
0.70635155048702
0.129364918303433
0.0452380282437327
0.0373812379101611
0.0225439800153797
0.0135287074026209
12714.4680851064 0.0456022121098875
0.705502193452666
0.129470903784587
0.045364790433208
0.0375782939003994
0.0227253095937958
0.0137562967254561
12723.1914893617 0.045612772813654
0.704621855113979
0.129579562548369
0.0454955870049491
0.0377820817596806
0.0229134253204157
0.0139947154389524
12731.914893617 0.0456232489498462
0.703707676522429
0.129691117755001
0.0456307758944415
0.0379932053660265
0.0231089480708089
0.0142450274414463
12740.6382978723 0.04563362772608
0.702756359755243
0.129805824781676
0.0457707687740159
0.0382123599284275
0.023312593654856
0.0145084653797008
12749.3617021277 0.0456438938626892
0.701764070637733
0.129923978042652
0.0459160427710552
0.0384403520132175
0.0235251937959238
0.0147864688767301
12758.085106383 0.045654028939367
0.70072631250411
0.130045919764884
0.0460671556304097
0.0386781254832079
0.0237477233426206
0.0150807343354009
12766.8085106383 0.0456640105173573
0.699637759891513
0.130172051444734
0.0462247656272472
0.0389267956008339
0.0239813360987627

0.0153932808195528
12775.5319148936 0.0456738109390918
0.698492035723781
0.130302849049546
0.0463896581582505
0.0391876946218903
0.0242274128021286
0.015726538705311
12784.2553191489 0.0456833956536874
0.697281407043596
0.130438883560728
0.0465627819253435
0.0394624339145179
0.0244876266042772
0.0160834712978508
12792.9787234043 0.0456927208158526
0.695996352952521
0.130580849993443
0.0467453002053776
0.0397529920104804
0.0247640359635015
0.0164677480588248
12800 0.0457
0.6949
0.1307
0.0469
0.04
0.025
0.0168
12801.7021276596 0.0457017298070152
0.694624974322038
0.130729605869306
0.0469386602792477
0.0400618343526157
0.0250592115875611
0.0168839837822171
12810.4255319149 0.0457103480042837
0.693152117098151
0.130886227942953
0.047144696254576
0.0403920907415212
0.0253764247613615
0.0173380951971531
12819.1489361702 0.0457184742843075
0.691557906264201
0.131052108478001
0.0473658015655381
0.0407478522288158
0.0257199616833464
0.01783789549579
12827.8723404255 0.045725967792377
0.689815718214727
0.131229079642305
0.0476051629894077
0.0411345777266608
0.0260955585720232
0.0183939350624991
12836.5957446809 0.0457326240661997
0.687888354076055
0.131419654525589
0.0478672049874967
0.0415598627309854
0.0265112209117071
0.019021078701967
12845.3191489362 0.0457381338245158
0.685722138561888
0.131627372699036

0.0481582609392964
0.0420346118125207
0.0269784868191246
0.0197409953436181
12854.0425531915 0.0457419962798721
0.683234141863019
0.131857562771829
0.0484880321449427
0.0425755788815416
0.0275151564463119
0.0205875316124835
12862.7659574468 0.0457433323646068
0.680286914846186
0.132118757665632
0.0488724204774925
0.0432103370849392
0.0281506810791997
0.0216175564819437
12871.4893617021 0.0457404053226612
0.676627234085463
0.1324259635799
0.0493402981236757
0.0439892183347713
0.0289391967857015
0.0229376837678267
12880.2127659574 0.0457291411604659
0.6717154728886
0.132808889286266
0.0499518454064226
0.0450180039885728
0.0299956850130369
0.0247809622566357
12888.9361702128 0.0456977739927767
0.664240975419445
0.133328312287827
0.0508464776322141
0.0465462353216671
0.0315975120659798
0.0277427132800898
12897.6595744681 0.0456272696648117
0.653395344985338
0.13395014412622
0.052067728000244
0.0486815291543227
0.0339039201972894
0.0323740638717743
12906.3829787234 0.0455559021977841
0.64486375441198
0.134333281123356
0.0529649119177265
0.0502914842373906
0.035699123856104
0.036291542255658
12915.1063829787 0.0455032469893961
0.639245938525627
0.134536184292465
0.053525404171665
0.05131770264838
0.0368704641377839
0.0390010592346832
12923.829787234 0.0454619189163562
0.635074234671103
0.134662067827007
0.0539261690452036
0.0520622815671522
0.0377342705152803
0.0410790574578978

12932.5531914894 0.0454274916852652
0.631710112983094
0.134748455237538
0.0542398180851626
0.052651868295642
0.0384269348132634
0.0427953189000353
12941.2765957447 0.0453977192789538
0.628861490949918
0.134811165248744
0.0544987710501794
0.0531435304450324
0.0390106308240572
0.0442766922031149
12950 0.0453713074456986
0.626370505838909
0.134858254780241
0.0547202537604282
0.0535677798591761
0.0395188656609985
0.0455930326545484

/

VITA

Name:

BULENT IZGEC

Permanent Address:

Me-Sa Gunes Sit. Turgutlu Sok. 13/8
G.O.P, Ankara, Turkey

Education:

B.S., Geophysics 1999
University of Ankara
Ankara, Turkey

M.S., Petroleum Engineering 2003
Texas A&M University
College Station, Texas